Clim. Past, 22, 747–781, 2026
https://doi.org/10.5194/cp-22-747-2026

Climate of the Past
Open Access
EGU

How unstable was the environment during the Penultimate Glacial in the South-Western Mediterranean? Vegetation, climate and human dynamics during MIS 6

Liz Charton[1,2], Nathalie Combourieu-Nebout[1], Adele Bertini[2], Odile Peyron[3], Mary Robles[3], Vincent Lebreton[1], and Marie-Hélène Moncel[1]

[1]UMR 7194 HNHP – "Histoire Naturelle des Humanités Préhistoriques", MNHN/CNRS/UPVD, Paris, France
[2]Dipartimento di Scienze della Terra, Università degli Studi di Firenze, Florence, Italy
[3]UMR 5554, ISEM-Institut des Sciences de l'Evolution de Montpellier, CNRS,
Université de Montpellier, Montpellier, France

Correspondence: Liz Charton (liz.charton@mnhn.fr)

Received: 10 October 2025 – Discussion started: 21 October 2025
Revised: 26 March 2026 – Accepted: 26 March 2026 – Published: 10 April 2026

Abstract. The impact of rapid climate variability on Neanderthal population in Europe during the Last Glacial (Marine Isotope Stages 4–2), including Dansgaard-Oeschger cycles and Heinrich stadials, has been the subject of a long-standing debate. However, few studies have focused on the nature and impact of such rapid variations on human population during earlier periods. A growing number of high-resolution paleoclimatic archives supports the persistence of rapid oscillations during the penultimate glaciation (Marine Isotope Stage – MIS 6), and the close response of Mediterranean ecosystems to these. Still, few palynological sequences in the Mediterranean region offer sufficient resolution to document vegetation dynamics during this time. Pollen records are especially lacking in the western Mediterranean, a key region to understand the connection between North Atlantic and Mediterranean climatic influences. This region is also traditionally considered a climatic refugium for human population during unfavourable periods. We provide new palynological data covering MIS 6 from the long and continuous marine record of the ODP site 976 in the Alboran Sea. A total of 200 samples, spanning the interval from 196 to 127 ka Before Present (BP), reveals both long-term trends and rapid fluctuations in the regional vegetation composition. A multi-method approach, including modern analogues, regression, and machine learning approaches, was applied to the ODP 976 pollen assemblages to reconstruct the annual/seasonal temperatures and precipitation. Results show that three phases can be identified. The first phase (187–166 ka BP) is characterized by significant oscillations of temperate trees and rather cool and humid conditions during early MIS 6, coincident with a sapropel layer deposition in both the western and eastern Mediterranean. In the second phase (165–144 ka BP), arid herbaceous vegetation is dominant, marking the main imprint of glacial maxima conditions and reduced climate variability. The third phase (144–129 ka BP) is marked by the development of Ericaceae and increased annual precipitation. At the end of MIS 6 glaciation, an episode of strong cooling and steppe and semi-desert expansion is identified as Heinrich Stadial 11 (135–129 ka BP), marking a distinct pattern for Termination II in the Western Mediterranean. Rapid oscillations appear like a pervasive feature of the Penultimate glacial in the SW Mediterranean, though they present reduced amplitude and frequency compared to the Last Glacial. A synthesis of human occupation during MIS 6 shows that a mosaic of traditional (Mode 2) and innovative (Mode 3) lithic technological features is observed in the archaeological record. Although the data are scarce, Neanderthals seem to have continuously inhabited Western Mediterranean regions across the penultimate glacial. The severe climate conditions during Heinrich Stadial 11 (∼ 133–129 ka BP) might have played a role in the apparent population contraction at the end of MIS 6, and perhaps also in the definitive abandonment of Lower Palaeolithic industries.

1 Introduction

Rapid climate oscillations occurred during the last Glacial period (MIS 4–2). Dansgaard-Oeschger (DO) cycles have been well identified in ice-core records (Bond et al., 1999; Dansgaard et al., 1993; Johnsen et al., 1992; Rasmussen et al., 2014) and recognized in Atlantic sedimentary cores (e.g. Bond et al., 1993, 1997; Roucoux et al., 2005; Sánchez Goñi et al., 2002; Shackleton et al., 2000; Zumaque et al., 2025). Short periods of intense cold named Heinrich Stadials (HS) and linked with intense iceberg discharges were also evidenced in Atlantic sediments (Bond et al., 1992; Heinrich, 1988; Hemming, 2004; Rasmussen et al., 2003; Ruddiman, 1977; Shackleton et al., 2004). Major cooling events also occurred during MIS 5 and the penultimate deglaciation (e.g. Chapman and Shackleton, 1999; Oppo et al., 2001). These high-frequency oscillations reflect major changes at global scale in the oceanic circulation and the Atlantic Meridional Overturning Circulation (AMOC), that are important features particularly during glacial terminations (Barker and Knorr, 2021). The Mediterranean region has been very sensitive to the rapid climate oscillations of MIS 5 to MIS 1, with changes recorded in both marine and continental environments (Cacho et al., 1999, 2006; Combourieu-Nebout et al., 2002, 2009; Fletcher et al., 2010; Martrat et al., 2007; Penaud et al., 2016; Sánchez Goñi et al., 2002; Sánchez Goñi, 2022).

The penultimate glacial (MIS 6) took place between ∼ 185 and 130 ka BP and presented a different ice-sheet and global climate configuration compared to the last glacial (MIS 4–2). It is considered among the coldest glacial periods of the past 800 ka BP (Masson-Delmotte et al., 2010), characterized by larger European Ice-Sheet and smaller Laurentide ice-sheet extension (Colleoni et al., 2016; Ehlers et al., 2018; Ehlers and Gibbard, 2007; Rohling et al., 2017). In Europe, it corresponds to the Riss glaciation in the Alpine area, and to the late Saalian glaciation complex in northern and central Europe, with two major ice-sheet advances identified in Germany: the Drenthe advance (∼ 170–155 ka BP) characterized by the maximum ice extent in Europe, and the less extensive Warthe advance during the younger stage of MIS 6 (Ehlers et al., 2011). The exact chronology of the Penultimate Glacial Maximum (i.e. the maximum extension of the northern hemisphere ice-sheet) is still not well constrained (Svendsen et al., 2004), but is usually considered around 140 ka BP (Colleoni et al., 2016). Five marine isotopic substages were identified from MIS 6e to 6a, reflecting variations of global sea temperatures : three cold substages (6e: ∼ 180 ka BP, 6c: ∼ 160 ka BP, 6a: ∼ 136 ka BP) with increasing cold intensity, and two warm substages (6d: ∼ 170 ka BP and 6b: ∼ 149 ka BP) (Railsback et al., 2015). Different speleothem records revealed that MIS 6 glaciation in Europe, including the Mediterranean region, was characterized by wetter conditions in comparison with the last glacial (Ayalon et al., 2002; Koltai et al., 2017; Nehme et al., 2018; Regattieri et al., 2014). Furthermore, various studies highlighted the apparent higher stability of the Laurentide ice-sheets during the penultimate glacial, leading to the absence of typical "Heinrich layers" in the North Atlantic sediments, with the exception of the large event recorded at the MIS 6 to MIS 5 transition, HS11 (∼ 135–129 ka BP) (de Abreu et al., 2003; McCarron et al., 2021; McManus et al., 1999; Obrochta et al., 2014; Ovsepyan and Murdmaa, 2017; Shackleton et al., 2003).

Human Palaeolithic groups in Europe were likely affected by rapid climate changes (Bradtmöller et al., 2012; Dennell et al., 2011; Raia et al., 2020; Willis et al., 2004). The South-Western Mediterranean probably played a major role as one of the climate refugia areas around the Mediterranean Basin during the most unfavourable climatic periods, permitting the persistence of "source" population able to recolonize the northernmost areas during more favourable periods (Bailey et al., 2008; Bicho and Carvalho, 2022). Neanderthal presence in very distinct ecotones in Eurasia proves they could adapt to a very wide range of environments. However, recent niche modelling approaches together with palaeoecological data from archaeological sites strengthened the view that warm forested landscapes like the MIS 5e environments represented the most suitable habitats for Neanderthals, where they could persist during colder periods (Carrión et al., 2026; Ochando et al., 2019; Stewart et al., 2019; Trájer, 2023). This conception leads to the overlap of the notions of refugium for vegetation and human populations, despite the greatest adaptability and niche extension of humans. Many studies focused on the potential impact of abrupt environmental changes on Neanderthal populations, especially those associated with Heinrich Stadials during MIS 3 (e.g. Charton et al., 2025; D'Errico and Sánchez Goñi, 2003; Finlayson and Carrión, 2007; Melchionna et al., 2018). During the previous climatic cycles of the Middle Pleistocene, when Early to Middle Palaeolithic cultures developed, repeated climate instability has been brought forward as an explanation for the large variability in the lithic production (Dennell et al., 2011; Foerster et al., 2022; Sánchez-Yustos and Diez-Martín, 2015), and the non-linearity of Neanderthal biological evolution (Bermúdez de Castro and Martinón-Torres, 2013; Hublin, 2009). Still, the short and long-term resilience of human populations in a globally unstable environment is poorly understood, and partially hindered by our limited knowledge of fast millennial-scale climate oscillations in older glaciations prior to MIS 4–2.

While the Greenland ice does not provide an adequate record for periods older than 123 ka BP (Chappellaz et al., 1997), the description of a precise stratigraphy of climatic events at sub millennial scale for the previous glacial/interglacial cycles remains complex, and relies on the Antarctic isotope record (Bazin et al., 2013; Jouzel et al., 2007), the study of marine sediments (de Abreu et al., 2003; Lisiecki and Raymo, 2005; Margari et al., 2010, 2014; McManus et al., 1999; Obrochta et al., 2014) and high-resolution conti-

nental archives such as speleothems (Burns et al., 2019; Held et al., 2024; Hodge et al., 2008; Wainer et al., 2013; Wang et al., 2018, 2001). Benthic and planktonic isotopic ratios together with Sea Surface Temperatures (SSTs) reconstructions in the North Atlantic and the Western Mediterranean showcased the persistence of millennial-scale events and interhemispheric bipolar see-saw heat transport during MIS 6, in addition to important reorganization of the water circulation during sapropel S6 deposition ∼ 175 ka BP (Margari et al., 2010, 2014; Martrat et al., 2004, 2007, 2014; Rousseau et al., 2020; Sierro and Andersen, 2022). Nevertheless, MIS 6 is much less well documented than the last glacial in Mediterranean Europe. Few palynological sequences are available to document the vegetation changes across this interval (Camuera et al., 2019, 2022; Follieri et al., 1988; Margari et al., 2010; Okuda et al., 2001; Roucoux et al., 2011; Sadori et al., 2016; Sinopoli et al., 2019; Tzedakis et al., 2006; Wilson et al., 2021). Among them, only one in SW Europe provides sufficient resolution to document high-frequency changes (Margari et al., 2010, 2014). This record from the deep-sea core MD01-2444 showed that several millennial-scale climatic events impacted the vegetation during the lower part of MIS 6 (Margari et al., 2010). The core is located out of the Mediterranean Sea, along the Portuguese margin in the Atlantic Ocean. Therefore, questions remain open concerning the impact of such rapid events on the Western Mediterranean region, considered a Pleistocene refugium for human populations.

To fill this gap, our study provides high-resolution pollen data and quantitative climate reconstructions from ODP site 976 in south-western Mediterranean focusing on MIS 6. We aim to (i) reconstruct the vegetation and climate changes in the SW Mediterranean during the penultimate glacial, (ii) identify millennial-scale climatic changes and correlate them with other Atlantic and Mediterranean paleoenvironmental records, (iii) compare the nature of millennial-scale climate and vegetation dynamics during the last glacial period and the penultimate glacial using a single, continuous pollen record and (iv) explore the potential impact of these climatic changes for Early Middle Palaeolithic human groups, with particular attention to the presence of climate refugia during the most extreme glacial phases.

2 Study site

Ocean Drilling Program (ODP) Site 976 (36°12′ N, 4°18′ W, 1108 m depth) core was retrieved in 1995 in the Alboran Sea (Zahn et al., 1999). The site is located about 110 km east of the Gibraltar Strait, 70 km south of the Spanish coast, and 100 km north of Morocco (Fig. 1).

The Alboran Sea is the westernmost extensional basin of the Mediterranean Sea, bordered to the north by the Betic Cordillera and to the south by the Moroccan Rif mountains. Oceanic currents result from the water masses exchanges between the Atlantic Ocean and the Mediterranean Sea through the Gibraltar Strait. The surface currents are governed by the inflow of low-salinity Atlantic waters (Atlantic Jet) forming two anticyclonic gyres named Western and Eastern Alboran Gyres (WAG and EAG) (Renault et al., 2012) (Fig. 1). The Mediterranean high-salinity water masses flow out in the Atlantic basin through the intermediate depth currents.

The modern climate in the Alboran Sea region is typically Mediterranean, defined by long, hot, dry summers and mild and cool winters (Lionello et al., 2006; Sánchez-Laulhé et al., 2021). Atlantic westerlies dominate during winter, while subtropical high pressure masses generate intense drought during summer (Sumner et al., 2001). The current vegetation distribution on the Alboran borderlands follows a strong altitudinal climatic gradient : dry steppe elements such as *Artemisia* and *Lygeum* grow in the most arid lowlands along the coast, sclerophyllous evergreen taxa, including *Quercus ilex*, *Olea* and *Pistacia* are the main representatives of the thermo-to meso-Mediterranean belts, while temperate vegetation with deciduous trees constitutes the overlying supra-Mediterranean belt (Quézel, 2000). Finally, coniferous forests of *Abies* and *Pinus* grow in the oro-Mediterranean belt (above approximately 1200 m), with the presence of *Cedrus* in altitudinal vegetation of the Moroccan Rif mountains.

The main sedimentation processes in the area originate from the strong erosion in the Betic Cordillera (Alonso et al., 1999; Liquete et al., 2005; Lobo et al., 2006) and the material transported by the surface Atlantic waters (Auffret et al., 1974), although a significant but unknown proportion of particles including pollen was transported by African winds as evidenced by the presence of Saharan clay particles and *Cedrus* pollen across the Pleistocene (Bout-Roumazeilles et al., 2007; Jiménez-Moreno et al., 2020; Magri and Parra, 2002). Therefore, the pollen assemblage is interpreted as reflecting the regional vegetation of the southern Iberian Peninsula, with smaller but variable contribution from Northern Africa. Previous studies have shown that the Alboran Sea palynological record displays close similarities with the Padul record in SE Spain (Camuera et al., 2019), indicating that ODP 976 is a valid archive to reconstruct the southern Iberian Peninsula vegetation changes (Fletcher and Sánchez Goñi, 2008; Charton et al., 2025).

Two Organic-Rich Layers (ORLs) were identified in ODP 976 core during the MIS 6 interval, bed 607 (50.43–49.93 m), and bed 606 (41.6–40.4 m) (Murat, 1999). The ages were recalculated based on the updated age model for MIS 6 presented here, giving 178.07–174.53 ka BP for bed 607, and 132.64–129.16 ka BP for bed 606. With a Total Organic Carbon (TOC) of 1.18 % and 1.85 % respectively, these layers have been described as "ghost sapropels", as they present a lower organic matter content than the Eastern Mediterranean sapropels (Rogerson et al., 2008). Their relevance for hydrological and climatic inferences in the Alboran Sea will be discussed in the light of the vegetation dynamics.

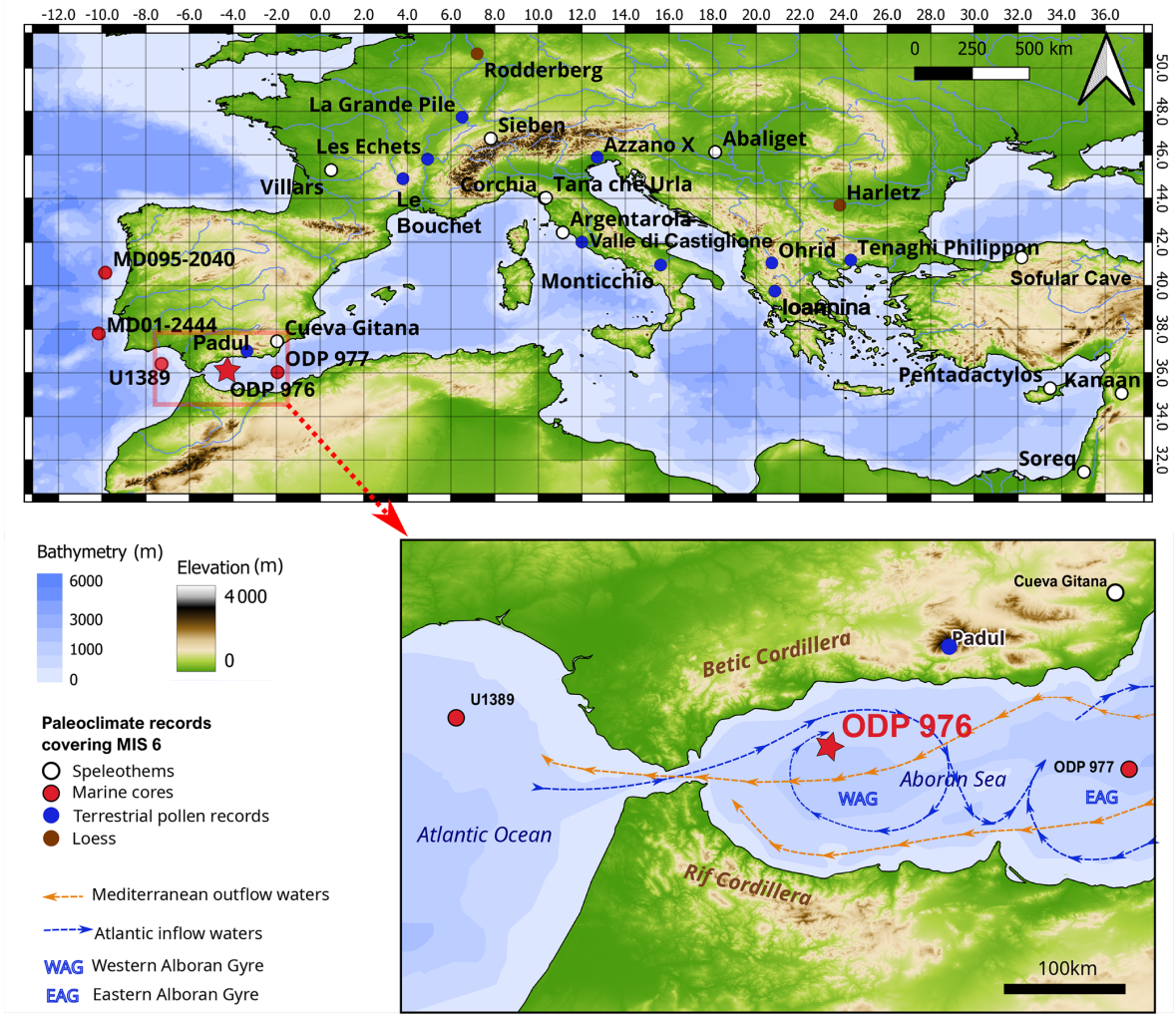

Figure 1. Map showing the location of ODP 976 core together with other paleoenvironmental and paleoclimate records covering part or all of MIS 6, as discussed in the text.

3 Methods

3.1 Age Model

The age model for the study interval uses three previously published tie-points between ODP 976 Mg / Ca-derived SST (Jiménez-Amat and Zahn, 2015) and the speleothem temperature records from Dongge cave in China (Kelly et al., 2006; see Fig. S1 in the Supplement). Several other marine records covering MIS 6 in the region are chronologically tuned to speleothems (e.g. Sierro and Andersen, 2022; Tzedakis et al., 2018). For the lower interval, the low resolution of planktonic isotopic data available for ODP 976 did not allow direct correlation to global temperature stacks or orbital configuration (von Grafenstein et al., 1999). Instead, we chose to align the higher-resolution pollen record produced in this study with the one from MD01-2444 core on the Portuguese margin (Margari et al., 2010, 2014; Tzedakis et al., 2018). Previous studies highlighted the strong similarities between pollen records on the Atlantic margin and the Alboran Sea during the last glacial period (Fletcher et al., 2010; Fletcher and Sánchez Goñi, 2008; Sánchez Goñi et al., 2002), supporting this approach. MD01-2444 chronology is based on the alignment of benthic isotopic events with the Antarctic temperature record, on AICC2012 timescale (Jouzel et al., 2007; Margari et al., 2010; Shin et al., 2020). The eleven tie-points between MD01-2444 core and EPICA Dome C can be found in the Supplement (Table S1). Five peaks of temperate forest in MD01-2444 were used as control-points for ODP 976 (Table 1). The main assumptions of these tuning approaches to the Dongge cave speleothem and the Antarctic record are discussed in detail in Jiménez-Amat and Zahn (2015) and Margari et al. (2010) respectively. The obtained chronology for ODP 976 core for MIS 6 prevents any assessment of the southwestern Mediterranean vegetation response to global climatic events.

Table 1. List of control points used to calibrate the ODP 976 record for the MIS 6 interval. The tie-points on MD01-2444 temperate pollen curve are on AICC2012 timescale.

Event type	ODP 976 meters composite depth (mcd)	Age (ka BP)	References
Dongge cave speleothem D3	40.25	128.73	Jiménez-Amat and Zahn (2015), Kelly et al. (2006)
Dongge cave speleothem D2	42.61	135.57	Jiménez-Amat and Zahn (2015), Kelly et al. (2006)
Dongge cave speleothem D1	44.14	142.09	Jiménez-Amat and Zahn (2015), Kelly et al. (2006)
Temperate pollen peak in MD01-2444	46.4	149.43	Margari et al. (2010), Shin et al. (2020)
Temperate pollen peak in MD01-2444	48.5	160.00	Margari et al. (2010), Shin et al. (2020)
Temperate pollen peak in MD01-2444	49.3	170.07	Margari et al. (2010), Shin et al. (2020)
Temperate pollen peak in MD01-2444	50.48	178.42	Margari et al. (2010), Shin et al. (2020)
Temperate pollen peak in MD01-2444	53.2	193.758	Margari et al. (2010), Shin et al. (2020)

A linear regression was applied to obtain a continuous age for the study interval, spanning from 126.4 to 196.6 ka BP, with a mean resolution of about 350 years for the record (Fig. 2).

3.2 Pollen analyses

Two hundred samples have been analysed in this study, between 40 and 54 m (mcd) depth. The sample processing followed the traditional steps used for pollen extraction (Faegri and Iversen, 1964) and previously applied to the ODP 976 core (Combourieu-Nebout et al., 2002; 2009; Sassoon et al., 2023, Charton et al., 2025). It included sample weighing between 5 and 10 g of sediments, a 150 µm sieving for retrieving macrofossils and macroparticles, followed by 10 % HCl, 40 % HF, 20 % HCl and a final 10 µm sieving.

A minimum of 150 pollen grains were counted for each sample, excluding *Pinus* as it is usually overrepresented in marine sequences (e.g. Combourieu-Nebout et al., 2002; Fletcher et al., 2010; Mudie, 2011, and references therein), and represents often more than 50 % of the total pollen sum in the study interval (see Fig. 3).

Ecological groups of pollen taxa were defined following previous studies of the ODP 976 record (Charton et al., 2025; Combourieu Nebout et al., 2009; Sassoon et al., 2023). The percentage pollen diagram was constructed using the *rioja* R package (Juggins, 2024). Constrained Incremental Sum-of-Squares (CONISS) cluster analysis was applied for pollen zonation, using the *vegan* package on R (Oksanen et al., 2026).

3.3 Pollen-inferred climate reconstructions: a multi-method approach

Four methods were applied to the ODP 976 record to reconstruct past climate changes during MIS 6. This is the first time this approach is used for the entire MIS 6 interval (Sinopoli et al., 2019). The multi-method approach allows for a more accurate climate reconstruction (trends and rapid events) compared to the traditional single-method approach (Chevalier et al., 2020; Peyron et al., 2011, 2013; Salonen et al., 2019; Sassoon et al., 2025). It also allows us to compare the reliability and biases of the different methods, which are based on different ecological principles and mathematical algorithms. Four methods were used in this study.

The Modern Analogue Technique (MAT) is the first "assemblage" method ever developed to estimate climate parameters based on pollen assemblages, and is still the most widely used (Guiot, 1990). It is based on the calculation of a dissimilarity index between the fossil samples and samples from a modern pollen dataset. The values of the closest modern analogues selected (here, 4) are averaged to reconstruct the climate parameters for each fossil sample. Weighted-Averaging Partial Least Squares (WA-PLS) (ter Braak and Juggins, 1993) is the second most widely used method, and is based on a different mathematical approach using non-linear regression. Assuming that taxa are most abundant where they find their optimum climatic conditions, WA-PLS models the plant/climate relationships from the modern calibration dataset, weighing the climatic values based on the pollen taxa percentage. These plant pollen abundance/climate transfer functions are then used to calculate the climate parameters of the fossil samples. The last two methods, Random Forest (RF) and Boosted Regression Trees (BRT), rely on a completely different approach using machine learning: they generate a large set of regression trees based on a randomised pollen dataset by bootstrapping (with pollen taxa selected randomly). Contrary to RF (Prasad et al., 2006), BRT (Salonen et al., 2012) assigns a higher probability to select samples that have not been selected before (boosting), increasing the performance of the model for elements that are less well predicted (Chevalier et al., 2020). The application of these machine learning methodologies in paleoclimatology is very promising, especially for BRT, and they have already been validated through different European and Mediterranean pollen records, for different time periods (Charton et al, 2025; d'Oliveira et al., 2023; Robles et

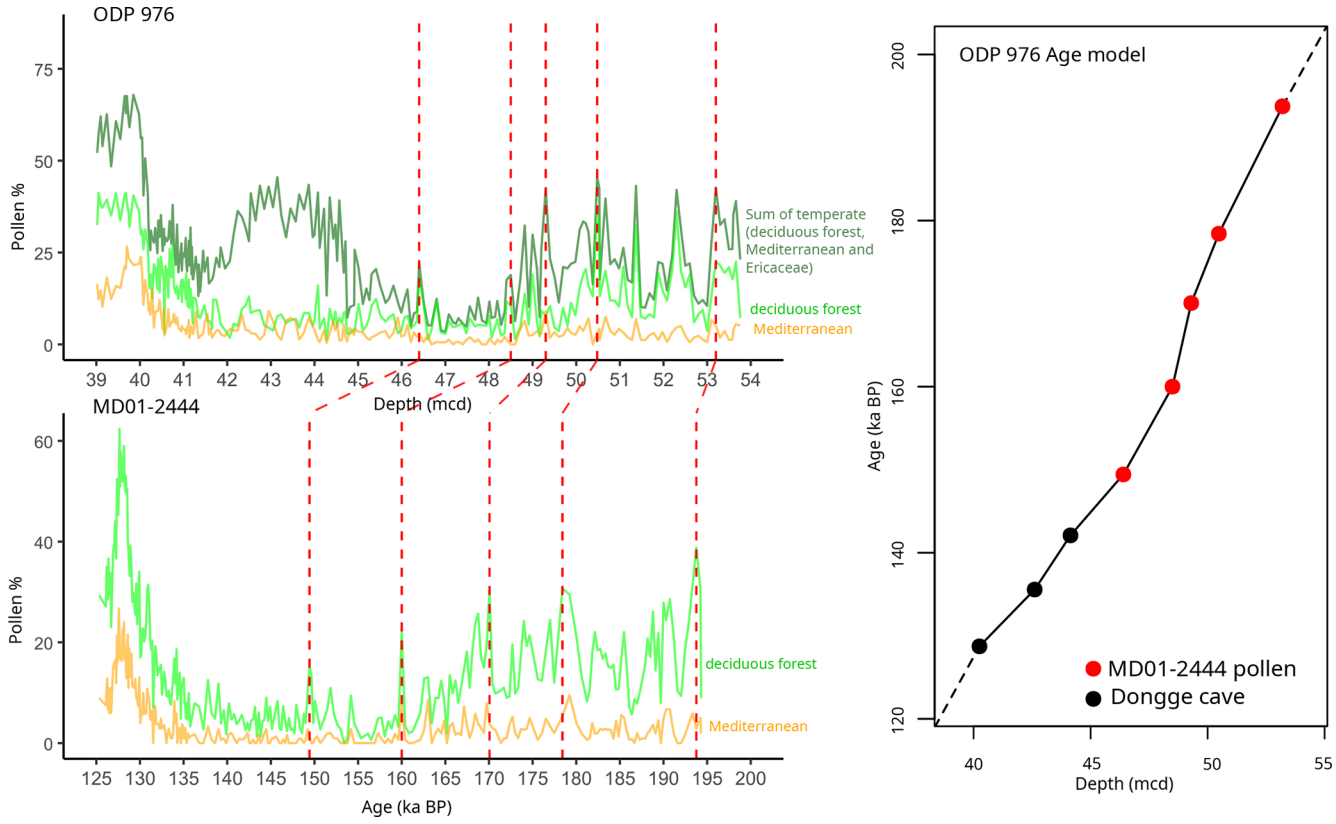

Figure 2. Age versus depth model for the MIS 6 part of ODP 976 record, based on correlation between the Mg / Ca-based SST curve (Jiménez-Amat and Zahn, 2015) and the Dongge cave speleothem temperature record (Kelly et al., 2006) (black dots), and graphical correlation of the temperate pollen curve with the MD01-2444 palynological record (red dots and dotted lines) on AICC2012 timescale (Margari et al., 2010; Shin et al., 2020).

al., 2023; Robles, 2022; Salonen et al., 2019; Sassoon et al., 2025).

The four methods were run on R using the *Rioja* package for MAT and WA-PLS (Juggins, 2024), *dismo* for BRT (Hijmans et al., 2024) and *randomForest* for RF (Liaw and Wiener, 2022).

We used the modern pollen dataset compiled by Peyron et al. (2013, 2017) and updated by Dugerdil et al. (2021) and Robles et al. (2023). Samples belonging to non-relevant biomes for this study were excluded (Taiga, Tundra, Pioneer Forest, warm steppe and hot desert), resulting in 2373 samples for calibration dataset spanning Eurasia and NW Africa (see Supplement, Fig. S2). A total of 103 harmonized pollen taxa are included in the dataset, excluding *Pinus* and aquatic taxa.

Six climate variables were reconstructed: PANN (annual precipitation), MAAT (annual temperatures), SUMMERPR (summer precipitation), WINTERPR (winter precipitation), MTWA (mean temperature of the warmest month) and MTCO (mean temperature of the coldest month). The climatic tolerance spectra of the ten most abundant pollen taxa in the ODP 976 record have been reconstructed based on the modern dataset (Fig. S3). They show that steppe and semi-desert taxa display the highest tolerance to low winter temperature and precipitation, while Mediterranean taxa (*Olea* and *Quercus ilex*-type) are the most tolerant taxa to high annual and summer temperature, and *Cedrus* and Ericaceae to higher annual and seasonal precipitation. SUMMERPR was poorly reconstructed according to the accuracy indicators (Table 2). This is in agreement with previous studies showing the poor reliability of summer parameters (e.g. Camuera et al., 2022). Therefore, we chose to represent seasonal parameters as contrast values for a better visualization: TCON (temperature contrast) = MTCO − MTWA, and PCON (precipitation contrast) = WINTERPR − SUMMERPR. The MTWA and SUMMERPR results can be found in the Supplement (Fig. S4).

For comparison with the present-day climate, and the calculation of anomalies, the modern values were extracted from ERA 5 reanalysis of the ECMWF (European Centre for Medium-Range Weather Forecasts), based on data assimilation into meteorological modelling from 1960 to 2022 (Hersbach et al., 2020). Pollen dispersal is reduced beyond a radius of 175 km (Rojo et al., 2016). However, other studies suggest that pollen can be transported up to distances of 200–300 km (Fernández-Rodríguez et al., 2014) and even

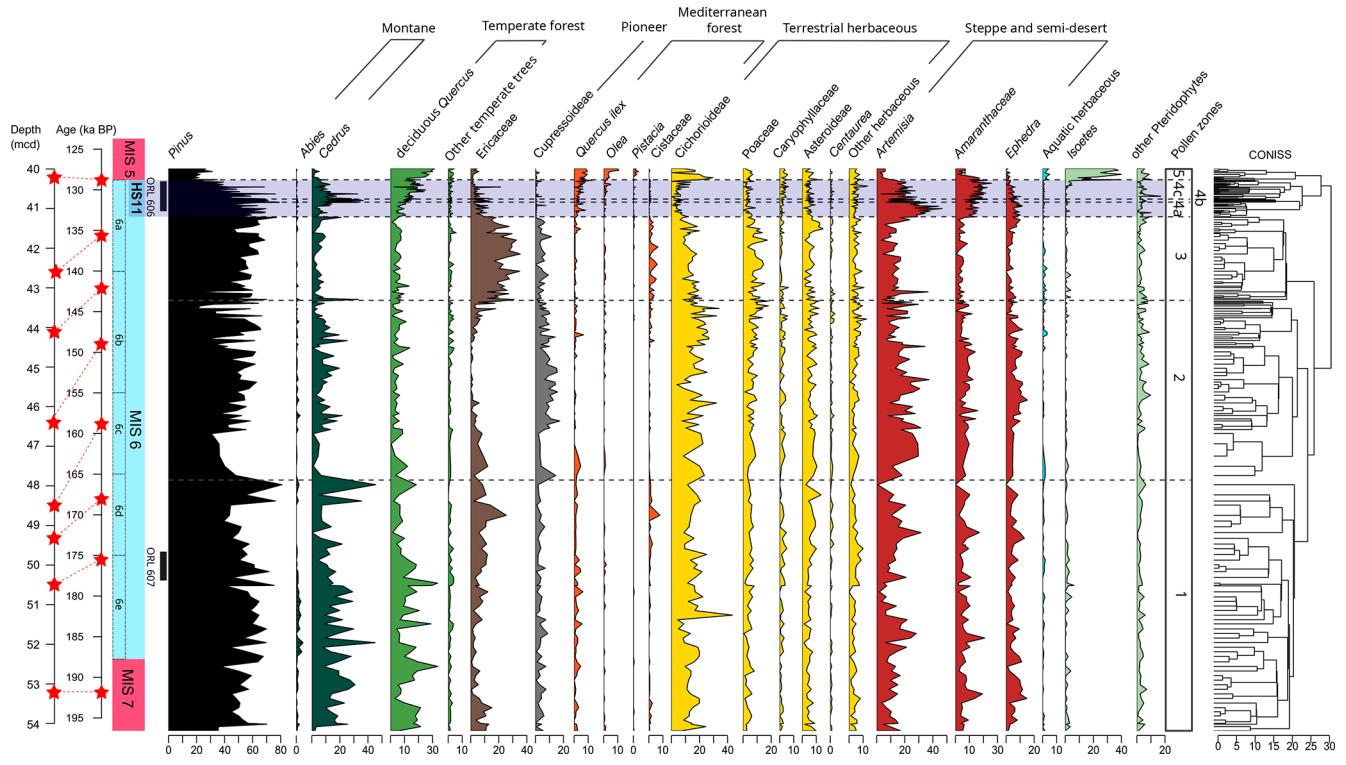

Figure 3. Pollen diagram of selected taxa for MIS 6 interval in the ODP 976 record, plotted against age. Taxa are grouped by ecological groups (see Table 2). Red stars indicate control points used for the age calibration, and their correspondence with mcd (meters composite depth) (see Table 1). The blue bar indicates Heinrich Stadial 11. ORL: Organic Rich Layers from ODP 976 (Murat, 1999).

over distances greater than 500 km (Bayr et al., 2023; Damialis et al., 2017). Sediments from marine cores such as ODP 976 can therefore include close and long-distance pollen. To account for these observations, an averaged value of the climate parameters on a 400 km radius around the ODP 976 site was extracted (Fig. S5), giving MAP = 478 mm, MAAT = 16.78 °C, MTCO = 13.78 °C, WINTERPR = 172 mm, TCON = −9.59, PCON = 141.5 mm. These values for modern climate, averaged temporally and spatially, provide a better basis for understanding the nature of the climate signal extracted from a marine palynological sequence at a regional pluri-annual scale.

The reliability of the different methods and climate parameters reconstructed is evaluated with bootstrapping cross-validation through two indicators: the correlation coefficient between the variables (R^2) and the root mean square error (RMSE).

4 Results

4.1 Pollen record

The pollen diagram shows the vegetation dynamics between 196.6 and 127.5 ka BP, spanning late MIS 7 to early MIS 5 (Fig. 3). Five pollen zones were separated by CONISS cluster analysis, with zone 4 being divided in three subzones (Table 2).

Zone 1 most represented taxa are deciduous *Quercus* and *Cedrus*, with important abundance variability showing an unstable phase at the transition from MIS 7 to MIS 6e and 6d. Zone 2 displays the maximum expansion of steppe and semi-desert vegetation together with other open vegetation taxa and Cupressoideae during the MIS 6b and 6c. An additional noteworthy observation within this interval is the presence of gastropod shells identified as *Limacina retroversa* (Jeanne Rampal, personal communication, 2023), recovered during sieving of a sample at 46.4 m, corresponding to around 155.5 ka BP (Fig. 4). This species is usually most abundant in temperate to subpolar waters in the North-Atlantic (Thabet et al., 2015). Zone 3 is mainly characterized by the abundance of Ericaceae at the final stage of MIS 6 (6b and 6a). Zone 4, at the end of MIS 6a, is divided into 3 subzones which display fast vegetation changes during the transition from MIS 6 to MIS 5 (Termination II), and Heinrich Stadial 11. The fast expansion of steppe and semi-desert taxa (*Artemisia*, Amaranthaceae, *Ephedra*) occurs simultaneously with the first increase of deciduous temperate and Mediterranean forest indicative of the initialization of interglacial conditions (zone 4a). This episode of arid vegetation dominance is interrupted in zone 4b by the fast expansion of mon-

Table 2. Description of the pollen zones identified through CONISS cluster analysis, including the main characteristics of their pollen assemblage and associated climate reconstructions.

Pollen zone	Depth (mcd) and Age (ka BP)	Description of the pollen assemblage (Fig. 3)	Climate reconstructions (Fig. 5)
5	40.25–39.98 m 128.73–127.47 ka BP	Peak abundance of deciduous *Quercus* (up to 32 %), *Quercus ilex* (4 %–10 %), *Olea* (2 %–11 %), *Pistacia* (up to 4 %), aquatic herbaceous (up to 5 %) and *Isoetes* (up to 38 %). High values of Cichorioideae (up to 30 %). Low percentages of *Pinus* (< 35 %), *Artemisia* (< 11 %), Amaranthaceae (< 18 %) and *Ephedra* (< 3 %).	Rapid increase of temperature, precipitation and seasonal contrast close to the modern value
4c	41.08–40.28 m 131.13–128.81 ka BP	New increase of *Artemisia* (up to 29 %) and Amaranthaceae (up to 26 %). High values of *Cedrus* (5 %–28 %), and increasing percentages of deciduous *Quercus* (10 %–23 %), Cichorioideae (0 %–14 %) and *Quercus ilex* (1 %–13 %). Decrease of Ericaceae (13 %–0 %). Increasing percentages of *Isoetes* (0 %–5 %) and Pteridophytes spores (0 %–17 %).	First decrease, and then increase in temperatures and precipitation, with low PCON.
4b	41.21–41.09 m 131.51–131.16 ka BP	Peak abundance of *Cedrus* (up to 37 %). Decrease of *Artemisia* (30 %–7 %), Amaranthaceae (6 %–13 %) and *Ephedra* (6 %–4 %). Notable abundance of deciduous *Quercus* (6 %–15 %) and *Quercus ilex* (1 %–3 %).	Abrupt rise in precipitation contrast, but still cold conditions.
4a	41.82–41.22 m 133.28–131.54 ka BP	Peak abundance of Artemisia, (24 %–47 %), Amaranthaceae (14 %–6 %) and *Ephedra* (5 %–11 %). Decreasing trend of Ericaceae percentages (12 %–2 %), and progressive increasing of deciduous *Quercus* (4 %–11 %) and *Quercus ilex* (1 %–8 %). Decrease of Cichorioideae (< 11 %) and Cupressoideae (< 8 %).	Rapid decrease in temperature, precipitation and seasonal contrast.
3	44.57–41.85 m 143.49–133.37 ka BP	Peak abundance of Ericaceae (12 %–35 %), and high values of Cichorioideae (8 %–22 %). Notable presence of Cupressoideae (2 %–11 %). Peak abundance of *Artemisia* (37 %) at 44.28 m/142.54 ka BP and *Cedrus* (33 %) at 44.57 m/143.49 ka BP.	Increase of temperatures (but still lower than present), and important precipitation rise until values higher-than-present. Seasonal contrast close to present-day.
2	48.91–44.63 m 165.16–143.68 ka BP	High percentages of Cichorioideae (11 %–34 %), Poaceae (4 %–18 %), *Artemisia* (4 %–37 %), Amaranthaceae (3 %–16 %) and *Ephedra* (3 %–12 %). Cupressoideae maximum between 150–160 ka BP (up to 17 %), and abundant *Cedrus* (up to 25 %). Very low values of deciduous *Quercus* (< 10 %), Mediterranean taxa (< 4 %) and Ericaceae (< 12 %), with minimum values between 150 and 158 ka BP.	Decline of temperatures and precipitation, both lower than the modern values, reaching a minimum between ∼ 164–155 ka BP. Afterwards, progressive rise in temperature, precipitation and seasonal contrast.
1	53.76–49 m 196.15–166.29 ka BP	High percentages of *Cedrus* (8 % to 45 %) and deciduous *Quercus* (4 % to 34 %), with important variations. Abundant Cichorioideae (up to 43 %) and Ericaceae (up to 25 %), with notable presence of *Abies* (up to 5 %), *Quercus ilex* (up to 6 %) and *Isoetes* (up to 6 %). Relatively low values of semi-desert elements (*Artemisia*, Amaranthaceae, *Ephedra*) but with two increases at 49.6 m/172 ka BP and at 51.6 m/185 ka BP.	Rather stable conditions expressed by the smoothed lines, but important and numerous rapid oscillations. In general, values of precipitation and seasonal contrast are close or higher that the modern value, while temperature is cooler than present.

tane vegetation mainly represented by *Cedrus*. A new steppe and semi-desert vegetation increase is observed in zone 4c, while the deciduous temperate forest and the Mediterranean vegetation continue to expand. Finally, zone 5 is characterized by the maximum abundance of mesophilous and thermophilous elements, mainly represented by deciduous *Quercus* and *Quercus ilex*, typical of the MIS 5 interglacial.

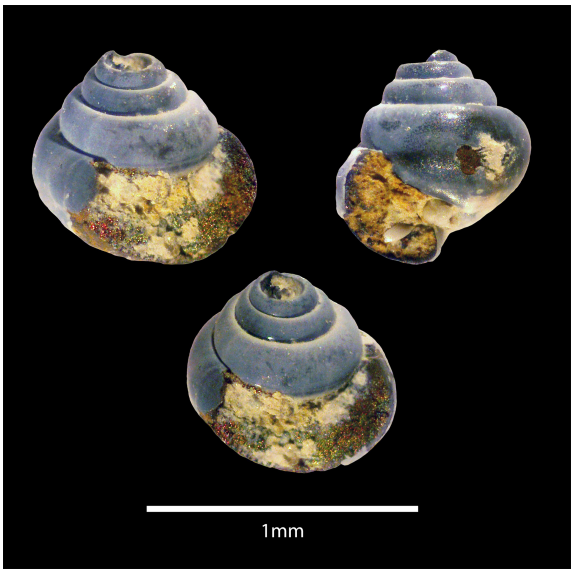

Figure 4. *Limacina retroversa* specimen found in sample B6H4 130–132 (identification: Jeanne Rampal, personal communication, 2023). Photo: Dael Sassoon.

4.2 Pollen-inferred climate reconstructions

Results show significant temperatures and precipitation variations in connection with the glacial/interglacial cyclicity and shorter-term variability (Fig. 5, Table 2). The most reliable methods according to the two R^2 and RMSE indicators are MAT and BRT, and the most accurately reconstructed parameters are MAAT and MTCO (Table 3). The four methods are in agreement for the general trends, although MAT shows the widest amplitude of variations, and RF has the smoothest curve.

Temperatures are lower than the present during the complete MIS 6 interval, except at the onset of MIS 5. A cooling trend is reconstructed during the final stage of MIS 7 (pollen zone 1, MIS 6e and 6d), while MTCO and the seasonal temperature contrast (TCON) are stable. The methods do not agree on the precipitation patterns during this phase, with MAT showing a trend toward aridity, decreasing WINTERPR and seasonal precipitation contrast (PCON), while the three other methods display a slight precipitation increase and stable PCON. From 166 ka BP onward (pollen zone 2, MIS 6c and 6b), both temperatures and precipitation decrease, and the seasonal contrast between winter and summer climate conditions reduced progressively. The MIS 6 minimum temperatures and precipitation are reconstructed in pollen zone 2 between around 150 and 160 ka BP, corresponding to the transition between MIS 6c and 6b. Subsequently, both temperatures and precipitation increase progressively in the late pollen zone 2 and early pollen zone 3 (MIS 6b to 6a). Between 140–135 ka BP (early MIS 6a), the four methods reconstruct temperatures similar to late MIS 7, a seasonal contrast close to the present, and precipitation higher than the present (except for BRT). This climate optimum is abruptly interrupted by the HS11 extreme arid event between ∼ 134 and ∼ 129 ka BP (pollen zone 4, late MIS 6a), during which temperatures, precipitation and seasonal contrasts are significantly reduced, reaching climate conditions similar to the MIS 6 glacial maxima ∼ 155 ka BP. A short climate amelioration is evidenced at ∼ 132 ka BP (pollen zone 4b), where precipitation and seasonal contrasts increase abruptly. Finally, after 130 ka BP the climate amelioration toward the MIS 5 interglacial conditions happens very fast (pollen zone 5).

5 Discussion

5.1 Paleoenvironment of MIS 6 and Termination II in the western Mediterranean

Important changes are recorded during MIS 6, that are consistent with orbital-scale variability during the different glacial substages.

Three phases can be discerned. The early phase (pollen zone 1) spans late MIS 7, MIS 6e and 6d (∼ 196–166 ka) and is characterized by high percentages of deciduous *Quercus*, *Cedrus* and Cichorioideae, with marked variability and several abrupt semi-desert and steppe increases under cool and humid climate conditions, with seasonal contrast similar to present-day. The middle phase (pollen zone 2) extends from MIS 6c to late 6b (∼ 165–143 ka), and displays the maximum expansion of steppe and semi-desert taxa together with very low temperatures and precipitation between ∼ 160 and ∼ 150 ka, a chronology compatible with the maximum Drenthe ice advance (Ehlers et al., 2011). Finally, the late phase (pollen zone 3), spanning late MIS 6b and 6a (∼ 143–133 ka), is marked by a major expansion of Ericaceae vegetation associated with higher reconstructed precipitation and winter temperatures, as well as enhanced seasonal contrast during this phase.

Previous studies are consistent with a subdivision of MIS 6 into three phases characterized by different general trends and amplitude of millennial-scale oscillations (Margari et al., 2014; Nehme et al., 2020). Margari et al. (2014) described an early phase between 185 and 160 ka BP, with warmer and wetter conditions and important rapid climate variability, a middle transitional phase between 160 and 150 ka BP, and a late phase with stable glacial conditions between 150 and 135 ka BP. This three-phasing for MIS 6 glaciation matches our interpretation of ODP 976 pollen zones 1, 2 and 3.

The final phase of MIS 6 is characterized by important changes in vegetation and climate, indicating a rapid modification of vegetation communities and atmospheric configuration at the transition between MIS 6 and MIS 5. Termination II (TII), defined as the period of fast reorganization of the climate system from full glacial (MIS 6) to full interglacial (MIS 5) conditions, is indeed characterized by extreme and fast internal dynamics including a major Heinrich

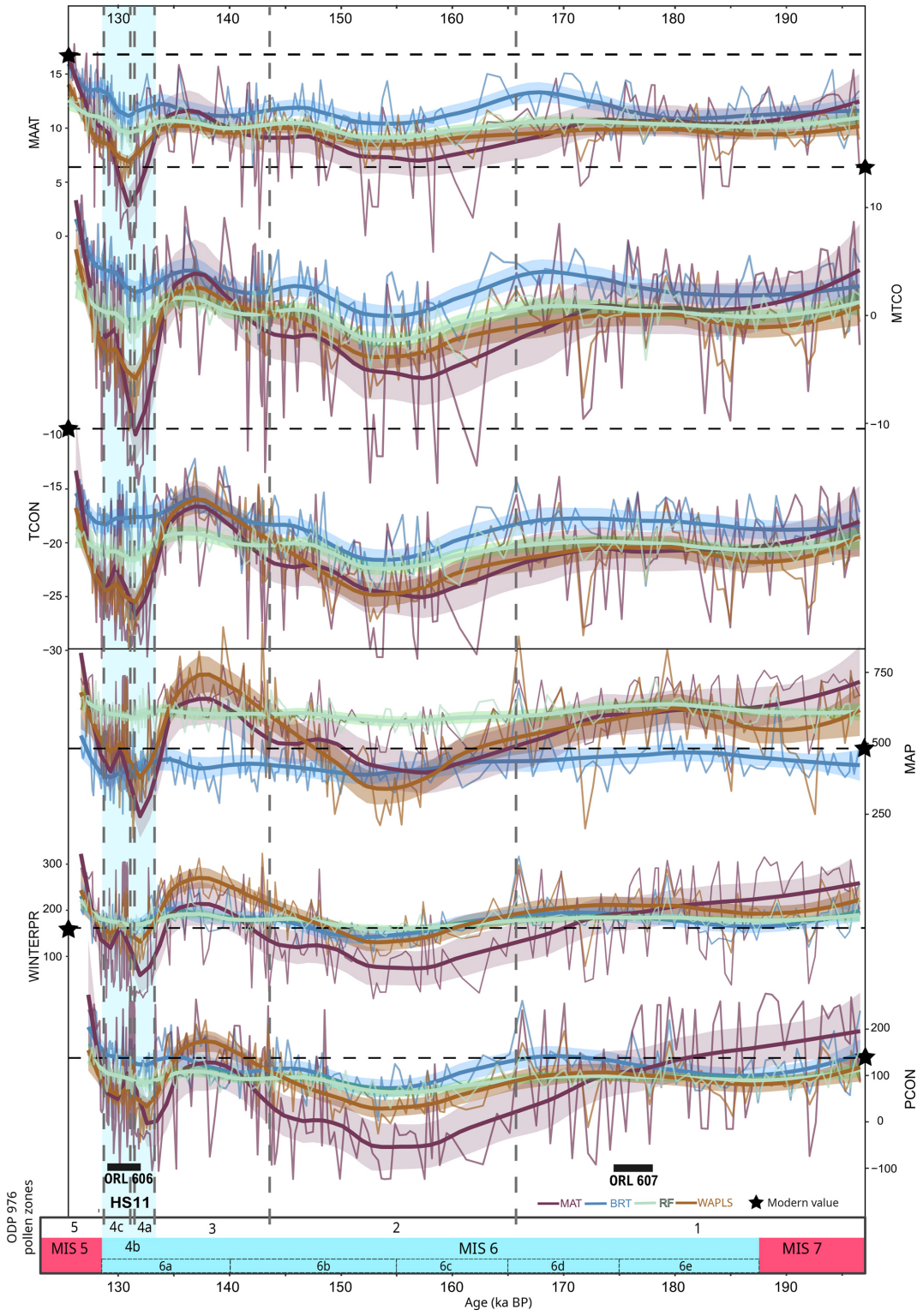

Figure 5. Pollen-based climate reconstructions for MIS 6 interval from the ODP 976 record. MAAT (Mean Annual Temperature), MTCO (Mean Temperature of the Coldest Month), TCON (Temperature Contrast, see methods), MAP (Mean Annual Precipitation), WINTERPR (Winter Precipitation) and PCON (Precipitation contrast, see methods) for the four different methods applied: MAT (Modern Analogue Technique), WA-PLS (Weighted Averaging Partial Least Square), BRT (Boosted Regression Trees) and RF (Random Forest). The light-coloured interval represents the 95 % confidence window, and the bold curves the loess smoothed values (alpha = 0.25). Modern values (see methods) are indicated by the horizontal dashed line and the black star. Grey vertical dashed lines separate the pollen zones defined by CONISS cluster analysis.

Table 3. R^2 (coefficient of determination) and RMSE (Root Mean Square Error) values for the different climate parameters reconstructed with the four methods applied. The lower the RMSE and the higher the R^2 (in bold), the more reliable the reconstruction.

	BRT		MAT		WA-PLS		RF	
	R^2	RMSE	R^2	RMSE	R^2	RMSE	R^2	RMSE
MTCO	**0.87**	2.96	**0.88**	3.19	**0.71**	4.44	**0.77**	3.88
MAAT	0.83	2.31	0.83	2.48	0.66	3.22	0.69	3.00
SUMMERPR	0.77	44.86	0.82	46.61	0.52	66.87	0.65	56.48
MAP	0.77	148.52	0.79	163.70	0.50	225.68	0.66	182.32
MTWA	0.76	2.25	0.79	2.33	0.53	3.16	0.61	2.81
WINTERPR	0.69	60.69	0.72	65.81	0.43	82.58	0.59	69.34

Stadial, HS11 (Broecker and Henderson, 1998; Gouzy et al., 2004; Martrat et al., 2014; Moseley et al., 2015; Ovsepyan and Murdmaa, 2017). The timing for TII has been estimated based on the initialisation and termination of Weak Asian Monsoon evidenced in the Dongge cave speleothems, lasting from ∼ 136 to 129 ka BP (Bajo et al., 2020; Kelly et al., 2006; Menviel et al., 2019). These boundaries for TII give a total duration of about 7 ka. The timing of TII in the ODP 976 marine record is directly dependent on the Dongge Cave chronology (see methods, Sect. 3.1). Approximately the same duration is observed in the vegetation response to TII, but with ∼ 1 ka delay: the imprint of HS11 on the vegetation in the Western Mediterranean region is indeed recorded here between 133.3–128.8 ka BP (pollen zone 4). This delay in marine and terrestrial proxies may reflect the vegetation response to the first cold pulse of HS11. ODP 976 provides for the first time a very detailed record of vegetation successions during this arid event (pollen zones 4a, 4b and 4c), in agreement with other SSTs and speleothem records that depict a three-phases or "W" pattern for the event (see Sect. 5.4). After the first rapid increase of steppe and semi-desert taxa (pollen zone 4a), the middle phase shows an abrupt decrease of steppe and semi-desert vegetation, and a fast increase of montane trees (mainly *Cedrus*) percentages (pollen zone 4b). Climate reconstructions reflect this event through a fast increase of both precipitation and temperatures. This pattern is fully compatible with the ODP 976 SSTs trend (Jiménez-Amat and Zahn, 2015; Martrat et al., 2014), although a delay of about 1 kyr is observed between the abrupt drop in alkenone-based SSTs at the onset of HS11 and the expansion of steppe and semi-desert vegetation. In the same way, the abrupt sea surface warming in the middle of HS11 (∼ 133 ka BP) is shifted in the pollen record, to around 131.5 ka BP (pollen zone 4b).

5.2 Hydroclimate connection with ORLs deposition during MIS 6

Pollen analyses help us to characterize the processes behind Organic Rich Layers (ORLs) deposition in this western Mediterranean region. Like sapropels, ORLs reveal important changes in the water stratification and circulation, with reduced bottom water ventilation and enhanced organic productivity in direct connection with (i) increase in the freshwaters Atlantic inflow at times of deglaciation and (ii) enhanced rivers runoff regionally linked with increased precipitation (Murat, 1999; Pérez-Asensio et al., 2020; Rogerson et al., 2008). Although they are often considered as "ghost sapropels", their timing and the mechanism behind them may differ from those of Eastern Mediterranean sapropels (Rogerson et al., 2008).

ORL bed 607 coincides with a period of enhanced precipitation around 176 ka reconstructed through our pollen-based approach (Fig. 7). Its basis appears almost synchronous with the onset of Sapropel S6 layer deposition in the Eastern Mediterranean (Emeis et al., 2003; Rohling et al., 2015; Savannah et al., 2024). Its duration also appears shorter than Sapropel S6, possibly indicating an interruption of favourable climate conditions in the Western Mediterranean region by a stadial event occurring around 172 ka BP and marked by an abrupt decrease in precipitation (Fig. 7).

ORL bed 606 was deposited during the second half of Termination II, at a time of deglaciation and directly following the first aridity pulse of HS11. Pollen-based reconstructions show enhanced precipitation and seasonal contrast during this time, suggesting intense precipitation together with deglacial freshwater input as combined causes for ORL deposition in the Western Mediterranean, which finds no counterpart in the Eastern Mediterranean. The implications of such organic layer deposition occurring at times of enhanced precipitation or deglaciation will be further discussed in Sect. 5.4.

5.3 Mediterranean vegetation changes during the penultimate glaciation: a synthesis

The ODP 976 pollen record documents MIS 6 vegetation changes in the Western Mediterranean with a temporal resolution comparable to the most detailed terrestrial palynological sequences from the Eastern Mediterranean (Tenaghi Philippon and Ioannina). A W-E transect of Mediterranean palynological records offers valuable insights on the spatial

pattern of vegetation changes during the penultimate glaciation (Fig. 6).

At the MIS 7–6 transition, no abrupt decline of temperate forest is recorded in the ODP 976 and Padul records, in contrast with central and Eastern pollen records such as Tenaghi Philippon, Ioannina, Ohrid and Castiglione where the transition is very abrupt (Follieri et al., 1988; Koutsodendris et al., 2023; Roucoux et al., 2011; Sadori et al., 2016). At these sites, a higher contrast has been described between interglacial periods with very high percentages of temperate deciduous forest taxa and glacial periods with very reduced tree cover (Tzedakis, 1993; Tzedakis et al., 2006). The western Mediterranean region, at the contrary, was generally characterized by a high proportion of herbaceous taxa, even during interglacial periods, attenuating the vegetation contrasts during transitions to glacial periods.

The first half of MIS 6 ($\sim$ 185–165 ka BP) is marked by relatively high percentages of arboreal pollen across all records, especially deciduous forest (Roucoux et al., 2011; Margari et al., 2010, 2014). The abundance of montane taxa (mainly *Cedrus*) is characteristic of ODP 976 record, and reflects the development of altitudinal trees on the Moroccan mountains. Montane elements also increase during early MIS 6 at Valle di Castiglione, mainly represented by *Fagus* and *Abies* (Follieri et al., 1988), and at Ioannina, mainly represented by *Pinus* (Roucoux et al., 2011). No equivalent pattern is recorded in Padul where herbaceous vegetation is largely dominant. The scarcity of palynological data from the western Mediterranean, especially from North Africa, limits our understanding of the spatio-temporal significance of *Cedrus* expansions during MIS 6, and past glaciations in general.

The main phase of steppe and semi-arid vegetation is recorded between $\sim$ 165–145 ka BP in the Alboran Sea record, consistent with Ohrid and Ioannina pollen sequences (Fig. 6). In Padul, however, the maximum expansion of steppe and semi-desert taxa occurs later, between $\sim$ 155 and $\sim$ 137 ka BP. This time window corresponds to the glacial maximum recorded at Azzano X (northern Italy) between 148 and 135 ka BP (Pini et al., 2009), and to a period of low pollen concentration at Valle di Castiglione, likely reflecting full glacial conditions. The $\sim$ 10 ka lag in the vegetation glacial maxima between ODP 976 and Padul is probably the result of the low temporal resolution of the latter, in addition to differences in the age models used. However, the presence of pioneer vegetation and to a lesser extent of montane elements in Padul during the maximum glacial phase matches the ODP 976 pattern in pollen zone 2, where Cupressoideae and *Cedrus* display high abundance.

A distinctive feature of the Western Mediterranean vegetation recorded during the final stage of MIS 6 (pollen zone 3) is the marked increase in Ericaceae observed in the ODP 976 record, whereas Ericaceae are almost absent in the rest of the Mediterranean region. A similar expansion is observed in the Atlantic margin, where core MD01-2444 recorded patterns of Ericaceae expansion matching the three insolation minima during MIS 6 (Margari et al., 2014). Ericaceae development during minimal summer insolation is particularly favoured by reduced summer evaporation at times of low seasonal contrast in precipitation, as already noted in the Alboran Sea during the last glacial (Fletcher and Sánchez Goñi, 2008). Following the same interpretation, the expansion of heathland vegetation in the Iberian Peninsula as recorded in ODP 976 during the final stage of MIS 6 may therefore mark the renewed influence of westerlies and Atlantic moisture preceding the onset of the transition to MIS 5 interglacial (Margari et al., 2014). Supporting this state, an increase in temperate deciduous forest at the end of MIS 6 is also seen in Padul, Ohrid and Ioannina records before the transition to MIS 5.

Despite some discrepancies due to the differences in age models and temporal resolutions, all records display comparable variations in temperate pollen percentages during the penultimate glacial. These variations support the persistent sensitivity of Mediterranean plant ecosystems to global-scale millennial climate variability during the penultimate glaciation, with modulation of the vegetation response depending on the local geography. Strong similarities can be observed between ODP 976 and Padul, despite the lower temporal resolution of Padul record. In both sequences, temperate pollen percentages reached $\sim$ 30 % of total pollen as a maximum during the rapid forest expansions events in the first half of MIS 6. This similarity supports the validity of the ODP 976 marine record to reconstruct the SW Iberian Peninsula temperate forest history. However, ODP 976 sequence provides a more regional image of the vegetation, including higher percentages of Ericaceae pollen coming from the Atlantic coast, and *Cedrus* pollen from the Moroccan mountains (Jiménez-Moreno et al., 2020), compared to Padul where percentages of Mediterranean taxa and hygrophyte herbaceous are higher due to the local nature of the signal (Camuera et al., 2019). Looking further east, Valle di Castiglione recorded various temperate trees expansions and contractions during the lower MIS 6, before the full glacial conditions. In the Italian Peninsula, various interstadials have also been identified further north at Azzano X (Pini et al., 2009). In the Balkans, Tenaghi Philippon shows the highest percentages of semi-desert and herbaceous vegetation throughout MIS 6, with more abrupt changes than all the other Mediterranean records, and more amplitude of the trees' contractions. This pattern was already described during the last climatic cycle and reflects the exacerbated vegetation dynamics locally, with episodes of rapid and enhanced colonization by tree vegetation (Koutsodendris et al., 2023; Tzedakis, 2005; Tzedakis et al., 2004). This has been mainly explained by the location of the site in a low altitudinal plain characterized by a more continental climate with lower winter precipitation: tree populations at lower altitudinal location are closer to their ecological threshold in term of precipitation, and are likely to be very affected even by minimal changes in the amount of rainfall. On the contrary, the Ioannina record shows the highest deciduous forest

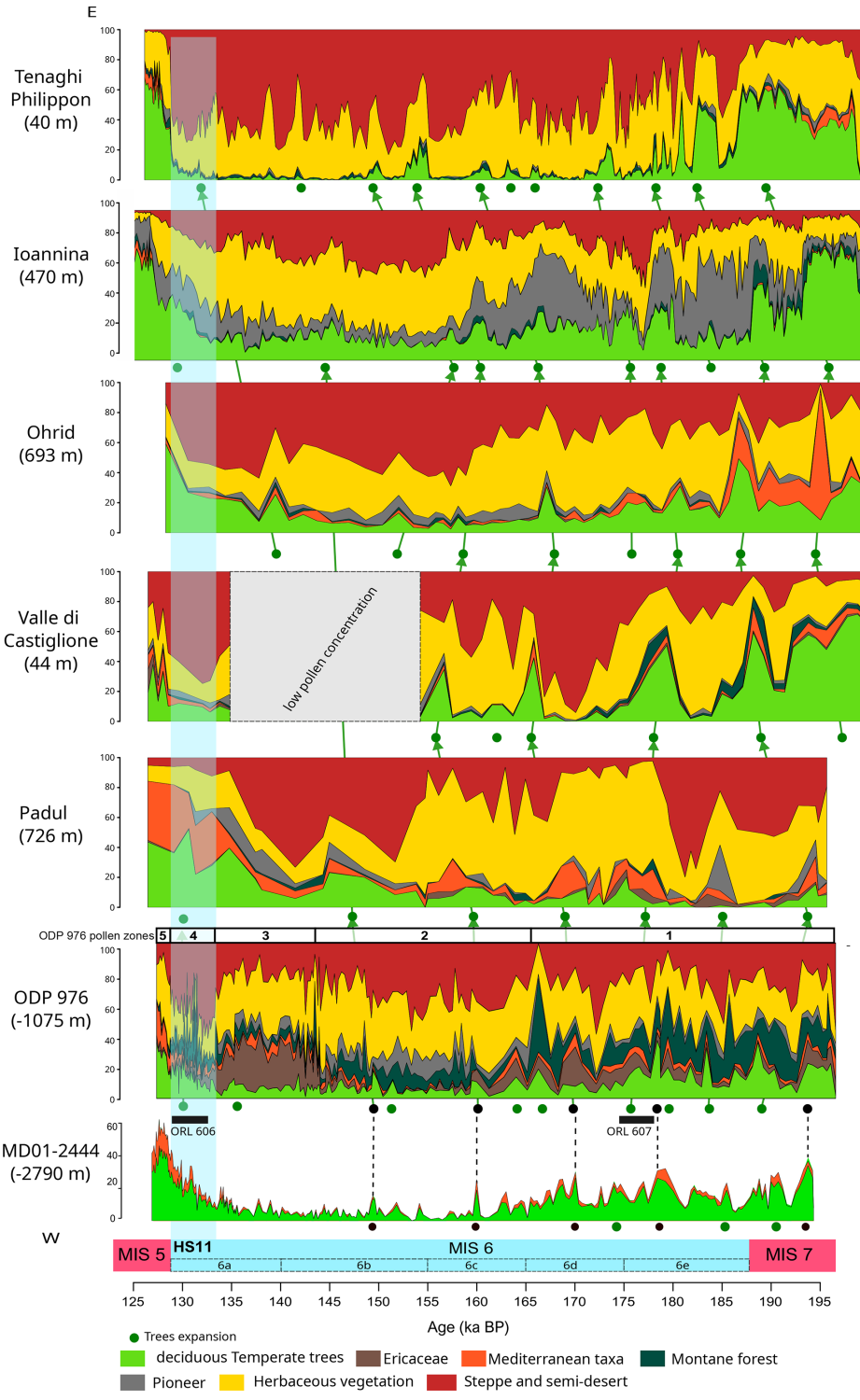

Figure 6. Synthesis of vegetation changes in the Mediterranean during MIS 6 based on available palynological sequences, from west (bottom) to east (top): MD01-2444 (Margari et al., 2010; Tzedakis et al., 2018), ODP 976 (this study), Padul (Camuera et al., 2019), Valle di Castiglione (Follieri et al., 1988), Ohrid (Sadori et al., 2016), Ioannina (Roucoux et al., 2011), Tenaghi Philippon (Koutsodendris et al., 2023). Each synthetic pollen diagram is plotted according to its own age model. ODP 976 and Ioannina's chronologies are based on alignment with MD01-2444 temperate pollen curve on AICC2012 timescale. The ecological groups are the same as for ODP 976, except *Pinus* was included in pioneer vegetation at Ioannina, as it is the only record where *Pinus* is not over-represented. Green dots indicate temperate vegetation increases, with tentative correlations between records. The two Organic Rich Layers (ORLs) identified in the ODP 976 core (Murat, 1999), were placed at the bottom.

percentages of all the records presented here, supporting its character as a local trees refugium (Roucoux et al., 2011).

Termination II displays a particular pattern in vegetation records from the Mediterranean region: while the expansion of trees and temperate vegetation is fast and continuous, HS11 represents at the same time a remarkable episode of abrupt steppe and semi-desert expansion. Although this event is visible in almost all the records, it is particularly prominent in the ODP 976 record (pollen zone 4), and appears less pronounced in the eastern Mediterranean sequences. This observation is compatible with previous observations that Heinrich stadials during the last glacial had a minor impact on the eastern Mediterranean vegetation compared to the western Mediterranean, likely due to the already limited presence of tree vegetation in the eastern records during glacials (Tzedakis, 2005). A similar interpretation can be proposed for the differential response of eastern and western Mediterranean vegetation to HS11, supporting the major sensitivity of the southwestern Mediterranean vegetation to North Atlantic cold events. In Padul, no major expansion of xerophyte vegetation is detected, but a small decrease of temperate deciduous taxa was interpreted as the HS11 imprint (Camuera et al., 2019), and the signal might be hindered by the low resolution of the record. A pattern of fast arid vegetation increase contemporaneous to the temperate forest expansion is also found in central Italy at Lago Grande di Monticchio, which was not presented in Fig. 6 as its record does not extend beyond 132 ka BP (Allen and Huntley, 2009; Brauer et al., 2007).

Finally, all palynological sequences reveal high-frequency oscillations of temperate and semi-desert pollen, compatible at first look with DO-like variability based on their duration and intensity. They represent a particularly distinctive feature of the lower part of MIS 6.

5.4 Rapid climate variability during MIS 6: a regional multiproxy comparison

In order to investigate the character of rapid climate variability during MIS 6, a comparison with regional and global climatic archives is essential. The events of arboreal pollen increase observed in the ODP 976 record show percentages and timing comparable to those from the Portuguese margin core MD01-2444 (Margari et al., 2010, 2014; Tzedakis et al., 2018) (Fig. 7m). However, the ODP 976 record generally presents lower values of temperate deciduous pollen percentages compared to the Atlantic record, due to its more semiarid Mediterranean influence as previously evidenced for the last glacial period (Charton et al., 2025; Fletcher et al., 2010). To better capture temperate vegetation dynamics, we added Ericaceae, a clear marker of Atlantic influence in the ODP 976 record, to the deciduous temperate forest, to obtain a "total temperate pollen sum" which enhances the main warming peaks and strengthens the correlation between the two marine cores on both sides of Gibraltar Strait (Fig. 7m and l). The ODP 976 pollen-inferred climate reconstructions show generally consistent patterns with the SSTs trends based on alkenones (Martrat et al., 2004, 2007), and the southern Iberian humidity recorded in the speleothem from Cueva Gitana (Hodge et al., 2008) (Fig. 7e and g). The ODP 976 pollen and climate record therefore appears to reflect well regional variations in both temperature and humidity across MIS 6.

Warm events in the northern hemisphere are generally well-correlated to peaks in the ODP 976 temperate pollen curve (Fig. 7c and l). An active bipolar seesaw dynamics was described during the penultimate glacial (Davtian and Bard, 2023; EPICA Community Members, 2006; Stocker, 1998), and the Antarctic record was used to elaborate the Greenland GL_T-syn (Greenland temperature synthetic) curve showing predicted $\delta^{18}O$ millennial-scale events for the past glacial eight climatic cycles, which are not directly recorded in Greenland ice (Barker et al., 2011; Bazin et al., 2013; Jouzel et al., 2007). Six Antarctic Isotopic maxima (AIM) events were recognized on the Deuterium curve during MIS 6 (6i to 6vi), correlated with increases in CO_2 concentrations and benthic isotope minima in the North Atlantic (Barker et al., 2011; Hodell et al., 2023; Margari et al., 2010, 2014; Shin et al., 2020) (Fig. 7a–c). These AIM and benthic minima in the Atlantic are not easily correlated with steppe expansions in the ODP 976 record, indicating a limited response of vegetation in the Western Mediterranean to the Antarctic warm events.

Barker et al. (2011) predicted the occurrence of eleven millennial-scale warming events during MIS 6 (Fig. 7c), while nine interstadials were recognized in the Alboran Sea from the alkenone record (Fig. 7e), (Martrat et al., 2004, 2007). In the loess record of Harletz in central Europe, ten interstadials were described (Rousseau et al., 2020), strongly matching the Chinese speleothems records of stadial and interstadial events related to the Asian Monsoon dynamics (Cheng et al., 2006; Li et al., 2014; Wang et al., 2018, 2001; Xue et al., 2019). The global nature of fast climate oscillations in the northern hemisphere thus appears controlled by the coupled influence of Atlantic cold events, and tropical monsoon variations as evidenced by the eastern Mediterranean speleothems records from Sofular, Soreq and Kanaan caves (Ayalon et al., 2002; Held et al., 2024; Matthews et al., 2021; Nehme et al., 2018).

The three phases identified during MIS 6 based on the ODP 976 vegetation and climate record can be compared with regional and global records to be interpreted in a broader context, based on general climatic trends and the expression of climatic instability.

5.4.1 Early MIS 6 (187–166 ka BP): warm/wet conditions and instability

The first phase encompasses the two substages MIS 6e and 6d, and is characterized by humid and rather warm climate

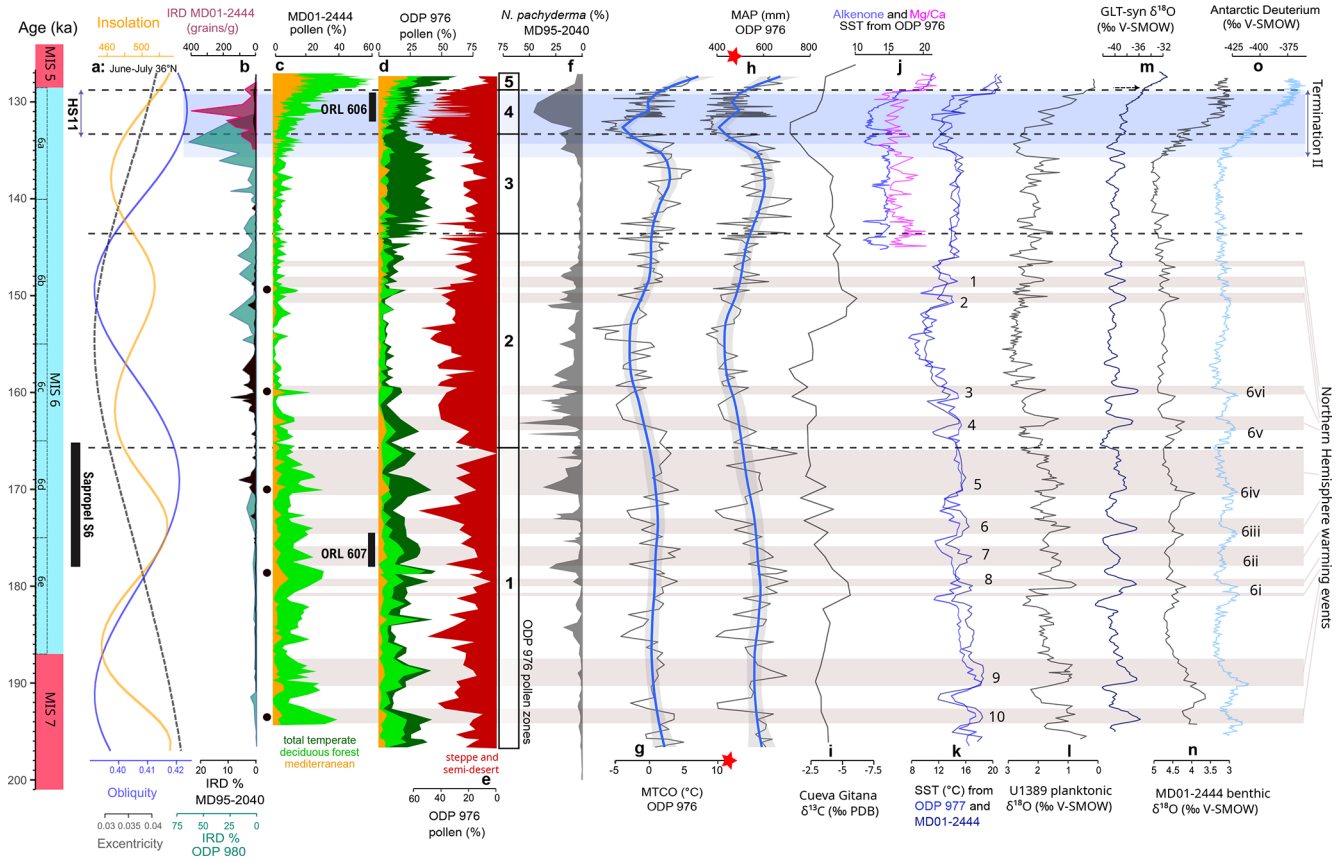

Figure 7. Millennial-scale climate changes during MIS 6. **(a)** Orbital parameters (Laskar et al., 2004) calculated for June–July at 36° N: Eccentricity (black), Obliquity (blue) and Insolation (yellow); **(b)** Ice-Rafted Debris (IRD) percentages from MD01-2444, 37° N (pink) (Skinner and Shackleton, 2006) redrawn from Tzedakis et al. (2018), MD95-2040 (black), 40° N (de Abreu et al., 2003) and ODP 980 (blue), 55° N (McManus et al., 1999; Oppo et al., 2001, 2006); **(c)** MD01-2444 pollen percentages of temperate tree (light green) and Mediterranean (orange) taxa (Margari et al., 2010; Tzedakis et al., 2018); **(d)** ODP 976 pollen percentages of total temperate taxa including temperate deciduous forest + Ericaceae + Mediterranean (dark green), deciduous forest (light green), Mediterranean (orange) (this study); **(e)** ODP 976 pollen percentages of semi-desert and steppe taxa, with ODP 976 pollen zones (this study); **(f)** *N. pachyderma* percentages from MD95-2040 (de Abreu et al., 2003; Voelker and de Abreu, 2011); **(g)** Mean Temperature of the Coldest Month (MTCO) reconstructed from ODP 976 pollen assemblage, mean of the four methods used in this study (MAT, WA-PLS, RF, BRT), with the red star showing the modern value; **(h)** Mean Annual Precipitation (MAP) reconstructed from ODP 976 pollen assemblage, mean of the four methods used in this study (MAT, WA-PLS, RF, BRT), with the red star showing the modern value; **(i)** δ^{18}C from Cueva Gitana (Hodge et al., 2008); **(j)** Alkenone-based SST (Martrat et al., 2014) and Mg / Ca-based SST (Jiménez-Amat and Zahn, 2015) from ODP 976; **(k)** Alkenone-based SST from ODP 977 (darker blue) and MD01-2444 (lighter blue) (Martrat et al., 2004, 2007); **(l)** Planktonic δ^{18}O from U1389 (Sierro and Andersen, 2022); **(m)** Greenland synthetic δ^{18}O (Barker et al., 2011); **(n)** Benthic δ^{18}O from MD01-2444 (Margari et al., 2010); **(o)** Antarctic Dome C δD (Bazin et al., 2013; Jouzel et al., 2007). The black rectangle indicates the interval of deposition of Sapropel layer S6 in the eastern Mediterranean (Ziegler et al., 2010). The marine substages MIS 6a–e follow (Railsback et al., 2015). All data are plotted on AICC2012 chronology (Bazin et al., 2013) following Sierro et al. (2020) and Sierro and Andersen (2022), except for the IRD records and Gitana Cave which is plotted on its own age model based on U-series absolute dating. The horizontal grey bars indicate the Northern Atlantic interstadial events based on the planktonic isotope record and the predicted millennial-scale warming events from Greenland synthetic record, with the numbers of the Alboran interstadials (AI-1 to AI-10) from Martrat et al. (2004, 2007). Numbers 6i–6vi correspond to the Antarctic Isotope Maxima (AIM) from Margari et al. (2010). The horizontal blue bar represents Heinrich Stadial 11 (HS11). Black dots show the five temperate pollen peaks in MD01-2444 used as control points for ODP 976 chronology.

conditions in the Mediterranean at the transition from MIS 7 to MIS 6. This phase aligns well with the deposition of ORL bed 607 in the Alboran Sea, and the sapropel layer S6 in the Eastern Mediterranean, associated with the maximum summer insolation and increased intensification of the summer monsoonal system in the eastern Mediterranean between 178.5 to 165.5 ka (Emeis et al., 2003; Rohling et al., 2015; Ziegler et al., 2010). At the same time of S6 deposition, Cheddadi and Rossignol-Strick (1995) described an increase in temperate pollen in the Nile region, and Soreq

cave speleothem records climatic conditions typical of an interglacial (Ayalon et al., 2002). Sapropel depositions usually occur during interglacial periods as MIS 1 (Holocene), which makes sapropel S6 an exceptional feature of early MIS 6. It reflects particularly warm and humid conditions, and intense freshwater input in the Mediterranean which can result from various sources, including increased rainfall and monsoon activity, Atlantic freshwater entrance, and enhanced river discharges (Sierro and Andersen, 2022). The long speleothem records in China report a period of northern shift of the Intertropical Convergence Zone associated with enhanced Asian Monsoon activity during this phase (Wang et al., 2018). Higher pluviometry is also supported by foraminifera isotopic and SSTs signal throughout the Mediterranean Sea, which were used to reconstruct past salinity and freshwater budget regionally (Kallel et al., 2000). Enhanced rainfall in the Balkans is evidenced by the Ioannina lake deepening (Wilson et al., 2021), and a more humid period is documented in speleothem records from Argentarola cave in Italy (Bard et al., 2002a) and Gitana cave in southern Spain (Hodge et al., 2008) (Fig. 7g). Therefore, humid conditions during this phase were not restricted to the eastern Mediterranean where the sapropel deposition occurred. ODP 976 organic layer 607 together with the pollen-based climate reconstructions support this view, with enhanced seasonal precipitation contrast during this interval driven by enhanced winter precipitation (Fig. 5). Comparison with Padul pollen-based hydroclimate reconstructions (Camuera et al., 2022) further strengthens this scenario: despite the chronological delay between the two sequences, this early MIS 6 humid phase and ORL deposition likely matches the Western Mediterranean Humid Period (WMHP 6) dated between 180–155 ka BP (Fig. 8). The same study made the case for a co-occurrence of humid periods in the Western Mediterranean and in West Africa (African Humid Periods) during periods of high precipitation seasonality and enhanced West African Monsoon. Pollen-inferred climate reconstructions from lake Ohrid have also shown the phase relationship between African Monsoons and periods of high winter precipitation in the Mediterranean region (Wagner et al., 2019; Sinopoli et al., 2019).

Another characteristic of this early MIS 6 phase is the strong variations in pollen and isotopic curves in the Atlantic and Western Mediterranean (Fig. 7a–d and l–m). Variations in temperate deciduous and Ericaceae percentages are observed in the ODP 976 record, in close correspondence with the Atlantic record from MD01-2444. The largest interstadial peak in ODP 976 around 179 ka BP is also identified in all the different records and marked by warmer conditions in the sea, and more effective precipitation in SE Iberia (Hodge et al., 2008). It is well correlated with the stadial following Antarctic event 6i (Margari et al., 2010), the associated predicted millennial-scale warming event in Greenland synthetic curve, and the Alboran Sea SST interstadial event 8 (Martrat et al., 2004). In Padul record, the temperate deciduous, Mediterranean and *Abies* percentages increase correlates well with this event (Camuera et al., 2019). It could also match the WMHP 6.1 interstadial (Camuera et al., 2022) (Fig. 8). This large interstadial was suggested to be at the origin of the initialisation of the sapropel S6 deposition (Sierro and Andersen, 2022), and could also have participated in the initialization of ORL 607 deposition in the Alboran Sea (Murat, 1999). On the other hand, the most important tree population decline and semi-desert expansion in ODP 976 is recorded at ∼ 172 ka BP, which could match Antarctic event 6iv, and is associated to a moderate increase of IRD deposition at the latitude of ODP 980 (Fig. 7n). A similar stadial can be observed in the Ioannina and Tenaghi Philippon records with a close chronology (Roucoux et al., 2011) (Fig. 6). Dry conditions at this time are also recorded in the eastern Mediterranean as shown in the Pentadactylos and Soreq speleothems (Ayalon et al., 2002; Nehme et al., 2018).

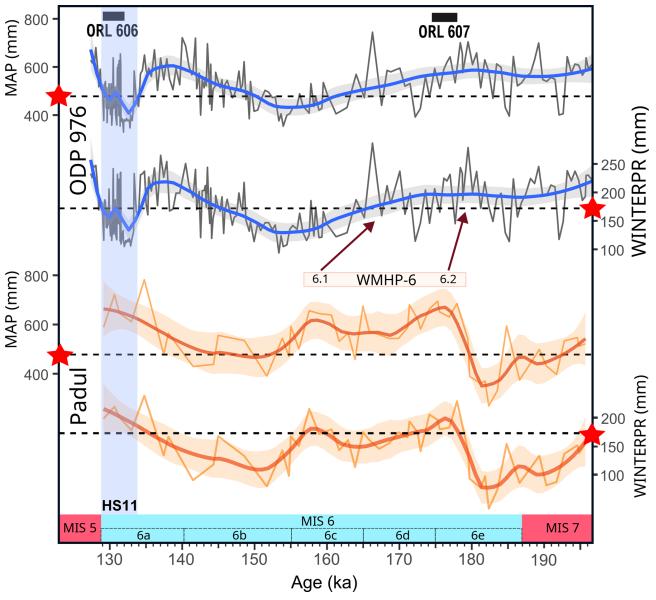

Figure 8. Comparison between the precipitation pattern reconstructed from ODP 976 with our multi-method approach (mean) (this study) and from Padul with only the WA-PLS method (Camuera et al., 2022). Mean Annual Precipitation (MAP) and Winter Precipitation (WINTERPR) are represented, together with the two Organic Rich Layers (ORLs) identified in ODP 976 (Murat, 1999) and the Western Mediterranean Humid Period (WMHP) 6 defined by Camuera et al. (2022). Red arrows indicate tentative correlation between the two phases of WMHP 6, and the precipitation reconstructions from ODP 976. Red stars and dashed lines indicate the modern climate value (see methods).

5.4.2 Middle MIS 6 (165–144 ka BP): maximum glacial conditions and stability

This phase is marked by the maximum expansion of semi-desert vegetation and the almost complete collapse of forest vegetation between ∼ 163 and 150 ka BP, according to the ODP 976 pollen and MD01-2444 records, synchronous with the minimum in orbital eccentricity. This is in agreement with the lowest SSTs values reconstructed in the Alboran Sea from the alkenone record occurring around 155 ka BP, and low SSTs in the Gulf of Lions too (Cortina et al., 2015). At the same time, high percentages of the cold species *N. pachyderma*, together with important ice-detritus pulses, are recorded on the Portuguese margin (de Abreu et al., 2003; Voelker and de Abreu, 2011) (Fig. 7j and n). The occurrence of the cold Atlantic species *Limacina retroversa* shells in the ODP 976 sediments at ∼ 155 ka BP is consistent with the enhanced entrance of cold subpolar water masses in the Alboran sea at the time of full glacial conditions. In parallel, there is an intensification of "Fleuve Manche" paleo river discharges evidenced in various sedimentary cores from the Bay of Biscay (Boswell et al., 2019; Eynaud et al., 2007; Penaud et al., 2009, 2016; Toucanne et al., 2009), and a fluvial aggradation linked with reduced vegetation cover in Spanish river basins (Macklin et al., 2002). A long-term aridification is recorded in SE Spain in Gitana cave close to the ODP 976 location (Hodge et al., 2008). The glacial maximum in Soreq cave speleothem is also recorded around 154 ka BP (Ayalon et al., 2002), and might be responsible for the hiatus in the Pentadactylos speleothem in Cyprus (Nehme et al., 2020). In Italy, the Tana che Urla cave also recorded cooling and aridification between 159–132 ka BP, indicated by both the carbon and oxygen isotopic ratio (Regattieri et al., 2014). The coolest phase in Abaliget Cave speleothem in central Europe is also recorded at that time (Koltai et al., 2017). Climate conditions reconstructed at ODP 976 site during this phase show the maximum aridity and cold temperatures, which are consistent and fall within the range of reconstructed temperatures and precipitation at the same time at Ohrid (Sinopoli et al., 2019). This main phase of glaciation in Europe took place after 163 ka BP, corresponding to the Drenthe glacial advance (Ehlers et al., 2018; Margari et al., 2014). The maximum ice expansion probably led to the almost complete collapse of temperate vegetation across the Mediterranean region, except in specific climate refugia like Ioannina or Padul (Fig. 6). The Mediterranean vegetation taxa were particularly affected and almost disappeared at this time in the ODP 976 record.

Few interstadial events are observed during this cold and dry phase, probably due to the extended ice volume reaching a critical threshold (McManus et al., 1999) and leading to higher climate stability at time of glacial maximum expansion (Sierro and Andersen, 2022). One moderate interstadial event around 150 ka BP is expressed in the ODP 976 and MD01-2444 records through an increase in temperate deciduous tree taxa (Fig. 7l and m). It may correspond to the interstadial recognized in Gitana Cave speleothem approximately at the same time, and is compatible with the Alboran Interstadial events 1 or 2 (Martrat et al., 2004), while a larger trees increase in Padul record is also observed (Camuera et al., 2019) (Fig. 6). It is also compatible with interstadials recognized in other speleothem records in eastern and central Mediterranean (Ayalon et al., 2002; Bard et al., 2002a; Regattieri et al., 2014). Sierro and Andersen (2002) described a major event of low Mediterranean overturning and high freshwater entrance through the Gibraltar Strait at that time and contemporaneous to the insolation maximum (Fig. 7o). This configuration was similar to the one contemporaneous to sapropel S6 and ORL 607 deposition during early MIS 6, but did not lead to any new sapropel deposition at 150 ka BP, probably because the climate conditions were more favourable but not enough for a sapropel deposition.

5.4.3 Late MIS 6 (144–129 ka BP): increased precipitation during the last glacial, and arid conditions during HS11

Between 150 and 140 ka BP, warmer and wetter conditions are indicated by ODP 976 pollen percentages of Ericaceae (pollen zone 3). Ericaceae expansions in the Iberian margin sediments were found to be associated to insolation minima in core MD01-2444 (Margari et al., 2014). This pattern is consistent with the ODP 976 Ericaceae curve (Fig. 7l). The climate reconstructions evidenced high precipitation and especially high WINTERPR values. These higher humidity and temperature values are supported by the carbon isotope record from Gitana Cave (Hodge et al., 2008) and the Alboran Sea SSTs (Martrat et al., 2007) (Fig. 7e–g). In central Europe, Abaliget Cave speleothem also shows more favourable climate conditions during this phase (Koltai et al., 2017). Climatic oscillations appear subdued in the Western Mediterranean pollen records during this last phase. The high resolution ODP 976 record shows some SST variations (Jiménez-Amat and Zahn, 2015; Martrat et al., 2014) : Ericaceae pollen contractions and semi-desert elements expansions could be correlated to three abrupt drops in alkenone-based SSTs at 144, 142, and 139 ka BP (Fig. 7f, k and l). Fifteen Chinese Interstadials (CIS) were identified at Hulu Cave during late MIS 6, linked with Asian Monsoon dynamics (Wang et al., 2018), and the ultra-high-resolution record of planktonic isotope ratio at U1389 by Sierro and Andersen (2022) also expresses some variability. However, the vegetation response in the SW Mediterranean was apparently limited.

Following the Ericaceae expansion, the most prominent feature of the late MIS 6 phase is the large and fast expansion of steppe and semi-desert vegetation during HS11, between 133 and 129 ka BP (pollen zone 4). It is characterized by a first large IRD peak at high latitude (ODP 980) around 134 ka BP, and later at the MD01-2444 latitude, around 131 ka BP (Skinner and Shackleton, 2006; Tzedakis et al., 2018). This event also corresponds to an increase in

the oxygen isotopic ratio at the Portuguese margin (especially planktonic, starting around 136 ka BP), also broadly synchronous to an important decrease in SSTs of the Atlantic and the Mediterranean Sea (Jiménez-Amat and Zahn, 2015; Martrat et al., 2004, 2007, 2014). A pronounced increase in *N. pachyderma* (sinistral) abundance is also recorded on the Portuguese margin (Voelker and de Abreu, 2011). Climate reconstructions show particularly harsh conditions in the Western Mediterranean region during this event, compatible with the reconstructions from Lake Ohrid (Sinopoli et al., 2019) and from three French sites (Les Echets, la Grande Pile and Le Bouchet) for the latest phase of MIS 6 (Guiot et al., 1989, 1993). An arid phase is also evidenced at Gitana Cave (Hodge et al., 2008), which closely matches the trend of the ODP 976 precipitation curve (Fig. 8). Aridity is evidenced in other speleothem records in Europe like Villars (Wainer et al., 2011), Sieben in the Alps (Moseley et al., 2015), and Abaliget cave in central Europe (Koltai et al., 2017). Dryness over western Europe is also supported by an episode of intense loess deposition in Rodderberg crater in northern Germany between 136–129 ka BP (Zhang et al., 2024). If HS11 is also recorded in China speleothems (Wang et al., 2018), it appears subdued in the eastern palynological Mediterranean records (Fig. 6), indicating that the Western Mediterranean region was more severely impacted by the dry and cold pulse of HS11. The "W" shape of HS11 described in Sect. 5.1 for the ODP 976 record matches well the Hulu cave record, where the particular event in the middle of HS11 was linked with a strong Asian Monsoon episode that could represent an analogue to the Bølling-Allerød during Termination I (Wang et al., 2018). The fast and multiphase vegetation and climate dynamics evidenced in the ODP 976 record is in agreement with the description of a "HS11 complex" with multiple phases (Tzedakis et al., 2018), and will require more focused attention in the future.

HS11 has been described as a "pause" in the glacial termination II (Gouzy et al., 2004; Hodge et al., 2008). However, in the ODP 976 and MD01-2444 records, temperate vegetation keeps increasing all along the event, despite the supposed cessation of the warming and moistening trend for almost 2000 years. Therefore, the trend toward increased temperate vegetation during Termination II did not seem to be strongly affected by the abrupt arid event, following the continuous climate amelioration described in various speleothem records from Italy covering Termination II, at Corchia cave, Tana che Urla and Argentarola (Bard et al., 2002b; Drysdale et al., 2005; Regattieri et al., 2014). On the contrary, the Gitana Cave speleothem records a strong moisture deficit (Fig. 7g), supporting a stronger impact of HS11 in the SW Mediterranean compared to the Italian Peninsula.

Finally, it is to be pointed out that HS12, occurring around 140 ka BP (Lisiecki and Stern, 2016), apparently did not have any imprint on the vegetation record of ODP 976, implying a subdued impact of this event on Mediterranean vegetation compared to HS11.

5.5 Comparison of MIS 6 with the last glacial period (MIS 4–2)

Various studies have pointed out strong similarities between the millennial-scale oscillations of the last glacial period and the penultimate glacial period, with the division between MIS 3 and MIS 2 being analogous to the early and mid-late phase of MIS 6 respectively (Held et al., 2024; Margari et al., 2010, 2014; Roucoux et al., 2011; Rousseau et al., 2020; Shin et al., 2020; Sierro et al., 2020). The same studies argued in favour of pervasive impact of stadial events on the continental climate and vegetation in the Mediterranean region, even in absence of typical Heinrich layers (Roucoux et al., 2011). The ODP 976 record shows a cooling and aridification trend during the first half of MIS 6 (Fig. 9), with decreasing intensity of interstadials events, that recalls the pattern of MIS 3 D–O cycles (Bond et al., 1993).

However, the absence of clear successions of stadial events and especially Heinrich stadials, together with the more subdued expression of interstadials in the vegetation record, limits the resemblance between the two glacial periods. The pacing of interstadial peaks also seems to be reduced compared to the last glacial period high-frequency oscillations, as previously highlighted from the high-resolution speleothem record from Sofular cave in Turkey (Held et al., 2024).

A comparison of millennial-scale changes during the past two glacial periods based on the ODP 976 and MD95-2040 records, on either side of the Gibraltar Strait, supports our view (Fig. 9). The last glacial period (encompassing MIS 4 to MIS 2) was characterized in the Alboran Sea by high-intensity oscillations in both temperate and semi-desert vegetation correlated with D–O cycles and intense ice-rafting events HE1 to HE7 in MD95-2040. During interstadial events, temperate and Mediterranean vegetation (deciduous forest + Mediterranean + Ericaceae) could reach values above 60 % of total pollen; during stadial events, the semi-desert pollen values reached values as high as 70 % of total pollen (during HS3, HS4 and HS5). In comparison, the penultimate glacial (MIS 6) displays much lower intensity events, with interstadials characterized by 45 % as a maximum value for temperate vegetation, and stadials with 65 % for the steppe and semi-desert vegetation (during HS11). High-intensity cold episodes during MIS 6 are limited to the HS11, and the ∼ 172 ka BP event. This is consistent with the multiproxy record of core MD95-2040 on the Portuguese margin, which evidenced reduced variability in the *N. pachyderma* abundance and IRD deposition during the penultimate glacial compared to the last glacial (de Abreu et al., 2003; Voelker and de Abreu, 2011). The ice rafting episodes appear to be of different nature during MIS 6 (Hodell et al., 2008; Liu et al., 2018; McCarron et al., 2021), with the main iceberg discharges originating from the European ice sheet, contrary to the typical Hudson Strait origin of the last glacial Heinrich layers. SST reconstructions in the western Mediterranean also show less intense cooling during MIS 6 than dur-

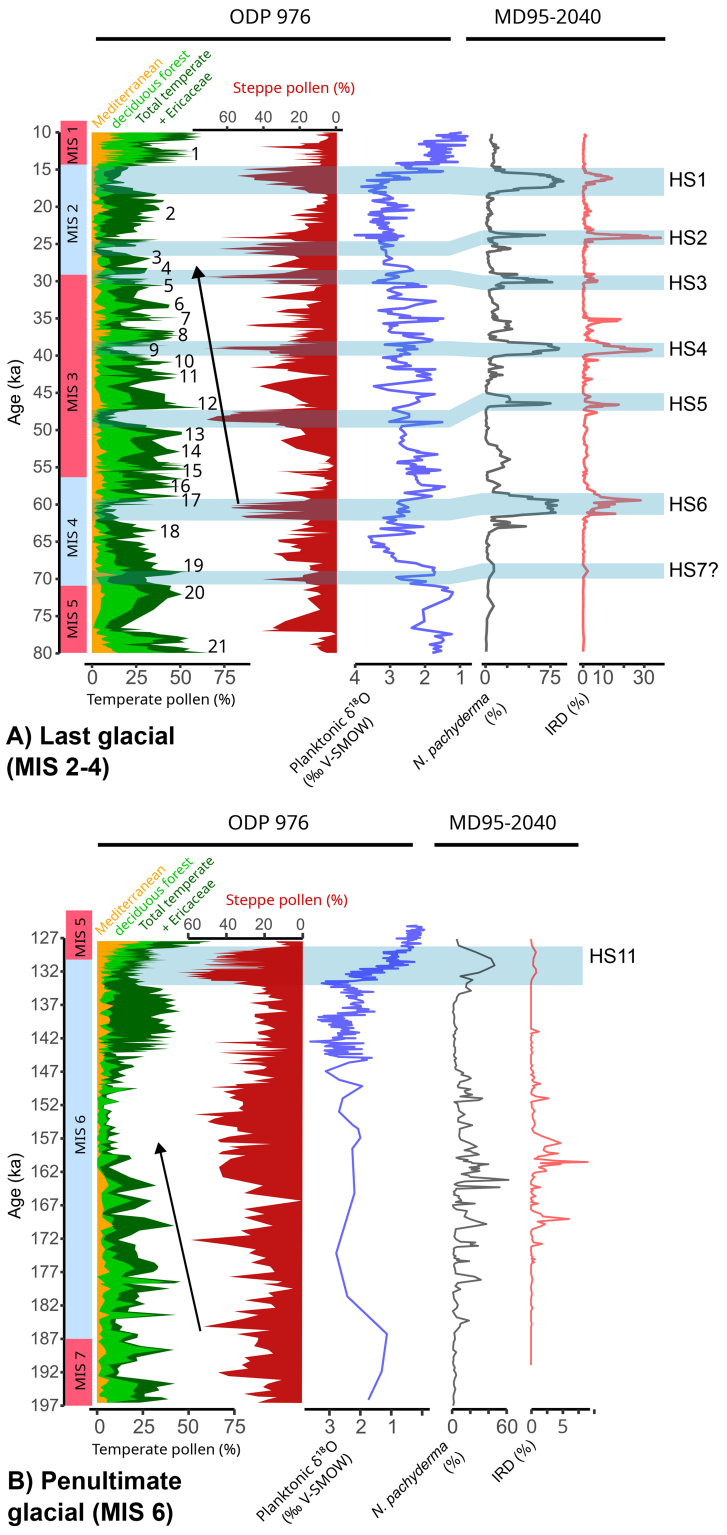

Figure 9. Comparison of millennial-scale changes during **(A)** the last glacial (MIS 2–4) and **(B)** the penultimate glacial (MIS 6), including the main pollen data from ODP 976 (Charton et al., 2025; Combourieu-Nebout et al., 2002, 2009, and unpublished data for the last climatic cycle, and this study for MIS 6), the ODP 976 planktonic isotopic ratio from *G. bulloides* (Combourieu-Nebout et al., 2002; Jiménez-Amat and Zahn, 2015; von Grafenstein et al., 1999, and unpublished data), and the *N. pachyderma* and IRD record from core MD95-2040 (de Abreu et al., 2003; Voelker and de Abreu, 2011). Marine Isotope Stages follow the boundaries from Lisiecki and Raymo (2005). Numbers on the Last Glacial correspond to the Greenland D-O events chronology (Fletcher et al., 2010; Rasmussen et al., 2014). Black arrows mark the aridification trend and decreasing interstadials intensity during MIS 3 and early MIS 6.

ing MIS 3 (Martrat et al., 2004, 2007), supporting limited incursions of polar waters in the Mediterranean during MIS 6 compared to MIS 3 coldest stadials, and especially Heinrich stadials (Cacho et al., 1999).

Like ODP 976, Ioannina records lower intensity arboreal pollen oscillations during early MIS 6 compared to the last glacial (Roucoux et al., 2011). In comparison, the Atlantic pollen record from MD01-2444 core displays similar amplitude of tree percentages during the last and the penultimate glacial (Margari et al., 2010). This difference can be explained by the different climate conditions, and the higher sensitivity to cold and aridity of sclerophyllous and deciduous forest vegetation on the Mediterranean side, as recorded in the ODP 976 and Ioannina palynological sequence. It appears that temperate vegetation in SW Mediterranean responded to millennial-scale climatic oscillations with higher intensity during the last glacial compared to the penultimate, probably because the climate in Europe was colder during MIS 6 compared to MIS 2. This is supported by larger European ice-sheet extension during the penultimate glacial (Ehlers et al., 2011; Ehlers and Gibbard, 2007; Shackleton, 1987), favouring the long-term establishment of open landscapes mainly composed by steppe and semi-desert plants. The differences in humidity might not be as easily interpretable, with an early MIS 6 more humid, and a MIS 6 glacial maximum more arid, compared to MIS 3 and MIS 2 as also suggested by the Ioannina record (Roucoux et al., 2011). Future climate reconstructions applied to the complete last glacial cycle in ODP 976 and other Mediterranean long pollen sequences will help understanding the different climate configurations between the last two glacial periods.

5.6 Human occupation during MIS 6 in SW Europe

Only a limited number of sites in South-Western Europe has yielded archaeological layers attributed to MIS 6, and even fewer of them have been radiometrically dated allowing for a robust comparison with the environmental changes (Fig. 10 and Table S2). The environmental proxies available in the archaeological layers (pollen, charcoal, macro and microfauna) can help the chronological attribution, but are often insufficient to establish a precise correlation with the high-resolution chrono-environmental framework of marine and glacial archives. Even when absolute dates are available, their large uncertainty range and the poor resolution of the archaeological record represent a major limitation and make it difficult to correlate the human occupation phases with a specific substage of MIS 6.

It is generally accepted that the northern part of Europe was almost completely depopulated during MIS 6, with very few sites identified compared to the southern European fringes, indicating discontinuous occupation during more favourable climatic episodes (Hérisson et al., 2016) or total abandonment like in the British lands (Scott, 2011; Shaw et al., 2016; White and Pettitt, 2011). Southern France, Italy and the Iberian Peninsula could have represented climate refugia during the most extreme ice-cap advances (Bicho and Carvalho, 2022). Notably, Italy is particularly deprived of sites well-dated to MIS 6 (Fig. 10) including the isolated Neanderthal of Altamura, the short episode of elephant scavenging at Poggetti Vecchi, and the long sequence of San Bernardino cave which chronological range extends up to $\sim$ 154 ka BP, a period marked by the most extensive glacial conditions of MIS 6. Some other few archaeological layers have been attributed to MIS 6, but they lack a robust chronological attribution (Aureli and Ronchitelli, 2018; Fontana et al., 2010; Fig. 10). One can hypothesise that regional climate conditions in the peninsula were particularly harsh after 150 ka, and that potential refugia sites remain to be identified in Italy. Palaeoecological reconstructions at the Poggetti Vecchi site indicated cold and dry open environment (Aranguren et al., 2019; Benvenuti et al., 2017). Interestingly, the chronological range for the site could coincide with a major stadial event at 171 ka BP identified in the ODP 976 core, and particularly well expressed in the Valle di Castiglione record (Fig. 6).

In Southern France and the Iberian Peninsula, according to available radiometric dates, human occupation appears to have been continuous across MIS 6, even during the glacial maximum, with both cave and open-air sites. France provides a comparable number of cave and open-air sites mainly concentrated in the southwestern region. The Portuguese record is mainly constituted by open-air sites in fluvial terrace systems of the lower Tagus, offering important insights into short-term occupations during the full-glacial stage, but with complex chronological attribution (Cunha et al., 2012, 2017; Pereira et al., 2019). The Spanish record includes various open-air settlements in the upper Tagus valley (Panera et al., 2011, 2014; Yravedra et al., 2019), as well as the Duero (Diez-Martín, 2010) and the Guadalquivir (Caro Gómez et al., 2011) valleys. Cave sites are fewer and are mainly located closer to the coast (Cueva del Bolomor, Cueva del Angel, Lezetxiki, Arlanpe, Ventalaperra), with the two exceptions of Cueva de Maltravieso and Villacastín. Key sites like Lazaret Cave (Late Acheulean, France) and Cueva del Bolomor (Middle Palaeolithic, Spain) evidence the persistence of human groups in possible climate refugia (Ochando et al., 2019; Valensi et al., 2005).

MIS 6 in Europe saw the final stage of the cultural transition from the Lower to the Middle Palaeolithic industries (MIS 8–5), mainly characterized by the emergence of more complex core technologies such as Levallois debitage and changes in subsistence strategies. No rupture is observed between the technocomplexes, as cultural diversity and the permanence of Acheulean bifacial tools associated to technological innovation mark these Early Middle Palaeolithic industries in Southern Europe (Santonja et al., 2016; Terradillos-Bernal et al., 2023). The distribution of archaeological sites and timing of human occupation in South-Western Mediterranean at that time reflect this pattern (Fig. 10). A mosaic of traditional and innovative behavioural traits can be observed,

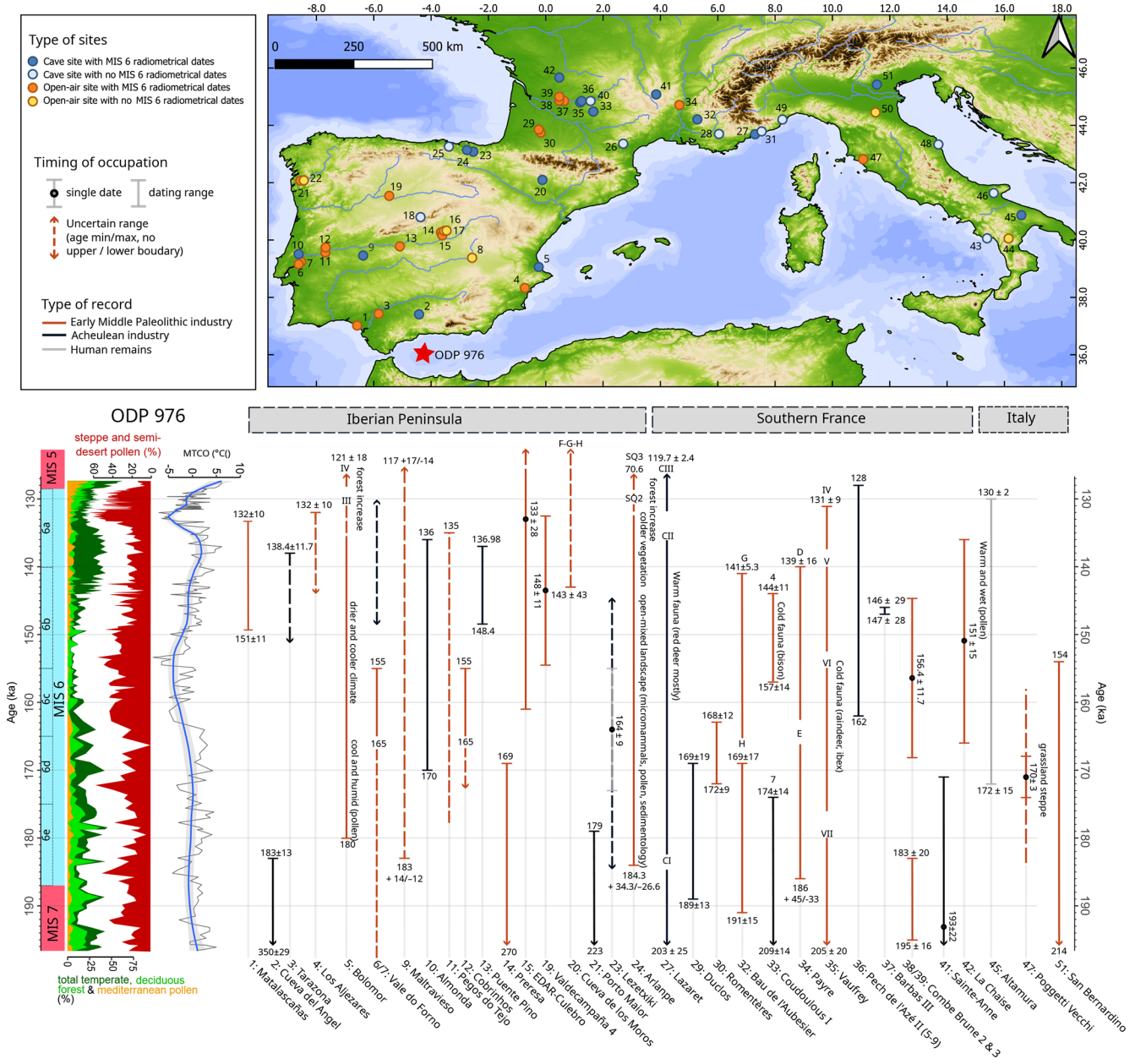

Figure 10. Distribution of archaeological sites and radiometrically dated human occupation in western Mediterranean attributed to MIS 6, with some relevant palaeoecological information when available. The dates used and references can be found in Table S2. Sites on the map are numbered from south to north in each country: 1: Matalascañas; 2: Cueva del Angel; 3: Tarazona; 4: Los Aljezares; 5: Cueva del Bolomor; 6: Vale do Forno; 7: VF3 (Milharos); 8: El Provencio; 9: Cueva de Maltravieso; 10: Almonda; 11: Pegos do Tejo; 12: Cobrinhos; 13: Puente Pino; 14: Preresa; 15: EDAR-Culebro 2; 16: Arriaga II/III; 17: Arganda II (Valdocarros); 18: Villacastin; 19: Valdecampana; 20: Cueva de los Moros de Gabasa; 21: Porto Maior; 22: Arbo; 23: Lezetxiki ; 24: Arlanpe ; 25: Ventalaperra; 26: Aldènes; 27: Grotte du Lazaret; 28 : Baume Bonne; 29: Duclos; 30: Romenteres; 31: Grotte du Prince; 32: Bau de l'Aubesier; 33: Coudoulous I; 34: Payre; 35: Grotte Vaufrey; 36: Pech de l'Aze II; 37: Barbas III; 38: Combe Brune 3; 39: Combe Brune 2; 40: Grotte Sirogne; 41: Sainte -Anne; 42: La Chaise; 43: Riparo del Poggio; 44: Rosaneto; 45: Altamura; 46: Riparo Paglicci; 47: Poggetti Vecchi; 48: Monte Conero; 49: Grotta del Colombo; 50: Due Pozzi/Scornetta; 51: Grotta di San Bernardino.

with late Acheulean and Early Middle Palaeolithic coexisting continuously (Cueto et al., 2016; de Lumley, 2018; Mathias et al., 2020; Moncel et al., 2025; Santonja et al., 2022; Torres et al., 2024; Valensi et al., 2013). Acheulean technocomplexes are progressively abandoned during MIS 6 in Europe (Álvarez-Alonso, 2014; Key et al., 2021), with the latest chronologies found possibly in the Manzanares basin in central Iberia at Arriaga sites (Panera et al., 2014; Rubio-Jara et al., 2016; Rubio-Jara and Panera, 2019; Silva et al., 2013), or at Lazaret cave (Michel et al., 2022), and dated to the beginning of MIS 5. No clear explanation is accepted for the emergence and generalization of the Levallois debitage, and while cognition might not be the only factor, some authors suggested that MIS 6 glaciation could have played a role in the final abandonment of Acheulean industries (Moncel et al., 2020; Valensi et al., 2005). It is hard to claim that specific environmental pressures favoured Levallois technology over bifacial production, as these lithic technologies seem to have co-existed in Western Europe since MIS 12–11 over several glacial/interglacial cycles (Baena et al., 2017; Moncel et al., 2020), including extremely cold stages (like MIS 12 and 10). This "mosaic" pattern for the Lower to Middle Palaeolithic transition, although at least partly imputable to the large dating uncertainties, points toward more complex processes leading to the generalization of Middle Palaeolithic industries from MIS 5. Interestingly, the end of the Lower to Middle Palaeolithic transition is also associated with a shift in the morphology of human remains, from "Early Neanderthals" (MIS 7–5) to "Classical Neanderthals" (MIS 5–3) (Di Vincenzo and Manzi, 2023). Sites like La Chaise (Abri Suard), Lazaret and Altamura provide fossil evidence for these "Early Neanderthals" which share characteristics with earlier Middle Pleistocene populations, and with later Neanderthals (Buzi et al., 2025; Couture-Veschambre et al., 2021; de Lumley, 2018). Genetic data also support an important population shift in western Europe sometimes around the transition from MIS 6 to MIS 5 (Peyrégne et al., 2019). Therefore, an important population reorganization seems to have occurred at the time of the final Acheulean industries, leading to the onset of the so-called "Classical neanderthal world" in western Eurasia, with generalized Middle Palaeolithic industries and established Neanderthal morphological features. The role of environmental changes occurring during MIS 6 in this population reorganization remains poorly understood.

Changes in land use and mobility pattern have been evidenced in north-central Iberia, and can be viewed as adaptations to the severe climatic conditions of MIS 6 evidenced in the ODP 976 sequence during pollen zone/phase 2: increasing mobility, more short-term occupations and reliance on more local resources for subsistence strategies (Diez-Martín, 2010; Diez-Martín et al., 2008; Rios-Garaizar, 2016; Sánchez-Yustos, 2009). However, identifying cultural phases in the archaeological sequences linked with specific climatic episodes is generally hindered by the poor resolution of the archaeological record and chronological data. Among the sites identified in this synthesis, Lazaret and Bolomor caves probably present the most informative and well-dated sequences with several archaeological layers dated to MIS 6.

Cueva del Bolomor stands out in the Iberian Peninsula record as it provided an exceptionally long and continuous record of human presence, and the oldest evidence of fire use in Spain during the Middle Palaeolithic (Vidal-Matutano et al., 2019). Climate changes during MIS 6 documented in Bolomor's sediments through multiple proxies are consistent with the different phases identified in the ODP 976 record, with a more humid and cool phase at the beginning of MIS 6, and the most arid phase taking place at the middle of Phase III (layers X–VIII) (Arsuaga et al., 2012; Fernández Peris et al., 2008). The site is described as a climatic refugium where Mediterranean vegetation persisted during the colder phase of MIS 6 thanks to the coastal reservoir character of the site (Ochando et al., 2019). No clear change in lithic production has been identified in the MIS 6 layers of Bolomor: according to Fernández Peris et al. (2008), archaeological layers XII to VII (Phase III, MIS 6) are all dominated by limestone flakes with few retouches, few recycling, and the presence non-Acheulean macro-lithic elements. These layers are characterized by expeditive flaking (including Levallois *débitage*) relying on local raw-material, pointing toward a high degree of mobility and search for immediate effectiveness. It is thus hard to distinguish different techno-cultural tendencies during this phase. The most visible change in the archaeological sequence occurs in layer VI (MIS 5) which shows an intensification of lithic production dominated by flint, the production of more specialized tools including microlithic elements and associated to more intense and stable occupation in the cave (Fernández Peris et al., 2008). Therefore, a clear behavioural change in the technological and economical exploitation of raw materials is identified at the beginning of MIS 5. Faunal remains show a large and constant diversity, including abundant micro supporting both short-term and long-term not-specialized occupation, with no clear change in the site's function across the sequence (Blasco et al., 2013).

Lazaret Cave, in south-eastern France, shows a very distinct scheme: the Lower to Middle Palaeolithic transition is well documented in the archaeological sequence (Unit CII and CIII), with the progressive replacement of large bifacial tools production by more standardized and smaller flakes (Cauche, 2012). Levallois *débitage* is already present and well-mastered in the lower MIS 6 levels, although rare, and becomes dominant in the upper levels (early MIS 5). Therefore, a subdivision of unit CII can be made with a lower interval rich in handaxes, and an upper layer characterized as "final Acheulean" with rare handaxes and more abundant flakes. Faunal assemblages are very constant throughout MIS 6, with the large dominance of red deers and rare presence of cold species (*Rangifer tarandus*, *Coelodonta antiquitatis*). Thus, the climatic oscillations of MIS 6 do not seem to have

influenced different hunting strategies or prey selection by human populations at Lazaret Cave, as large game hunting of red deer prevailed (Valensi et al., 2013).

Therefore, Lazaret and Bolomor caves are examples of different strategies of site exploitation and technological evolution during MIS 6: Lazaret Cave represents a specialized red-deer hunting camp evidencing a progressive change from Lower to Middle Palaeolithic tools, while Cueva del Bolomor can be characterized as a short-term camp with more generalized hunting and stable expeditive Middle Palaeolithic industry. Despite these differences both sites provide evidence for a change in lithic assemblages occurring at the end of MIS 6/beginning of MIS 5: the disappearance of handaxes and generalization of Levallois flakes in Lazaret, and the intensification and standardization of flint flakes in Bolomor.

The fast climate dynamics during Termination II as evidenced in the ODP 976 paleoenvironmental record could have represented a critical period for human population. At the end of MIS 6, more sites have been identified in the Iberian Peninsula than Southern France, showing the latter could have represented a climate refugium at the time of maximum glacial expansion, with more intense human occupation regionally. Many of these late MIS 6 sites present a chronological boundary at the top of the sequence compatible with the onset of Termination II around 136 ka BP, and with HS11, within the dating uncertainty: Matalascañas, Tarrazona, Los Aljezares, Bolomor Unit III, Almonda, Pegos do Tejo, Puente Pino, Arlanpe Unit SQ2, Lazaret Unit CII, Payre layer D, Vauffrey unit IV, and Pech de l'Azé II layer 5. The extreme character of this event in the South-Western Mediterranean as expressed in the ODP 976 sequence could have put further environmental pressure on hominin groups already diminished. A niche modelling approach based on 41 sites of Western Eurasia since 145 ka BP has shown that the projected potential niche space for Neanderthals at the end of MIS 6 ($\sim$ 145 ka BP) was very reduced and concentrated in Western Europe (Yaworsky et al., 2024). This coincides with the end of pollen zone/phase 2 in the ODP 976 record, the most cold and arid phase of the penultimate Glacial before HS11. Then, the authors reconstruct a progressive expansion of Neanderthal potential niche space between 145 and 130 ka, compatible with the climatic warming and moistening during pollen zone/phase 3 in the ODP 976 record (Yaworsky et al., 2024). The temporal resolution of the model (1000 years) does not allow to detect the impact of HS11 on the niche projection, and only a small slowdown and decline of the projected niche is visible at $\sim$ 130 ka BP, before the MIS 5e optimum (Yaworsky et al., 2024; Fig. 5). A regional study focused on North-Western Spain argued in favour of a demographic vacuum at the end of MIS 6, compatible with HS11 and leading to a population reorganization implying contraction or micro-extinction, before the generalization of Middle Palaeolithic industries during MIS 5 (Sánchez-Yustos and Diez-Martín, 2015). According to the same authors, following this crisis, Neanderthal population entered a "reorganisation phase" leading to demographical stability and more technological standardization, visible in the explosion of the number of sites in Europe in general, especially after the MIS 5e climatic optimum (Bringmans, 2007; Lewis et al., 2011; Wenzel, 2007). This statement is supported by niche modelling which shows a peak in projected potential niche space of Neanderthal during MIS 5e (Yaworsky et al., 2024), and by recent genetic data which provided evidence for at least two radiation events linked with the environmental conditions of the last interglacial (Vernot et al., 2021), and Neanderthal population continuity since $\sim$ 120 ka BP (Peyrégne et al., 2019). Thus, HS11 did not lead to complete extinction of hominin groups but might have induced deep demographical and technological reorganization, representing the first and one of the most intense abrupt changes that Neanderthal population had to face in South-Western Europe before the Last Glacial largest oscillations (HS6–4). According to this view, the emergence of the "classical Neanderthal" world in Europe after the MIS 6/5 transition corresponds to the initialization of dynamics of repeated population contraction and expansion in response to the Upper Pleistocene instability, especially during MIS 4–2 (Sánchez-Yustos, 2009). This view is increasingly supported by genetic data (Fotiadou et al., 2026). In that sense, the subdued environmental instability during MIS 6 evidenced in the ODP site 976 record compared to the last glacial period (Sect. 5.5 and Fig. 9) could also have implications for human populations, with less fragmented (although harsh) habitats and more stable (although reduced) population during MIS 6. This hypothesis remains however hard to test based on the very different nature and quality of preservation of the archaeological record during MIS 6 compared to MIS 4–2 (e.g. Charton et al., 2025).

6 Conclusion

The ODP site 976 record sheds light on the environmental and climate changes during MIS 6 in the SW Mediterranean. The sequence is characterized by the high representation of *Cedrus* and Ericaceae pollen, resulting from the combined influence of African and Atlantic input respectively. ODP 976 position, at the confluence of Mediterranean versus Atlantic, and Eurasian versus African climatic areas, is ideal to decipher the processes behind orbital and sub-orbital climate dynamics during past glaciations. Three main phases have been distinguished during MIS 6 with different trends in vegetation and climate changes. Millennial-scale oscillations are recorded especially during the early part of MIS 6 ($\sim$ 187–166 ka BP) through the rapid increases of temperate and Mediterranean pollen, some of which are similar to millennial-scale warming events identified in the ice-core and marine temperature records, as well as other palynological sequences in the Mediterranean region. This Early MIS 6 phase is characterized by overall warmer and wetter climate conditions, in agreement with other paleoclimate archives in

the Mediterranean showing enhanced moisture availability at the beginning of MIS 6. This phase of enhanced moisture availability was likely connected with enhanced Asian and African monsoon activity and was probably at the origin of the deposition of the Organic Rich Layer 607 in the Alboran Sea and sapropel S6 in the eastern Mediterranean. The second phase (165–144 ka BP) shows the establishment of full glacial conditions in the Mediterranean, with the maximum spread of steppe and semi-desert vegetation associated to cold and arid climate conditions and limited rapid oscillations. Finally, the final stages of MIS 6 are marked by increased humidity and the development of Ericaceae, with moderate millennial-scale oscillations seen in the vegetation record. Termination II is very particular in the ODP 976 record, with the continuous increase of temperate and Mediterranean vegetation being contemporaneous to a major episode of steppe expansion and aridity increase identified as HS11. This event shows a particular three phases or "W" shape, in agreement with other records, and had a major impact on the SW Mediterranean environments. A comparison with the changes occurring during the last glacial period (MIS 4–2) inferred from the same core highlighted the limited duration, frequency and intensity of MIS 6 millennial-scale climatic events compared to the last Glacial D-O cycles and Heinrich Stadials (MIS 4–2). These results support a subdued impact of the millennial-scale climatic oscillations on the continental vegetation in the Mediterranean region during the Penultimate glaciation compared to the Last Glacial. The only exception is HS11, which stands out by its notable intensity and duration and is of particular interest to understand the mechanisms behind Termination II.

Human populations continuously inhabited the SW Mediterranean territory during MIS 6. While few sites are available and robustly dated to MIS 6 in Italy, Southern France and the Iberian Peninsula appear to have been intensely populated, supporting their nature of Pleistocene Climate refugia. More ecological data from well-dated archaeological sites during MIS 6 would be needed to increase the quality of human-environmental dynamics comparison. However, the synthesis drawn in the present study highlights the extreme nature of events characterizing Termination II, and particularly HS11, which could have represented an important environmental crisis for human population at that time, catalysing the end of the Lower to Middle Palaeolithic Transition and the onset of the "classical" Neanderthal world through a drastic population bottleneck.

Data availability. Pollen counts and climate reconstruction results from ODP 976 have been submitted to PANGAEA data repository and will be available in the next months (https://www.pangaea.de/, last access: 1 April 2026).

Supplement. The supplement related to this article is available online at https://doi.org/10.5194/cp-22-747-2026-supplement.

Author contributions. LC, NC, AB and VL designed the project. LC and NC carried out the palynological analyses. LC, OP and MR applied the four methods of pollen-based climate reconstruction to the ODP 976 record. LC and MHM led the archaeological synthesis. LC made the figures and wrote the text. All authors contributed to improve the manuscript by their expertise.

Competing interests. At least one of the (co-)authors is a member of the editorial board of *Climate of the Past*. The peer-review process was guided by an independent editor, and the authors also have no other competing interests to declare.

Disclaimer. Publisher's note: Copernicus Publications remains neutral with regard to jurisdictional claims made in the text, published maps, institutional affiliations, or any other geographical representation in this paper. The authors bear the ultimate responsibility for providing appropriate place names. Views expressed in the text are those of the authors and do not necessarily reflect the views of the publisher.

Acknowledgements. We want to thank the three anonymous reviewers and the editor for their very helpful comments on this manuscript. We acknowledge the International Ocean Drilling Project and the MARUM Bremen Core Repository for making available the ODP 976 samples. We thank Lionel Dubost for assistance in laboratory treatment of samples to HF. We are grateful to Francisco Sierro for sharing the isotopic data on AICC2012 timescale, to Jon Camuera for the pollen data from Padul and to Katherine Roucoux for the pollen data from Ioannina. This is an ISEM contribution.

Financial support. The ODP 976 core sampling and samples preparation were funded by the Centre National de la Recherche Scientifique and the Muséum National d'Histoire Naturelle. This publication has been supported by the European Research Council, HORIZON EUROPE European Research Council (grant no. 101052653). The doctoral contract of Liz Charton was funded by the Ministère de l'Enseignement supérieur et de la Recherche (doctoral school ED 227 DIVONA). The co-tutorship with the Unversity of Florence was supported by the Università Italo Francese (Vinci program, grant no. C2-166).

Review statement. This paper was edited by Antje Voelker and reviewed by three anonymous referees.

References

Allen, J. R. M. and Huntley, B.: Last Interglacial palaeovegetation, palaeoenvironments and chronology: a new record from Lago Grande di Monticchio, southern Italy, Quaternary Sci. Rev., 28, 1521–1538, https://doi.org/10.1016/j.quascirev.2009.02.013, 2009.

Alonso, B., Ercilla, G., Martínez-Ruíz, F., Baraza, J., and Galimont, A. (Eds.): Pliocene–Pleistocene sedimentary facies at site 976: depositional history in the northwestern Alboran Aea, in: Proceedings of the Ocean Drilling Program, 161 Scientific Results, vol. 161, Ocean Drilling Program, https://doi.org/10.2973/odp.proc.sr.161.1999, 1999.

Álvarez-Alonso, D.: First Neanderthal settlements in northern Iberia: The Acheulean and the emergence of Mousterian technology in the Cantabrian region, Quatern. Int., 326–327, 288–306, https://doi.org/10.1016/j.quaint.2012.12.023, 2014.

Aranguren, B., Grimaldi, S., Benvenuti, M., Capalbo, C., Cavanna, F., Cavulli, F., Ciani, F., Comencini, G., Giuliani, C., Grandinetti, G., Mariotti Lippi, M., Masini, F., Mazza, P. P. A., Pallecchi, P., Santaniello, F., Savorelli, A., and Revedin, A.: Poggetti Vecchi (Tuscany, Italy): A late Middle Pleistocene case of human–elephant interaction, J. Hum. Evol., 133, 32–60, https://doi.org/10.1016/j.jhevol.2019.05.013, 2019.

Arsuaga, J. L., Fernández Peris, J., Gracia-Téllez, A., Quam, R., Carretero, J. M., Barciela González, V., Blasco, R., Cuartero, F., and Sañudo, P.: Fossil human remains from Bolomor Cave (Valencia, Spain), J. Hum. Evol., 62, 629–639, https://doi.org/10.1016/j.jhevol.2012.02.002, 2012.

Auffret, G.-A., Pastouret, L., Chamley, H., and Lanoix, F.: Influence of the prevailing current regime on sedimentation in the Alboran Sea, Deep Sea Research and Oceanographic Abstracts, 21, 839–849, https://doi.org/10.1016/0011-7471(74)90003-5, 1974.

Aureli, D. and Ronchitelli, A.: The Lower Tyrrhenian Versant: was it a techno-cultural area during the Middle Palaeolithic? Evolution of the lithic industries of the Riparo del Molare sequence in the frame of Neanderthal peopling dynamics in Italy, in: Palaeolithic Italy. Advanced studies on early human adaptations in the Apennine peninsula, edited by: Borgia, V. and Cristiani, E., Leiden, 59–94, ISBN 9789088905834, 2018.

Ayalon, A., Bar-Matthews, M., and Kaufman, A.: Climatic conditions during marine oxygen isotope stage 6 in the eastern Mediterranean region from the isotopic composition of speleothems of Soreq Cave, Israel, Geology, 30, 303, https://doi.org/10.1130/0091-7613(2002)030<0303:CCDMOI>2.0.CO;2, 2002.

Baena, J., Moncel, M.-H., Cuartero, F., Chacón Navarro, M. G., and Rubio, D.: Late Middle Pleistocene genesis of Neanderthal technology in Western Europe: The case of Payre site (south-east France), Quatern. Int., 436, 212–238, https://doi.org/10.1016/j.quaint.2014.08.031, 2017.

Bailey, G., Carrión, J., Fa, D., Finlayson, C., Finlayson, G., and Vidal, J.: The coastal shelf of the Mediterranean and beyond: Corridor and refugium for human populations in the Pleistocene Introduction, Quaternary Sci. Rev., 27, 2095–2099, https://doi.org/10.1016/j.quascirev.2008.08.005, 2008.

Bajo, P., Drysdale, R. N., Woodhead, J. D., Hellstrom, J. C., Hodell, D., Ferretti, P., Voelker, A. H. L., Zanchetta, G., Rodrigues, T., Wolff, E., Tyler, J., Frisia, S., Spötl, C., and Fallick, A. E.: Persistent influence of obliquity on ice age terminations since the Middle Pleistocene transition, Science, 367, 1235–1239, https://doi.org/10.1126/science.aaw1114, 2020.

Bard, E., Delaygue, G., Rostek, F., Antonioli, F., Silenzi, S., and Schrag, D. P.: Hydrological conditions over the western Mediterranean basin during the deposition of the cold Sapropel 6 (ca. 175 kyr BP), Earth Planet. Sc. Lett., 202, 481–494, https://doi.org/10.1016/S0012-821X(02)00788-4, 2002a.

Bard, E., Antonioli, F., and Silenzi, S.: Sea-level during the penultimate interglacial period based on a submerged stalagmite from Argentarola Cave (Italy), Earth Planet. Sc. Lett., 196, 135–146, https://doi.org/10.1016/S0012-821X(01)00600-8, 2002b.

Barker, S. and Knorr, G.: Millennial scale feedbacks determine the shape and rapidity of glacial termination, Nat. Commun., 12, 2273, https://doi.org/10.1038/s41467-021-22388-6, 2021.

Barker, S., Knorr, G., Edwards, R. L., Parrenin, F., Putnam, A. E., Skinner, L. C., Wolff, E., and Ziegler, M.: 800 000 Years of Abrupt Climate Variability, Science, 334, 347–351, https://doi.org/10.1126/science.1203580, 2011.

Bayr, D., Plaza, M. P., Gilles, S., Kolek, F., Leier-Wirtz, V., Traidl-Hoffmann, C., and Damialis, A.: Pollen long-distance transport associated with symptoms in pollen allergics on the German Alps: An old story with a new ending?, Sci. Total Environ., 881, 163310, https://doi.org/10.1016/j.scitotenv.2023.163310, 2023.

Bazin, L., Landais, A., Lemieux-Dudon, B., Toyé Mahamadou Kele, H., Veres, D., Parrenin, F., Martinerie, P., Ritz, C., Capron, E., Lipenkov, V., Loutre, M.-F., Raynaud, D., Vinther, B., Svensson, A., Rasmussen, S. O., Severi, M., Blunier, T., Leuenberger, M., Fischer, H., Masson-Delmotte, V., Chappellaz, J., and Wolff, E.: An optimized multi-proxy, multi-site Antarctic ice and gas orbital chronology (AICC2012): 120–800 ka, Clim. Past, 9, 1715–1731, https://doi.org/10.5194/cp-9-1715-2013, 2013.

Benvenuti, M., Bahain, J.-J., Capalbo, C., Capretti, C., Ciani, F., D'Amico, C., Esu, D., Giachi, Gi., Giuliani, C., Gliozzi, E., Lazzeri, S., Macchioni, N., Lippi, M. M., Masini, F., Mazza, P. P. A., Pallecchi, P., Revedin, A., Savorelli, A., Spadi, M., Sozzi, L., Vietti, A., Voltaggio, M., and Aranguren, B.: Paleoenvironmental context of the early Neanderthals of Poggetti Vecchi for the late middle Pleistocene of Central Italy, Quat. res., 88, 327–344, https://doi.org/10.1017/qua.2017.51, 2017.

Bermúdez de Castro, J. M. and Martinón-Torres, M.: A new model for the evolution of the human Pleistocene populations of Europe, Quatern. Int., 295, 102–112, https://doi.org/10.1016/j.quaint.2012.02.036, 2013.

Bicho, N. and Carvalho, M.: Peninsular southern Europe refugia during the Middle Palaeolithic: an introduction, J. Quaternary Sci., 37, 133–135, https://doi.org/10.1002/jqs.3410, 2022.

Blasco, R., Rosell, J., Fernández Peris, J., Arsuaga, J. L., Bermúdez de Castro, J. M., and Carbonell, E.: Environmental availability, behavioural diversity and diet: a zooarchaeological approach from the TD10-1 sublevel of Gran Dolina (Sierra de Atapuerca, Burgos, Spain) and Bolomor Cave (Valencia, Spain), Quaternary Sci. Rev., 70, 124–144, https://doi.org/10.1016/j.quascirev.2013.03.008, 2013.

Bond, G., Heinrich, H., Broecker, W., Labeyrie, L., McManus, J., Andrews, J., Huon, S., Jantschik, R., Clasen, S., Simet, C., Tedesco, K., Klas, M., Bonani, G., and Ivy, S.: Evidence for massive discharges of icebergs into the North Atlantic

ocean during the last glacial period, Nature, 360, 245–249, https://doi.org/10.1038/360245a0, 1992.

Bond, G., Broecker, W., Johnsen, S., McManus, J., Labeyrie, L., Jouzel, J., and Bonani, G.: Correlations between climate records from North Atlantic sediments and Greenland ice, Nature, 365, 143–147, https://doi.org/10.1038/365143a0, 1993.

Bond, G., Showers, W., Cheseby, M., Lotti, R., Almasi, P., Demenocal, P., Priore, P., Cullen, H., Hajdas, I., and Bonani, G.: A pervasive millennial-scale cycle in the North Atlantic Holocene and glacial climates, Science, 278, 1257, https://doi.org/10.1126/science.278.5341.1257, 1997.

Bond, G. C., Showers, W., Elliot, M., Evans, M., Lotti, R., Hajdas, I., Bonani, G., and Johnson, S.: The North Atlantic's 1–2 kyr climate rhythm: Relation to Heinrich events, Dansgaard/Oeschger cycles and the Little Ice Age, Washington DC American Geophysical Union Geophysical Monograph Series, 112, 35–58, https://doi.org/10.1029/GM112p0035, 1999.

Boswell, S. M., Toucanne, S., Pitel-Roudaut, M., Creyts, T. T., Eynaud, F., and Bayon, G.: Enhanced surface melting of the Fennoscandian Ice Sheet during periods of North Atlantic cooling, Geology, 47, 664–668, https://doi.org/10.1130/G46370.1, 2019.

Bout-Roumazeilles, V., Combourieu Nebout, N., Peyron, O., Cortijo, E., Landais, A., and Masson-Delmotte, V.: Connection between South Mediterranean climate and North African atmospheric circulation during the last 50 000 yr BP North Atlantic cold events, Quaternary Sci. Rev., 26, 3197–3215, https://doi.org/10.1016/j.quascirev.2007.07.015, 2007.

Bradtmöller, M., Pastoors, A., Weninger, B., and Weniger, G.-C.: The repeated replacement model – Rapid climate change and population dynamics in Late Pleistocene Europe, Quatern. Int., 247, 38–49, https://doi.org/10.1016/j.quaint.2010.10.015, 2012.

Brauer, A., Allen, J. R. M., Mingram, J., Dulski, P., Wulf, S., and Huntley, B.: Evidence for last interglacial chronology and environmental change from Southern Europe, P. Natl. Acad. Sci. USA, 104, 450–455, https://doi.org/10.1073/pnas.0603321104, 2007.

Bringmans, P.: First Evidence of Neanderthal Presence in Northwest Europe during the Late Saalian "Zeifen Interstadial" (MIS 6.01) found at the VLL and VLB Sites at Veldwezelt-Hezerwater, Belgium, Journal of Archaeology of Northwest Europe, 1, https://www.researchgate.net/publication/228873892_First_Evidence_of_Neanderthal_Presence_in_Northwest_Europe_during_the_Late_Saalian_%27Zeifen_Interstadial%27_MIS_601_found_at_the_VLL_and_VLB_Sites_at_Veldwezelt-Hezerwater_Belgium (last access: 2 April 2026), 2007.

Broecker, W. S. and Henderson, G. M.: The sequence of events surrounding Termination II and their implications for the cause of glacial-interglacial CO_2 changes, Paleoceanography, 13, 352–364, 1998.

Burns, S. J., Welsh, L. K., Scroxton, N., Cheng, H., and Edwards, R. L.: Millennial and orbital scale variability of the South American Monsoon during the penultimate glacial period, Sci. Rep., 9, 1234, https://doi.org/10.1038/s41598-018-37854-3, 2019.

Buzi, C., Profico, A., Lorenzo, C., and Manzi, G.: The first preserved nasal cavity in the human fossil record: The Neanderthal from Altamura, P. Natl. Acad. Sci. USA, 122, e2426309122, https://doi.org/10.1073/pnas.2426309122, 2025.

Cacho, I., Grimalt, J. O., Pelejero, C., Canals, M., Sierro, F. J., Flores, J. A., and Shackleton, N.: Dansgaard-Oeschger and Heinrich event imprints in Alboran Sea paleotemperatures, Paleoceanography, 14, 698–705, https://doi.org/10.1029/1999PA900044, 1999.

Cacho, I., Shackleton, N., Elderfield, H., Sierro, F. J., and Grimalt, J. O.: Glacial rapid variability in deep-water temperature and δ18O from the Western Mediterranean Sea, Quaternary Sci. Rev., 25, 3294–3311, https://doi.org/10.1016/j.quascirev.2006.10.004, 2006.

Camuera, J., Jiménez-Moreno, G., Ramos-Román, M. J., García-Alix, A., Toney, J. L., Anderson, R. S., Jiménez-Espejo, F., Bright, J., Webster, C., Yanes, Y., and Carrión, J. S.: Vegetation and climate changes during the last two glacial-interglacial cycles in the western Mediterranean: A new long pollen record from Padul (southern Iberian Peninsula), Quaternary Sci. Rev., 205, 86–105, https://doi.org/10.1016/j.quascirev.2018.12.013, 2019.

Camuera, J., Ramos-Román, M. J., Jiménez-Moreno, G., García-Alix, A., Ilvonen, L., Ruha, L., Gil-Romera, G., González-Sampériz, P., and Seppä, H.: Past 200 kyr hydroclimate variability in the western Mediterranean and its connection to the African Humid Periods, Sci. Rep., 12, 9050, https://doi.org/10.1038/s41598-022-12047-1, 2022.

Caro Gómez, J. A., Díaz Del Olmo, F., Artigas, R. C., Recio Espejo, J. M., and Barrera, C. B.: Geoarchaeological alluvial terrace system in Tarazona: Chronostratigraphical transition of Mode 2 to Mode 3 during the middle-upper pleistocene in the Guadalquivir River valley (Seville, Spain), Quatern. Int., 243, 143–160, https://doi.org/10.1016/j.quaint.2011.04.022, 2011.

Carrión, J., Amorós, G., Amorós, A., and Marín-Arroyo, A. B.: Beyond the cold steppes: Neanderthal landscapes and the neglect of flora, Quaternary Sci. Rev., 371, 109673, https://doi.org/10.1016/j.quascirev.2025.109673, 2026.

Cauche, D.: Productions lithiques et comportements techno-économiques de groupes humains acheuléens et moustériens en région liguro-provençale, C. R. Palevol., 11, 519–527, https://doi.org/10.1016/j.crpv.2011.12.008, 2012.

Chapman, M. R. and Shackleton, N. J.: Global ice-volume fluctuations, North Atlantic ice-rafting events, and deep-ocean circulation changes between 130 and 70 ka, Geology, 27, 795, https://doi.org/10.1130/0091-7613(1999)027<0795:GIVFNA>2.3.CO;2, 1999.

Chappellaz, J., Brook, E., Blunier, T., and Malaizé, B.: CH_4 and δ^{18} O of O_2 records from Antarctic and Greenland ice: A clue for stratigraphic disturbance in the bottom part of the Greenland Ice Core Project and the Greenland Ice Sheet Project 2 ice cores, J. Geophys. Res., 102, 26547–26557, https://doi.org/10.1029/97JC00164, 1997.

Charton, L., Combourieu-Nebout, N., Bertini, A., Lebreton, V., Peyron, O., Robles, M., Sassoon, D., and Moncel, M.-H.: Vegetation and climate changes during the Middle to Upper Palaeolithic transition in the southwestern Mediterranean: What happened to the last Neanderthals during Heinrich stadial 4?, Quaternary Sci. Rev., 359, 109345, https://doi.org/10.1016/j.quascirev.2025.109345, 2025.

Cheddadi, R. and Rossignol-Strick, M.: Eastern Mediterranean Quaternary paleoclimates from pollen and isotope records of ma-

rine cores in the Nile Cone Area, Paleoceanography, 10, 291–300, https://doi.org/10.1029/94PA02672, 1995.

Cheng, H., Edwards, R. L., Wang, Y., Kong, X., Ming, Y., Kelly, M. J., Wang, X., Gallup, C. D., and Liu, W.: A penultimate glacial monsoon record from Hulu Cave and two-phase glacial terminations, Geology, 34, 217–220, https://doi.org/10.1130/G22289.1, 2006.

Chevalier, M., Davis, B. A. S., Heiri, O., Seppä, H., Chase, B. M., Gajewski, K., Lacourse, T., Telford, R. J., Finsinger, W., Guiot, J., Kühl, N., Maezumi, S. Y., Tipton, J. R., Carter, V. A., Brussel, T., Phelps, L. N., Dawson, A., Zanon, M., Vallé, F., Nolan, C., Mauri, A., de Vernal, A., Izumi, K., Holmström, L., Marsicek, J., Goring, S., Sommer, P. S., Chaput, M., and Kupriyanov, D.: Pollen-based climate reconstruction techniques for late Quaternary studies, Earth-Sci. Rev., 210, https://doi.org/10.1016/j.earscirev.2020.103384, 2020.

Colleoni, F., Wekerle, C., Näslund, J.-O., Brandefelt, J., and Masina, S.: Constraint on the penultimate glacial maximum Northern Hemisphere ice topography (∼ 140 kyrs BP), Quaternary Sci. Rev., 137, 97–112, https://doi.org/10.1016/j.quascirev.2016.01.024, 2016.

Combourieu-Nebout, N., Turon, J. L., Zahn, R., Capotondi, L., Londeix, L., and Pahnke, K.: Enhanced aridity and atmospheric high-pressure stability over the western Mediterranean during the North Atlantic cold events of the past 50 k.y., Geol., 30, 863, https://doi.org/10.1130/0091-7613(2002)030<0863:EAAAHP>2.0.CO;2, 2002.

Combourieu Nebout, N., Peyron, O., Dormoy, I., Desprat, S., Beaudouin, C., Kotthoff, U., and Marret, F.: Rapid climatic variability in the west Mediterranean during the last 25 000 years from high resolution pollen data, Clim. Past, 5, 503–521, https://doi.org/10.5194/cp-5-503-2009, 2009.

Cortina, A., Sierro, F. J., Flores, J. A., Martrat, B., and Grimalt, J. O.: The response of SST to insolation and ice sheet variability from MIS 3 to MIS 11 in the northwestern Mediterranean Sea (Gulf of Lions), Geophys. Res. Lett., 42, 10366–10374, https://doi.org/10.1002/2015GL065539, 2015.

Couture-Veschambre, C., López-Onaindia, D., Sala, N., Arlegi, M., Balzeau, A., Crevecoeur, I., Maureille, B., Tournepiche, J.-F., and Gómez-Olivencia, A.: Reassessment of the Neandertal fossil collection from Abri Suard (La Chaise de Vouthon, Charente, France), B. Mem. Soc. Anthro. Par., 33, https://doi.org/10.4000/bmsap.6982, 2021.

Cueto, S., Preysler, J., Pérez-González, A., Torres, C., Pérez, I., and Miguel, J.: Acheulian flint quarries in the Madrid Tertiary basin, central Iberian Peninsula: First data obtained from geoarchaeological studies, Quatern. Int., 411, https://doi.org/10.1016/j.quaint.2016.01.041, 2016.

Cunha, P. P., Almeida, N. A. C., Aubry, T., Martins, A. A., Murray, A. S., Buylaert, J.-P., Sohbati, R., Raposo, L., and Rocha, L.: Records of human occupation from Pleistocene river terrace and aeolian sediments in the Arneiro depression (Lower Tejo River, central eastern Portugal), Geomorphology, 165–166, 78–90, https://doi.org/10.1016/j.geomorph.2012.02.017, 2012.

Cunha, P. P., Martins, A. A., Buylaert, J.-P., Murray, A. S., Raposo, L., Mozzi, P., and Stokes, M.: New data on the chronology of the Vale do Forno sedimentary sequence (Lower Tejo River terrace staircase) and its relevance as a fluvial archive of the Middle Pleistocene in western Iberia, Quaternary Sci. Rev., 166, 204–226, https://doi.org/10.1016/j.quascirev.2016.11.001, 2017.

Damialis, A., Kaimakamis, E., Konoglou, M., Akritidis, I., Traidl-Hoffmann, C., and Gioulekas, D.: Estimating the abundance of airborne pollen and fungal spores at variable elevations using an aircraft: how high can they fly?, Sci. Rep., 7, 44535, https://doi.org/10.1038/srep44535, 2017.

Dansgaard, W., Johnsen, S. J., Clausen, H. B., Dahl-Jensen, D., Gundestrup, N. S., Hammer, C. U., Hvidberg, C. S., Steffensen, J. P., Sveinbjörnsdottir, A. E., and Jouzel, J.: Evidence for general instability of past climate from a 250-kyr ice-core record, Nature, 364, 218–220, 1993.

Davtian, N. and Bard, E.: A new view on abrupt climate changes and the bipolar seesaw based on paleotemperatures from Iberian Margin sediments, P. Natl. Acad. Sci. USA, 120, e2209558120, https://doi.org/10.1073/pnas.2209558120, 2023.

de Abreu, L., Shackleton, N. J., Schönfeld, J., Hall, M., and Chapman, M.: Millennial-scale oceanic climate variability off the Western Iberian margin during the last two glacial periods, Mar. Geol., 196, 1–20, https://doi.org/10.1016/S0025-3227(03)00046-X, 2003.

de Lumley, M. A.: Les restes humains fossiles de la grotte du Lazaret. Généralités, approche démographique, in: Les restes humains fossiles de la grotte du Lazaret, Nice, Alpes-Maritimes. Des Homo erectus européens évolués en voie de néandertalisation, CNRS Editions, 217–220, ISBN 978-2-271-12018-2, 2018.

Dennell, R. W., Martinón-Torres, M., and Bermúdez de Castro, J. M.: Hominin variability, climatic instability and population demography in Middle Pleistocene Europe, Quaternary Sci. Rev., 30, 1511–1524, https://doi.org/10.1016/j.quascirev.2009.11.027, 2011.

D'Errico, F. and Sánchez Goñi, M. F. S.: Neandertal extinction and the millennial scale climatic variability of OIS 3, Quaternary Sci. Rev., 22, 769–788, https://doi.org/10.1016/S0277-3791(03)00009-X, 2003.

Diez-Martín, F.: Evaluating the effect of plowing on the archaeological record: The early middle palaeolithic in the river Duero basin plateaus (north-central Spain), Quatern. Int., 214, 30–43, https://doi.org/10.1016/j.quaint.2009.10.024, 2010.

Diez-Martín, F., Sánchez-Yustos, P., Gómez-González, J. Á., and Gómez De La Rúa, D.: Earlier Palaeolithic Settlement Patterns: Landscape Archaeology on the River Duero Basin Plateaus (Castilla y León, Spain), J. World Prehist., 21, 103–137, https://doi.org/10.1007/s10963-008-9012-0, 2008.

Di Vincenzo, F. and Manzi, G.: Homo heidelbergensis as the Middle Pleistocene common ancestor of Denisovans, Neanderthals and modern humans, Journal of Mediterranean Earth Sciences, 15, https://doi.org/10.13133/2280-6148/18074, 2023.

d'Oliveira, L., Dugerdil, L., Ménot, G., Evin, A., Muller, S. D., Ansanay-Alex, S., Azuara, J., Bonnet, C., Bremond, L., Shah, M., and Peyron, O.: Reconstructing 15 000 years of southern France temperatures from coupled pollen and molecular (branched glycerol dialkyl glycerol tetraether) markers (Canroute, Massif Central), Clim. Past, 19, 2127–2156, https://doi.org/10.5194/cp-19-2127-2023, 2023.

Drysdale, R. N., Zanchetta, G., Hellstrom, J. C., Fallick, A. E., and Zhao, J.: Stalagmite evidence for the onset of the Last Interglacial in southern Europe at 129 ± 1 ka, Geophys. Res. Lett., 32, https://doi.org/10.1029/2005GL024658, 2005.

Dugerdil, L., Joannin, S., Peyron, O., Jouffroy-Bapicot, I., Vannière, B., Boldgiv, B., Unkelbach, J., Behling, H., and Ménot, G.: Climate reconstructions based on GDGT and pollen surface datasets from Mongolia and Baikal area: calibrations and applicability to extremely cold–dry environments over the Late Holocene, Clim. Past, 17, 1199–1226, https://doi.org/10.5194/cp-17-1199-2021, 2021.

Ehlers, J. and Gibbard, P. L.: The extent and chronology of Cenozoic Global Glaciation, Quatern. Int., 164–165, 6–20, https://doi.org/10.1016/j.quaint.2006.10.008, 2007.

Ehlers, J., Grube, A., Stephan, H.-J., and Wansa, S.: Pleistocene Glaciations of North Germany – New Results, in: Developments in Quaternary Sciences, Elsevier, vol. 15, 149–162, https://doi.org/10.1016/B978-0-444-53447-7.00013-1, 2011.

Ehlers, J., Gibbard, P. L., and Hughes, P. D.: Chapter 4 – Quaternary Glaciations and Chronology, in: Past Glacial Environments, 2nd edn., edited by: Menzies, J. and van der Meer, J. J. M., Elsevier, 77–101, https://doi.org/10.1016/B978-0-08-100524-8.00003-8, 2018.

Emeis, K., Schulz, H., Struck, U., Rossignol-Strick, M., Erlenkeuser, H., Howell, M., Kroon, D., Mackensen, A., Ishizuka, S., Oba, T., Sakamoto, T., and Koizumi, I.: Eastern Mediterranean surface water temperatures and δ18O composition during deposition of sapropels in the late Quaternary, Paleoceanography, 18, 1005, https://doi.org/10.1029/2000PA000617, 2003.

EPICA Community Members: One-to-one coupling of glacial climate variability in Greenland and Antarctica, Nature, 444, 195–198, https://doi.org/10.1038/nature05301, 2006.

Eynaud, F., Zaragosi, S., Scourse, J. D., Mojtahid, M., Bourillet, J. F., Hall, I. R., Penaud, A., Locascio, M., and Reijonen, A.: Deglacial laminated facies on the NW European continental margin: The hydrographic significance of British-Irish Ice Sheet deglaciation and Fleuve Manche paleoriver discharges, Geochem. Geophy. Geosy., 8, https://doi.org/10.1029/2006GC001496, 2007.

Faegri, K. and Iversen, J.: Textbook of Pollen Analysis, 4th edn., John Wiley and Sons, Chichester, UK, 338 pp., ISBN 0-471-92178-5, 1964.

Fernández Peris, J., Barciela, V., Blasco, R., Cuartero, F., and Sañudo, P.: El Paleolítico Medio en el territorio valenciano y la variabilidad tecno-económica de la Cova del Bolomor, Treballs d'Arqueologia, 141–169, https://dialnet.unirioja.es/servlet/articulo?codigo=3184845 (last access: 2 April 2026), 2008.

Fernández-Rodríguez, S., Skjøth, C. A., Tormo-Molina, R., Brandao, R., Caeiro, E., Silva-Palacios, I., Gonzalo-Garijo, A., and Smith, M.: Identification of potential sources of airborne Olea pollen in the Southwest Iberian Peninsula, Int. J. Biometeorol., 58, 337–348, https://doi.org/10.1007/s00484-012-0629-4, 2014.

Finlayson, C. and Carrión, J. S.: Rapid ecological turnover and its impact on Neanderthal and other human populations, Trends Ecol. Evol., 22, 213–222, https://doi.org/10.1016/j.tree.2007.02.001, 2007.

Fletcher, W. J. and Sánchez Goñi, M. F.: Orbital- and sub-orbital-scale climate impacts on vegetation of the western Mediterranean basin over the last 48 000 yr, Quaternary Res., 70, 451–464, https://doi.org/10.1016/j.yqres.2008.07.002, 2008.

Fletcher, W. J., Sánchez Goñi, M. F., Allen, J. R. M., Cheddadi, R., Combourieu-Nebout, N., Huntley, B., Lawson, I., Londeix, L., Magri, D., Margari, V., Müller, U. C., Naughton, F., Novenko, E., Roucoux, K., and Tzedakis, P. C.: Millennial-scale variability during the last glacial in vegetation records from Europe, Quaternary Sci. Rev., 29, 2839–2864, https://doi.org/10.1016/j.quascirev.2009.11.015, 2010.

Foerster, V., Asrat, A., Bronk Ramsey, C., Brown, E. T., Chapot, M. S., Deino, A., Duesing, W., Grove, M., Hahn, A., Junginger, A., Kaboth-Bahr, S., Lane, C. S., Opitz, S., Noren, A., Roberts, H. M., Stockhecke, M., Tiedemann, R., Vidal, C. M., Vogelsang, R., Cohen, A. S., Lamb, H. F., Schaebitz, F., and Trauth, M. H.: Pleistocene climate variability in eastern Africa influenced hominin evolution, Nat. Geosci., 15, 805–811, https://doi.org/10.1038/s41561-022-01032-y, 2022.

Follieri, M., Magri, D., and Sadori, L.: A 250 000-years pollen record from Valle di Castiglione (Roma), Pollen et Spores, 30, 329–356, 1988.

Fontana, F., Nenzioni, G., and Peretto, C.: The southern Po plain area (Italy) in the mid-late Pleistocene: Human occupation and technical behaviours, Quatern. Int., 223, 465–471, https://doi.org/10.1016/j.quaint.2010.02.013, 2010.

Fotiadou, C. M., Pedersen, J. B., Rougier, H., Roksandic, M., Spyrou, M. A., Nägele, K., Reiter, E., Bocherens, H., Kandel, A. W., Haidle, M. N., Streicher, T. P., Conard, N. J., Schilt, F., Godinho, R. M., Uthmeier, T., Doyon, L., Semal, P., Krause, J., Barbieri, A., Mihailović, D., Crevecoeur, I., and Posth, C.: Archaeogenetic insights into the demographic history of Late Neanderthals, P. Natl. Acad. Sci. USA, 123, e2520565123, https://doi.org/10.1073/pnas.2520565123, 2026.

Gouzy, A., Malaizé, B., Pujol, C., and Charlier, K.: Climatic "pause" during Termination II identified in shallow and intermediate waters off the Iberian margin, Quaternary Sci. Rev., 23, 1523–1528, https://doi.org/10.1016/j.quascirev.2004.03.002, 2004.

Guiot, J.: Methodology of the last climatic cycle reconstruction in France from pollen data, Palaeogeogr. Palaeocl., 80, 49–69, https://doi.org/10.1016/0031-0182(90)90033-4, 1990.

Guiot, J., Pons, A., De Beaulieu, J. L., and Reille, M.: A 140 000-year continental climate reconstruction from two European pollen records, Nature, 338, 309–313, https://doi.org/10.1038/338309a0, 1989.

Guiot, J., De Beaulieu, J. L., Cheddadi, R., David, F., Ponel, P., and Reille, M.: The climate in Western Europe during the last Glacial/Interglacial cycle derived from pollen and insect remains, Palaeogeogr. Palaeocl., 103, 73–93, https://doi.org/10.1016/0031-0182(93)90053-L, 1993.

Heinrich, H.: Origin and Consequences of Cyclic Ice Rafting in the Northeast Atlantic Ocean During the Past 130 000 Years, Quaternary Res., 29, 142–152, https://doi.org/10.1016/0033-5894(88)90057-9, 1988.

Held, F., Cheng, H., Edwards, R. L., Tüysüz, O., Koç, K., and Fleitmann, D.: Dansgaard-Oeschger cycles of the penultimate and last glacial period recorded in stalagmites from Türkiye, Nat. Commun., 15, 1183, https://doi.org/10.1038/s41467-024-45507-5, 2024.

Hemming, S. R.: Heinrich events: Massive late Pleistocene detritus layers of the North Atlantic and their global climate imprint, Rev. Geophys., 42, https://doi.org/10.1029/2003RG000128, 2004.

Hérisson, D., Brenet, M., Cliquet, D., Moncel, M.-H., Richter, J., Scott, B., Van Baelen, A., Di Modica, K., Loecker, D., Ashton, N., Bourguignon, L., Delagnes, A., Faivre, J.-P., Folgado-Lopez,

M., Locht, J.-L., Pope, M., Raynal, J.-P., Roebroeks, W., Santagata, C., and Peer, P.: The emergence of the Middle Palaeolithic in north-western Europe and its southern fringes, Quatern. Int., 411, https://doi.org/10.1016/j.quaint.2016.02.049, 2016.

Hersbach, H., Bell, B., Berrisford, P., Hirahara, S., Horányi, A., Muñoz-Sabater, J., Nicolas, J., Peubey, C., Radu, R., Schepers, D., Simmons, A., Soci, C., Abdalla, S., Abellan, X., Balsamo, G., Bechtold, P., Biavati, G., Bidlot, J., Bonavita, M., De Chiara, G., Dahlgren, P., Dee, D., Diamantakis, M., Dragani, R., Flemming, J., Forbes, R., Fuentes, M., Geer, A., Haimberger, L., Healy, S., Hogan, R. J., Hólm, E., Janisková, M., Keeley, S., Laloyaux, P., Lopez, P., Lupu, C., Radnoti, G., de Rosnay, P., Rozum, I., Vamborg, F., Villaume, S., and Thépaut, J.-N.: The ERA5 global reanalysis, Q. J. Roy. Meteor. Soc., 146, 1999–2049, https://doi.org/10.1002/qj.3803, 2020.

Hijmans, R. J., Phillips, S., Leathwick, J., and Elith, J.: dismo: Species Distribution Modeling, R package version 1.3-15, https://cran.r-project.org/web/packages/dismo/index.html (last access: 2 April 2026), 2024.

Hodell, D. A., Channell, J. E. T., Curtis, J. H., Romero, O. E., and Röhl, U.: Onset of "Hudson Strait" Heinrich events in the eastern North Atlantic at the end of the middle Pleistocene transition (~640 ka)?, Paleoceanography, 23, 2008PA001591, https://doi.org/10.1029/2008PA001591, 2008.

Hodell, D. A., Crowhurst, S. J., Lourens, L., Margari, V., Nicolson, J., Rolfe, J. E., Skinner, L. C., Thomas, N. C., Tzedakis, P. C., Mleneck-Vautravers, M. J., and Wolff, E. W.: A 1.5-million-year record of orbital and millennial climate variability in the North Atlantic, Clim. Past, 19, 607–636, https://doi.org/10.5194/cp-19-607-2023, 2023.

Hodge, E., Richards, D., Smart, P., Andreo, B., Hoffmann, D., Mattey, D., and González-Ramón, A.: Effective precipitation in southern Spain (~266 to 46 ka) based on a speleothem stable carbon isotope record, Quaternary Res., 69, 447–457, https://doi.org/10.1016/j.yqres.2008.02.013, 2008.

Hublin, J. J.: The origin of Neandertals, P. Natl. Acad. Sci. USA, 106, 16022–16027, https://doi.org/10.1073/pnas.0904119106, 2009.

Jiménez-Amat, P. and Zahn, R.: Offset timing of climate oscillations during the last two glacial-interglacial transitions connected with large-scale freshwater perturbation, Paleoceanography, 30, 768–788, https://doi.org/10.1002/2014PA002710, 2015.

Jiménez-Moreno, G., Anderson, R. S., Ramos-Román, M. J., Camuera, J., Mesa-Fernández, J. M., García-Alix, A., Jiménez-Espejo, F. J., Carrión, J. S., and López-Avilés, A.: The Holocene Cedrus pollen record from Sierra Nevada (S Spain), a proxy for climate change in N Africa, Quaternary Sci. Rev., 242, 106468, https://doi.org/10.1016/j.quascirev.2020.106468, 2020.

Johnsen, S. J., Clausen, H. B., Dansgaard, W., Fuhrer, K., Gundestrup, N., Hammer, C. U., Iversen, P., Jouzel, J., Stauffer, B., and Steffensen, J. P.: Irregular glacial interstadials recorded in a new Greenland record, Nature, 359, 311–313, 1992.

Jouzel, J., Masson-Delmotte, V., Cattani, O., Dreyfus, G., Falourd, S., Hoffmann, G., Minster, B., Nouet, J., Barnola, J. M., Chappellaz, J., Fischer, H., Gallet, J. C., Johnsen, S., Leuenberger, M., Loulergue, L., Luethi, D., Oerter, H., Parrenin, F., Raisbeck, G., Raynaud, D., Schilt, A., Schwander, J., Selmo, E., Souchez, R., Spahni, R., Stauffer, B., Steffensen, J. P., Stenni, B., Stocker, T. F., Tison, J. L., Werner, M., and Wolff, E. W.: Orbital and millennial Antarctic climate variability over the past 800 000 years, Science, 317, 793–796, https://doi.org/10.1126/science.1141038, 2007.

Juggins, S.: rioja: Analysis of Quaternary Science Data, R package version 1.0-7, https://cran.r-project.org/package=rioja (last access: 2 April 2026), 2024.

Kallel, N., Duplessy, J.-C., Labeyrie, L., Fontugne, M., Paterne, M., and Montacer, M.: Mediterranean pluvial periods and sapropel formation over the last 200 000 years, Palaeogeogr. Palaeocl., 157, 45–58, https://doi.org/10.1016/S0031-0182(99)00149-2, 2000.

Kelly, M., Edwards, R., Cheng, H., Yuan, D., Cai, Y., Zhang, M., Lin, Y., and An, Z.: High resolution characterization of the Asian Monsoon between 146 000 and 99 000 years B.P. from Dongge Cave, China and global correlation of events surrounding Termination II, Palaeogeogr. Palaeocl., 236, 20–38, https://doi.org/10.1016/j.palaeo.2005.11.042, 2006.

Key, A. J. M., Jarić, I., and Roberts, D. L.: Modelling the end of the Acheulean at global and continental levels suggests widespread persistence into the Middle Palaeolithic, Humanit. Soc. Sci. Commun., 8, 55, https://doi.org/10.1057/s41599-021-00735-8, 2021.

Koltai, G., Spötl, C., Shen, C.-C., Wu, C.-C., Rao, Z., Palcsu, L., Kele, S., Surányi, G., and Bárány-Kevei, I.: A penultimate glacial climate record from southern Hungary, J. Quaternary Sci., 32, 946–956, https://doi.org/10.1002/jqs.2968, 2017.

Koutsodendris, A., Dakos, V., Fletcher, W. J., Knipping, M., Kotthoff, U., Milner, A. M., Müller, U. C., Kaboth-Bahr, S., Kern, O. A., Kolb, L., Vakhrameeva, P., Wulf, S., Christanis, K., Schmiedl, G., and Pross, J.: Atmospheric CO_2 forcing on Mediterranean biomes during the past 500 kyrs, Nat. Commun., 14, 1664, https://doi.org/10.1038/s41467-023-37388-x, 2023.

Laskar, J., Robutel, P., Joutel, F., Gastineau, M., Correia, A. C. M., and Levrard, B.: A long-term numerical solution for the insolation quantities of the Earth, Astron. Astrophys., 428, 261–285, https://doi.org/10.1051/0004-6361:20041335, 2004.

Lewis, S., Ashton, N., and Jacobi, R.: 9 – Testing Human Presence During the Last Interglacial (MIS 5e): A Review of the British Evidence, in: Developments in Quaternary Sciences, vol. 14, edited by: Ashton, N., Lewis, S. G., and Stringer, C., Elsevier, 125–164, https://doi.org/10.1016/B978-0-444-53597-9.00009-1, 2011.

Li, T.-Y., Shen, C.-C., Huang, L.-J., Jiang, X.-Y., Yang, X.-L., Mii, H.-S., Lee, S.-Y., and Lo, L.: Stalagmite-inferred variability of the Asian summer monsoon during the penultimate glacial–interglacial period, Clim. Past, 10, 1211–1219, https://doi.org/10.5194/cp-10-1211-2014, 2014.

Liaw, A. and Wiener, M.: Classification and Regression by randomForest, https://doi.org/10.32614/CRAN.package.randomForest, 2002.

Lionello, P., Malanotte-Rizzoli, P., Boscolo, R., Alpert, P., Artale, V., Li, L., Luterbacher, J., May, W., Trigo, R., Tsimplis, M., Ulbrich, U., and Xoplaki, E.: The Mediterranean climate: An overview of the main characteristics and issues, in: Developments in Earth and Environmental Sciences, vol. 4, edited by: Lionello, P., Malanotte-Rizzoli, P., and Boscolo, R., Elsevier, 1–26, https://doi.org/10.1016/S1571-9197(06)80003-0, 2006.

Liquete, C., Arnau, P., Canals, M., and Colas, S.: Mediterranean river systems of Andalusia, southern Spain, and associated

deltas: A source to sink approach, Mar. Geol., 222–223, 471–495, https://doi.org/10.1016/j.margeo.2005.06.033, 2005.

Lisiecki, L. and Raymo, M.: Pliocene-Pleistocene stack of 57 globally distributed benthic 18O records, Paleoceanography, 20, https://doi.org/10.1029/2004PA001071, 2005.

Lisiecki, L. E. and Stern, J. V.: Regional and global benthic δ18O stacks for the last glacial cycle, Paleoceanography, 31, 1368–1394, https://doi.org/10.1002/2016PA003002, 2016.

Liu, J., Fang, N., Wang, F., Yang, F., and Ding, X.: Features of ice-rafted debris (IRD) at IODP site U1312 and their palaeoenvironmental implications during the last 2.6 Myr, Palaeogeogr. Palaeocl., 511, 364–378, https://doi.org/10.1016/j.palaeo.2018.09.002, 2018.

Lobo, F. J., Fernández-Salas, L. M., Moreno, I., Sanz, J. L., and Maldonado, A.: The sea-floor morphology of a Mediterranean shelf fed by small rivers, northern Alboran Sea margin, Cont. Shelf Res., 26, 2607–2628, https://doi.org/10.1016/j.csr.2006.08.006, 2006.

Macklin, M. G., Fuller, I. C., Lewin, J., Maas, G. S., Passmore, D. G., Rose, J., Woodward, J. C., Black, S., Hamlin, R. H. B., and Rowan, J. S.: Correlation of fluvial sequences in the Mediterranean basin over the last 200 ka and their relationship to climate change, Quaternary Sci. Rev., 21, 1633–1641, https://doi.org/10.1016/S0277-3791(01)00147-0, 2002.

Magri, D. and Parra, I.: Late Quaternary western Mediterranean pollen records and African winds, Earth Planet. Sc. Lett., 200, 401–408, https://doi.org/10.1016/S0012-821X(02)00619-2, 2002.

Margari, V., Skinner, L. C., Tzedakis, P. C., Ganopolski, A., Vautravers, M., and Shackleton, N. J.: The nature of millennial-scale climate variability during the past two glacial periods, Nat. Geosci., 3, 127–131, https://doi.org/10.1038/ngeo740, 2010.

Margari, V., Skinner, L., Hodell, D., Martrat, B., Toucanne, S., Gibbard, P., Lunkka, J., and Tzedakis, C.: Land-ocean changes on orbital and millennial time scales and the penultimate glaciation, Geology, https://doi.org/10.1130/G35070.1, 2014.

Martrat, B., Grimalt, J. O., Lopez-Martinez, C., Cacho, I., Sierro, F. J., Flores, J. A., Zahn, R., Canals, M., Curtis, J. H., and Hodell, D. A.: Abrupt Temperature Changes in the Western Mediterranean over the Past 250 000 Years, Science, 306, 1762–1765, https://doi.org/10.1126/science.1101706, 2004.

Martrat, B., Grimalt, J. O., Shackleton, N. J., de Abreu, L., Hutterli, M. A., and Stocker, T. F.: Four Climate Cycles of Recurring Deep and Surface Water Destabilizations on the Iberian Margin, Science, 317, 502–507, https://doi.org/10.1126/science.1139994, 2007.

Martrat, B., Jimenez-Amat, P., Zahn, R., and Grimalt, J. O.: Similarities and dissimilarities between the last two deglaciations and interglaciations in the North Atlantic region, Quaternary Sci. Rev., 99, 122–134, https://doi.org/10.1016/j.quascirev.2014.06.016, 2014.

Masson-Delmotte, V., Stenni, B., Pol, K., Braconnot, P., Cattani, O., Falourd, S., Kageyama, M., Jouzel, J., Landais, A., Minster, B., Barnola, J. M., Chappellaz, J., Krinner, G., Johnsen, S., Röthlisberger, R., Hansen, J., Mikolajewicz, U., and Otto-Bliesner, B.: EPICA Dome C record of glacial and interglacial intensities, Quaternary Sci. Rev., 29, 113–128, https://doi.org/10.1016/j.quascirev.2009.09.030, 2010.

Mathias, C., Bourguignon, L., Brenet, M., Grégoire, S., and Moncel, M.-H.: Between new and inherited technical behaviours: a case study from the Early Middle Palaeolithic of Southern France, Archaeol. Anthropol. Sci., 12, 146, https://doi.org/10.1007/s12520-020-01114-1, 2020.

Matthews, A., Affek, H. P., Ayalon, A., Vonhof, H. B., and Bar-Matthews, M.: Eastern Mediterranean climate change deduced from the Soreq Cave fluid inclusion stable isotopes and carbonate clumped isotopes record of the last 160 ka, Quaternary Sci. Rev., 272, 107223, https://doi.org/10.1016/j.quascirev.2021.107223, 2021.

McCarron, A. P., Bigg, G. R., Brooks, H., Leng, M. J., Marshall, J. D., Ponomareva, V., Portnyagin, M., Reimer, P. J., and Rogerson, M.: Northwest Pacific ice-rafted debris at 38° N reveals episodic ice-sheet change in late Quaternary Northeast Siberia, Earth Planet. Sc. Lett., 553, 116650, https://doi.org/10.1016/j.epsl.2020.116650, 2021.

McManus, J. F., Oppo, D. W., and Cullen, J. L.: A 0.5-Million-Year Record of Millennial-Scale Climate Variability in the North Atlantic, Science, 283, 971–975, https://doi.org/10.1126/science.283.5404.971, 1999.

Melchionna, M., Di Febbraro, M., Carotenuto, F., Rook, L., Mondanaro, A., Castiglione, S., Serio, C., Vero, V. A., Tesone, G., Piccolo, M., Diniz-Filho, J. A. F., and Raia, P.: Fragmentation of Neanderthals' pre-extinction distribution by climate change, Palaeogeogr. Palaeocl., 496, 146–154, https://doi.org/10.1016/j.palaeo.2018.01.031, 2018.

Menviel, L., Capron, E., Govin, A., Dutton, A., Tarasov, L., Abe-Ouchi, A., Drysdale, R. N., Gibbard, P. L., Gregoire, L., He, F., Ivanovic, R. F., Kageyama, M., Kawamura, K., Landais, A., Otto-Bliesner, B. L., Oyabu, I., Tzedakis, P. C., Wolff, E., and Zhang, X.: The penultimate deglaciation: protocol for Paleoclimate Modelling Intercomparison Project (PMIP) phase 4 transient numerical simulations between 140 and 127 ka, version 1.0, Geosci. Model Dev., 12, 3649–3685, https://doi.org/10.5194/gmd-12-3649-2019, 2019.

Michel, V., Shen, G., Shen, C.-C., Duval, M., Woodhead, J., Chou, Y.-M., Hu, H.-M., Wu, C.-C., Kan, Y.-C., Yang, H., Yu, T.-L., Gallet, S., and Valensi, P.: Datations radioisotopiques (U-Th, U-Pb) et paléodosimétriques (ESR) des plus anciens sites préhistoriques des Alpes-Maritimes: la grotte du Vallonnet, le site de plein air de Terra Amata et la grotte du Lazaret, in: Bulletin du Musée d'Anthropologie préhistorique de Monaco, vol. 61, 65–80, https://hal.science/hal-04026546v2 (last access: 2 April 2026), 2022.

Moncel, M., Vaissié, E., Marin, J., Fernandes, P., Abrunhosa, A., Hardy, B., Richard, M., Torres, C., and Baena, J.: Early Middle Palaeolithic Occupations Dated to MIS 7 at the Abri du Maras (Ardèche, Southeast France), Journal of Paleolithic Archaeology, 8, 21, https://doi.org/10.1007/s41982-025-00221-6, 2025.

Moncel, M.-H., Ashton, N., Arzarello, M., Fontana, F., Lamotte, A., Scott, B., Muttillo, B., Berruti, G., Nenzioni, G., Tuffreau, A., and Peretto, C.: Early Levallois core technology between Marine Isotope Stage 12 and 9 in Western Europe, J. Hum. Evol., 139, 102735, https://doi.org/10.1016/j.jhevol.2019.102735, 2020.

Moseley, G. E., Spötl, C., Cheng, H., Boch, R., Min, A., and Edwards, R. L.: Termination-II interstadial/stadial climate change recorded in two stalagmites from the

north European Alps, Quaternary Sci. Rev., 127, 229–239, https://doi.org/10.1016/j.quascirev.2015.07.012, 2015.

Mudie, P.: Pollen distribution in recent marine sediments, eastern Canada, Can. J. Earth Sci., 19, 729–747, https://doi.org/10.1139/e82-062, 2011.

Murat, A. (Ed.): Chapitre 41: Pliocene–pleistocene occurrence of sapropels in the western mediterranean sea and their relation to eastern mediterranean sapropels, in: Proceedings of the Ocean Drilling Program, 161 Scientific Results, vol. 161, Ocean Drilling Program, https://doi.org/10.2973/odp.proc.sr.161.1999, 1999.

Nehme, C., Verheyden, S., Breitenbach, S. F. M., Gillikin, D. P., Verheyden, A., Cheng, H., Edwards, R. L., Hellstrom, J., Noble, S. R., Farrant, A. R., Sahy, D., Goovaerts, T., Salem, G., and Claeys, P.: Climate dynamics during the penultimate glacial period recorded in a speleothem from Kanaan Cave, Lebanon (central Levant), Quaternary Res., 90, 10–25, https://doi.org/10.1017/qua.2018.18, 2018.

Nehme, C., Kluge, T., Verheyden, S., Nader, F., Charalambidou, I., Weissbach, T., Gucel, S., Cheng, H., Edwards, R. L., Satterfield, L., Eiche, E., and Claeys, P.: Speleothem record from Pentadactylos cave (Cyprus): new insights into climatic variations during MIS 6 and MIS 5 in the Eastern Mediterranean, Quaternary Sci. Rev., 250, 106663, https://doi.org/10.1016/j.quascirev.2020.106663, 2020.

Obrochta, S. P., Crowley, T. J., Channell, J. E. T., Hodell, D. A., Baker, P. A., Seki, A., and Yokoyama, Y.: Climate variability and ice-sheet dynamics during the last three glaciations, Earth Planet. Sc. Lett., 406, 198–212, https://doi.org/10.1016/j.epsl.2014.09.004, 2014.

Ochando, J., Carrión, J. S., Blasco, R., Fernández, S., Amorós, G., Munuera, M., Sañudo, P., and Fernández Peris, J.: Silvicolous Neanderthals in the far West: the mid-Pleistocene palaeoecological sequence of Bolomor Cave (Valencia, Spain), Quaternary Sci. Rev., 217, 247–267, https://doi.org/10.1016/j.quascirev.2019.03.015, 2019.

Oksanen, J., Simpson, G., Blanchet, F., Kindt, R., Legendre, P., Minchin, P., O'Hara, R., Solymos, P., Stevens, M., Szoecs, E., Wagner, H., Barbour, M., Bedward, M., Bolker, B., Borcard, D., Borman, T., Carvalho, G., Chirico, M., De Caceres, M., Durand, S., Evangelista, H., FitzJohn, R., Friendly, M., Furneaux, B., Hannigan, G., Hill, M., Lahti, L., Martino, C., McGlinn, D., Ouellette, M., Ribeiro Cunha, E., Smith, T., Stier, A., Ter Braak, C., and Weedon, J.: vegan: Community Ecology Package, R package version 2.8-0, https://vegandevs.github.io/vegan/ (last access: 2 April 2026), 2026

Okuda, M., Yasuda, Y., and Setoguchi, T.: Middle to Late Pleistocene vegetation history and climatic changes at Lake Kopais, Southeast Greece, Boreas, 30, 73–82, https://doi.org/10.1111/j.1502-3885.2001.tb00990.x, 2001.

Oppo, D. W., Keigwin, L. D., McManus, J. F., and Cullen, J. L.: Persistent suborbital climate variability in marine isotope stage 5 and termination II, Paleoceanography, 16, 280–292, https://doi.org/10.1029/2000PA000527, 2001.

Oppo, D. W., McManus, J. F., and Cullen, J. L.: Evolution and demise of the Last Interglacial warmth in the subpolar North Atlantic, Quaternary Sci. Rev., 25, 3268–3277, https://doi.org/10.1016/j.quascirev.2006.07.006, 2006.

Ovsepyan, E. A. and Murdmaa, I. O.: Response of the bering sea to Heinrich Event 11, Lithol. Miner. Resour., 52, 442–446, https://doi.org/10.1134/S0024490217060062, 2017.

Panera, J., Torres, T., Pérez-González, A., Ortiz, J. E., Rubio-Jara, S., and del Val, D. U.: Geocronología de la Terraza Compleja de Arganda en el valle del río Jarama (Madrid, España), Estud. Geol., 67, 495–504, https://doi.org/10.3989/egeol.40550.204, 2011.

Panera, J., Rubio-Jara, S., Yravedra, J., Blain, H.-A., Sesé, C., and Pérez-González, A.: Manzanares Valley (Madrid, Spain): A good country for Proboscideans and Neanderthals, Quatern. Int., 326–327, 329–343, https://doi.org/10.1016/j.quaint.2013.09.009, 2014.

Penaud, A., Eynaud, F., Turon, J. L., Zaragosi, S., Malaizé, B., Toucanne, S., and Bourillet, J. F.: What forced the collapse of European ice sheets during the last two glacial periods (150 ka B.P. and 18 ka cal B.P.)? Palynological evidence, Palaeogeogr. Palaeocl., 281, 66–78, https://doi.org/10.1016/j.palaeo.2009.07.012, 2009.

Penaud, A., Eynaud, F., Voelker, A. H. L., and Turon, J.-L.: Palaeohydrological changes over the last 50 ky in the central Gulf of Cadiz: complex forcing mechanisms mixing multi-scale processes, Biogeosciences, 13, 5357–5377, https://doi.org/10.5194/bg-13-5357-2016, 2016.

Pereira, T., Cunha, P. P., Martins, A. A., Nora, D., Paixão, E., Figueiredo, O., Raposo, L., Henriques, F., Caninas, J., Moura, D., and Bridgland, D. R.: Geoarchaeology of the Cobrinhos site (Vila Velha de Ródão, Portugal) – a record of the earliest Mousterian in western Iberia, J. Archaeol. Sci. Reports, 24, 640–654, https://doi.org/10.1016/j.jasrep.2018.11.026, 2019.

Pérez-Asensio, J. N., Frigola, J., Pena, L. D., Sierro, F. J., Reguera, M. I., Rodríguez-Tovar, F. J., Dorador, J., Asioli, A., Kuhlmann, J., Huhn, K., and Cacho, I.: Changes in western Mediterranean thermohaline circulation in association with a deglacial Organic Rich Layer formation in the Alboran Sea, Quaternary Sci. Rev., 228, 106075, https://doi.org/10.1016/j.quascirev.2019.106075, 2020.

Peyrégne, S., Slon, V., Mafessoni, F., de Filippo, C., Hajdinjak, M., Nagel, S., Nickel, B., Essel, E., Le Cabec, A., Wehrberger, K., Conard, N. J., Kind, C. J., Posth, C., Krause, J., Abrams, G., Bonjean, D., Di Modica, K., Toussaint, M., Kelso, J., Meyer, M., Pääbo, S., and Prüfer, K.: Nuclear DNA from two early Neandertals reveals 80 000 years of genetic continuity in Europe, Sci. Adv., 5, eaaw5873, https://doi.org/10.1126/sciadv.aaw5873, 2019.

Peyron, O., Goring, S., Dormoy, I., Kotthoff, U., Pross, J., de Beaulieu, J.-L., Drescher-Schneider, R., Vannière, B., and Magny, M.: Holocene seasonality changes in the central Mediterranean region reconstructed from the pollen sequences of Lake Accesa (Italy) and Tenaghi Philippon (Greece), Holocene, 21, 131–146, https://doi.org/10.1177/0959683610384162, 2011.

Peyron, O., Magny, M., Goring, S., Joannin, S., de Beaulieu, J.-L., Brugiapaglia, E., Sadori, L., Garfi, G., Kouli, K., Ioakim, C., and Combourieu-Nebout, N.: Contrasting patterns of climatic changes during the Holocene across the Italian Peninsula reconstructed from pollen data, Clim. Past, 9, 1233–1252, https://doi.org/10.5194/cp-9-1233-2013, 2013.

Peyron, O., Combourieu-Nebout, N., Brayshaw, D., Goring, S., Andrieu-Ponel, V., Desprat, S., Fletcher, W., Gambin, B., Ioakim,

C., Joannin, S., Kotthoff, U., Kouli, K., Montade, V., Pross, J., Sadori, L., and Magny, M.: Precipitation changes in the Mediterranean basin during the Holocene from terrestrial and marine pollen records: a model–data comparison, Clim. Past, 13, 249–265, https://doi.org/10.5194/cp-13-249-2017, 2017.

Pini, R., Ravazzi, C., and Donegana, M.: Pollen stratigraphy, vegetation and climate history of the last 215 ka in the Azzano Decimo core (plain of Friuli, northeastern Italy), Quaternary Sci. Rev., 28, 1268–1290, https://doi.org/10.1016/j.quascirev.2008.12.017, 2009.

Prasad, A. M., Iverson, L. R., and Liaw, A.: Newer Classification and Regression Tree Techniques: Bagging and Random Forests for Ecological Prediction, Ecosystems, 9, 181–199, https://doi.org/10.1007/s10021-005-0054-1, 2006.

Quézel, P.: Réflexions sur l'évolution de la flore et de la végétation au Maghreb Méditerranéen, Ibis Press, Paris, 117 pp., ISBN 2910728153, 2000.

Raia, P., Mondanaro, A., Melchionna, M., Di Febbraro, M., Diniz-Filho, J. A., Rangel, T., Holden, P., Carotenuto, F., Edwards, N., Lima-Ribeiro, M., Profico, A., Maiorano, L., Castiglione, S., Serio, C., and Rook, L.: Past Extinctions of Homo Species Coincided with Increased Vulnerability to Climatic Change, One Earth, 3, 480–490, https://doi.org/10.1016/j.oneear.2020.09.007, 2020.

Railsback, L. B., Gibbard, P. L., Head, M. J., Voarintsoa, N. R. G., and Toucanne, S.: An optimized scheme of lettered marine isotope substages for the last 1.0 million years, and the climatostratigraphic nature of isotope stages and substages, Quaternary Sci. Rev., 111, 94–106, https://doi.org/10.1016/j.quascirev.2015.01.012, 2015.

Rasmussen, S. O., Bigler, M., Blockley, S. P., Blunier, T., Buchardt, S. L., Clausen, H. B., Cvijanovic, I., Dahl-Jensen, D., Johnsen, S. J., Fischer, H., Gkinis, V., Guillevic, M., Hoek, W. Z., Lowe, J. J., Pedro, J. B., Popp, T., Seierstad, I. K., Steffensen, J. P., Svensson, A. M., Vallelonga, P., Vinther, B. M., Walker, M. J. C., Wheatley, J. J., and Winstrup, M.: A stratigraphic framework for abrupt climatic changes during the Last Glacial period based on three synchronized Greenland ice-core records: refining and extending the INTIMATE event stratigraphy, Quaternary Sci. Rev., 106, 14–28, https://doi.org/10.1016/j.quascirev.2014.09.007, 2014.

Rasmussen, T. L., Oppo, D. W., Thomsen, E., and Lehman, S. J.: Deep sea records from the southeast Labrador Sea: Ocean circulation changes and ice-rafting events during the last 160 000 years, Paleoceanography, 18, https://doi.org/10.1029/2001PA000736, 2003.

Regattieri, E., Zanchetta, G., Drysdale, R. N., Isola, I., Hellstrom, J. C., and Roncioni, A.: A continuous stable isotope record from the penultimate glacial maximum to the Last Interglacial (159–121 ka) from Tana Che Urla Cave (Apuan Alps, central Italy), Quaternary Res., 82, 450, https://doi.org/10.1016/j.yqres.2014.05.005, 2014.

Renault, L., Oguz, T., Pascual, A., Vizoso, G., and Tintore, J.: Surface circulation in the Alborán Sea (western Mediterranean) inferred from remotely sensed data, J. Geophys. Res., 117, 2011JC007659, https://doi.org/10.1029/2011JC007659, 2012.

Rios-Garaizar, J.: Early Middle Palaeolithic occupations at Ventalaperra cave (Cantabrian Region, Northern Iberian Peninsula), Journal of Lithic Studies, 3, https://doi.org/10.2218/jls.v3i1.1287, 2016.

Robles, M.: Vegetation, climate, and human history of the Mediterranean basin: A Late-Glacial to Holocene reconstruction from Italy (Lake Matese) to Armenia (Lake Sevan) inferred from a multi-proxy approach (pollen, NPPs, brGDGTs, XRF), PhD thesis, University of Molise, University of Montpellier, Campobasso, Montpellier, https://www.theses.fr/s217687 (last access: 2 April 2026), 2022.

Robles, M., Peyron, O., Ménot, G., Brugiapaglia, E., Wulf, S., Appelt, O., Blache, M., Vannière, B., Dugerdil, L., Paura, B., Ansanay-Alex, S., Cromartie, A., Charlet, L., Guédron, S., de Beaulieu, J.-L., and Joannin, S.: Climate changes during the Late Glacial in southern Europe: new insights based on pollen and brGDGTs of Lake Matese in Italy, Clim. Past, 19, 493–515, https://doi.org/10.5194/cp-19-493-2023, 2023.

Rogerson, M., Cacho, I., Jimenez-Espejo, F., Reguera, M. I., Sierro, F. J., Martinez-Ruiz, F., Frigola, J., and Canals, M.: A dynamic explanation for the origin of the western Mediterranean organic-rich layers, Geochem. Geophy. Geosy., 9, https://doi.org/10.1029/2007GC001936, 2008.

Rohling, E. J., Marino, G., and Grant, K. M.: Mediterranean climate and oceanography, and the periodic development of anoxic events (sapropels), Earth-Sci. Rev., 143, 62–97, https://doi.org/10.1016/j.earscirev.2015.01.008, 2015.

Rohling, E. J., Hibbert, F. D., Williams, F. H., Grant, K. M., Marino, G., Foster, G. L., Hennekam, R., de Lange, G. J., Roberts, A. P., Yu, J., Webster, J. M., and Yokoyama, Y.: Differences between the last two glacial maxima and implications for ice-sheet, δ18O, and sea-level reconstructions, Quaternary Sci. Rev., 176, 1–28, https://doi.org/10.1016/j.quascirev.2017.09.009, 2017.

Rojo, J., Orlandi, F., Pérez-Badia, R., Aguilera, F., Ben Dhiab, A., Bouziane, H., Díaz de la Guardia, C., Galán, C., Gutiérrez-Bustillo, A. M., Moreno-Grau, S., Msallem, M., Trigo, M. M., and Fornaciari, M.: Modeling olive pollen intensity in the Mediterranean region through analysis of emission sources, Sci. Total Environ., 551–552, 73–82, https://doi.org/10.1016/j.scitotenv.2016.01.193, 2016.

Roucoux, K. H., de Abreu, L., Shackleton, N. J., and Tzedakis, P. C.: The response of NW Iberian vegetation to North Atlantic climate oscillations during the last 65 kyr, Quaternary Sci. Rev., 24, 1637–1653, https://doi.org/10.1016/j.quascirev.2004.08.022, 2005.

Roucoux, K. H., Tzedakis, P. C., Lawson, I. T., and Margari, V.: Vegetation history of the penultimate glacial period (Marine isotope stage 6) at Ioannina, north-west Greece, J. Quaternary Sci., 26, 616–626, https://doi.org/10.1002/jqs.1483, 2011.

Rousseau, D.-D., Antoine, P., Boers, N., Lagroix, F., Ghil, M., Lomax, J., Fuchs, M., Debret, M., Hatté, C., Moine, O., Gauthier, C., Jordanova, D., and Jordanova, N.: Dansgaard–Oeschger-like events of the penultimate climate cycle: the loess point of view, Clim. Past, 16, 713–727, https://doi.org/10.5194/cp-16-713-2020, 2020.

Rubio-Jara, S. and Panera, J.: Unravelling an essential archive for the European Pleistocene. The human occupation in the Manzanares valley (Madrid, Spain) throughout nearly 800 000 years, Quatern. Int., 520, 5–22, https://doi.org/10.1016/j.quaint.2018.08.007, 2019.

Rubio-Jara, S., Panera, J., Rodríguez-de-Tembleque, J., Santonja, M., and Pérez-González, A.: Large flake Acheulean in the middle of Tagus basin (Spain): Middle stretch of

the river Tagus valley and lower stretches of the rivers Jarama and Manzanares valleys, Quatern. Int., 411, 349–366, https://doi.org/10.1016/j.quaint.2015.12.023, 2016.

Ruddiman, W. F.: Late Quaternary deposition of ice-rafted sand in the subpolar North Atlantic (lat 40° to 65° N), Geol. Soc. Am. Bull., 88, 1813, https://doi.org/10.1130/0016-7606(1977)88<1813:LQDOIS>2.0.CO;2, 1977.

Sadori, L., Koutsodendris, A., Panagiotopoulos, K., Masi, A., Bertini, A., Combourieu-Nebout, N., Francke, A., Kouli, K., Joannin, S., Mercuri, A. M., Peyron, O., Torri, P., Wagner, B., Zanchetta, G., Sinopoli, G., and Donders, T. H.: Pollen-based paleoenvironmental and paleoclimatic change at Lake Ohrid (south-eastern Europe) during the past 500 ka, Biogeosciences, 13, 1423–1437, https://doi.org/10.5194/bg-13-1423-2016, 2016.

Salonen, J. S., Seppä, H., Luoto, M., Bjune, A. E., and Birks, H. J. B.: A North European pollen–climate calibration set: analysing the climatic responses of a biological proxy using novel regression tree methods, Quaternary Sci. Rev., 45, 95–110, https://doi.org/10.1016/j.quascirev.2012.05.003, 2012.

Salonen, J. S., Korpela, M., Williams, J. W., and Luoto, M.: Machine-learning based reconstructions of primary and secondary climate variables from North American and European fossil pollen data, Sci. Rep., 9, 15805, https://doi.org/10.1038/s41598-019-52293-4, 2019.

Sánchez Goñi, M.: The climatic and environmental context of the Late Pleistocene, in: Updating Neanderthals. Understanding Behavioural Complexity in the Late Middle Palaeolithic, Elsevier/Academic Press, London, 165–169, https://doi.org/10.1016/B978-0-12-823498-3.00012-1, 2022.

Sánchez Goñi, M. F., Cacho, I., Jean Louis, T., Joel, G., Sierro, F., Peypouquet, J., Grimalt, J., and Shackleton, N.: Synchroneity between marine and terrestrial responses to millennial scale climatic variability during the last glacial period in the Mediterranean region, Clim. Dynam., 19, 95, https://doi.org/10.1007/s00382-001-0212-x, 2002.

Sánchez-Laulhé, J. M., Jansa, A., and Jiménez, C.: Alboran Sea Area Climate and Weather, in: Alboran Sea – Ecosystems and Marine Resources, edited by: Báez, J. C., Vázquez, J.-T., Camiñas, J. A., and Malouli Idrissi, M., Springer International Publishing, Cham, 31–83, https://doi.org/10.1007/978-3-030-65516-7_3, 2021.

Sánchez-Yustos, P.: El paleolítico antiguo en la cuenca del Duero. Instrumentos teóricos para la construcción de un modelo interpretativo de arqueología económica, http://uvadoc.uva.es/handle/10324/8989 (last access: 2 April 2026), 2009.

Sánchez-Yustos, P. and Diez-Martín, F.: Dancing to the rhythms of the Pleistocene? Early Middle Paleolithic population dynamics in NW Iberia (Duero Basin and Cantabrian Region), Quaternary Sci. Rev., 121, https://doi.org/10.1016/j.quascirev.2015.05.005, 2015.

Santonja, M., Pérez-González, A., Panera, J., Rubio-Jara, S., and Méndez-Quintas, E.: The coexistence of Acheulean and Ancient Middle Palaeolithic techno-complexes in the Middle Pleistocene of the Iberian Peninsula, Quatern. Int., 411, 367–377, https://doi.org/10.1016/j.quaint.2015.04.056, 2016.

Santonja, M., Pérez-González, A., Baena, J., Panera, J., Méndez-Quintas, E., Uribelarrea, D., Demuro, M., Arnold, L., Abrunhosa, A., and Rubio-Jara, S.: The Acheulean of the Upper Guadiana River Basin (Central Spain). Morphostratigraphic Context and Chronology, Front. Earth Sci., 10, https://doi.org/10.3389/feart.2022.912007, 2022.

Sassoon, D., Lebreton, V., Combourieu-Nebout, N., Peyron, O., and Moncel, M.-H.: Palaeoenvironmental changes in the southwestern Mediterranean (ODP site 976, Alboran sea) during the MIS 12/11 transition and the MIS 11 interglacial and implications for hominin populations, Quaternary Sci. Rev., 304, 108010, https://doi.org/10.1016/j.quascirev.2023.108010, 2023.

Sassoon, D., Combourieu-Nebout, N., Peyron, O., Bertini, A., Toti, F., Lebreton, V., and Moncel, M.-H.: Pollen-based climatic reconstructions for the interglacial analogues of MIS 1 (MIS 19, 11, and 5) in the southwestern Mediterranean: insights from ODP Site 976, Clim. Past, 21, 489–515, https://doi.org/10.5194/cp-21-489-2025, 2025.

Savannah, M., Eelco, R., Timme, D., Katharine, G., Jörg, K., Gianluca, M., Francesca, S., Francesca, C., Caterina, M., Anna, S., and Alessandra, N.: The "glacial" sapropel S6 (172 ka; MIS 6): A multiproxy approach to solve a Mediterranean "cold case", Palaeogeogr. Palaeocl., 650, 112384, https://doi.org/10.1016/j.palaeo.2024.112384, 2024.

Scott, B.: Becoming Neanderthals: the earlier British middle palaeolithic, Oxbow books, Oxford, ISBN 978-1-84217-973-4, 2011.

Shackleton, N. J.: Oxygen isotopes, ice volume and sea level, Quaternary Sci. Rev., 6, 183–190, https://doi.org/10.1016/0277-3791(87)90003-5, 1987.

Shackleton, N. J., Hall, M. A., and Vincent, E.: Phase relationships between millennial-scale events 64 000–24 000 years ago, Paleoceanography, 15, 565–569, https://doi.org/10.1029/2000PA000513, 2000.

Shackleton, N. J., Sánchez-Goñi, M. F., Pailler, D., and Lancelot, Y.: Marine Isotope Substage 5e and the Eemian Interglacial, Glob. Planet. Change, 36, 151–155, https://doi.org/10.1016/S0921-8181(02)00181-9, 2003.

Shackleton, N. J., Fairbanks, R. G., Chiu, T., and Parrenin, F.: Absolute calibration of the Greenland time scale: implications for Antarctic time scales and for Δ14C, Quaternary Sci. Rev., 23, 1513–1522, https://doi.org/10.1016/j.quascirev.2004.03.006, 2004.

Shaw, A., Bates, M., Conneller, C., Gamble, C., Julien, M.-A., McNabb, J., Pope, M., and Scott, B.: The archaeology of persistent places: the Palaeolithic case ofLa Cotte de St Brelade, Jersey, Antiquity, 90, 1437–1453, https://doi.org/10.15184/aqy.2016.212, 2016.

Shin, J., Nehrbass-Ahles, C., Grilli, R., Chowdhry Beeman, J., Parrenin, F., Teste, G., Landais, A., Schmidely, L., Silva, L., Schmitt, J., Bereiter, B., Stocker, T. F., Fischer, H., and Chappellaz, J.: Millennial-scale atmospheric CO_2 variations during the Marine Isotope Stage 6 period (190–135 ka), Clim. Past, 16, 2203–2219, https://doi.org/10.5194/cp-16-2203-2020, 2020.

Sierro, F. J. and Andersen, N.: An exceptional record of millennial-scale climate variability in the southern Iberian Margin during MIS 6: Impact on the formation of sapropel S6, Quaternary Sci. Rev., 286, 107527, https://doi.org/10.1016/j.quascirev.2022.107527, 2022.

Sierro, F. J., Hodell, D. A., Andersen, N., Azibeiro, L. A., Jimenez-Espejo, F. J., Bahr, A., Flores, J. A., Ausin, B., Rogerson, M., Lozano-Luz, R., Lebreiro, S. M., and Hernandez-Molina, F. J.: Mediterranean Overflow Over the Last 250 kyr: Freshwater Forcing From the Tropics to the Ice Sheets, Pa-

leoceanography and Paleoclimatology, 35, e2020PA003931, https://doi.org/10.1029/2020PA003931, 2020.

Silva, P. G., López-Recio, M., Tapias, F., Roquero, E., Morín, J., Rus, I., Carrasco-García, P., Giner-Robles, J. L., Rodríguez-Pascua, M. A., and Pérez-López, R.: Stratigraphy of the Arriaga Palaeolithic sites. Implications for the geomorphological evolution recorded by thickened fluvial sequences within the Manzanares River valley (Madrid Neogene Basin, Central Spain), Geomorphology, 196, 138–161, https://doi.org/10.1016/j.geomorph.2012.10.019, 2013.

Sinopoli, G., Peyron, O., Masi, A., Holtvoeth, J., Francke, A., Wagner, B., and Sadori, L.: Pollen-based temperature and precipitation changes in the Ohrid Basin (western Balkans) between 160 and 70 ka, Clim. Past, 15, 53–71, https://doi.org/10.5194/cp-15-53-2019, 2019.

Skinner, L. C. and Shackleton, N. J.: Deconstructing Terminations I and II: revisiting the glacioeustatic paradigm based on deep-water temperature estimates, Quaternary Sci. Rev., 25, 3312–3321, https://doi.org/10.1016/j.quascirev.2006.07.005, 2006.

Stewart, J. R., García-Rodríguez, O., Knul, M. V., Sewell, L., Montgomery, H., Thomas, M. G., and Diekmann, Y.: Palaeoecological and genetic evidence for Neanderthal power locomotion as an adaptation to a woodland environment, Quaternary Sci. Rev., 217, 310–315, https://doi.org/10.1016/j.quascirev.2018.12.023, 2019.

Stocker, T. F.: The Seesaw Effect, Science, 282, 61–62, https://doi.org/10.1126/science.282.5386.61, 1998.

Sumner, G., Homar, V., and Ramis, C.: Precipitation seasonality in eastern and southern coastal Spain, Int. J. Climatol., 21, 219–247, https://doi.org/10.1002/joc.600, 2001.

Svendsen, J. I., Alexanderson, H., Astakhov, V. I., Demidov, I., Dowdeswell, J. A., Funder, S., Gataullin, V., Henriksen, M., Hjort, C., Houmark-Nielsen, M., Hubberten, H. W., Ingólfsson, Ó., Jakobsson, M., Kjær, K. H., Larsen, E., Lokrantz, H., Lunkka, J. P., Lysså, A., Mangerud, J., Matiouchkov, A., Murray, A., Möller, P., Niessen, F., Nikolskaya, O., Polyak, L., Saarnisto, M., Siegert, C., Siegert, M. J., Spielhagen, R. F., and Stein, R.: Late Quaternary ice sheet history of northern Eurasia, Quaternary Sci. Rev., 23, 1229–1271, https://doi.org/10.1016/j.quascirev.2003.12.008, 2004.

ter Braak, C. and Juggins, S.: Weighted Averaging Partial Least Squares Regression (WA-PLS): An Improved Method for Reconstructing Environmental Variables from Species Assemblages, Hydrobiologia, 269–270, 485–502, https://doi.org/10.1007/BF00028046, 1993.

Terradillos-Bernal, M., Demuro, M., Arnold, L. J., Jordá-Pardo, J. F., Clemente-Conte, I., Benito-Calvo, A., and Díez Fernández-Lomana, J. C.: San Quirce (Palencia, Spain): new chronologies for the Lower to Middle Palaeolithic transition of south-west Europe, J. Quaternary Sci., 38, 21–37, https://doi.org/10.1002/jqs.3460, 2023.

Thabet, A. A., Maas, A. E., Lawson, G. L., and Tarrant, A. M.: Life cycle and early development of the thecosomatous pteropod Limacina retroversa in the Gulf of Maine, including the effect of elevated CO_2 levels, Mar. Biol., 162, 2235–2249, https://doi.org/10.1007/s00227-015-2754-1, 2015.

Torres, C., Tapias, F., Demuro, M., Arnold, L., Arriolabengoa, M., Pérez, S., and Preysler, J.: The Acheulian site of Cantera Vieja (Madrid, Spain) and the Lower to Middle Palaeolithic transition in central Spain, Rersearch Square, preprint, https://doi.org/10.21203/rs.3.rs-4195503/v1, 2024.

Toucanne, S., Zaragosi, S., Bourillet, J. F., Cremer, M., Eynaud, F., Van Vliet-Lanoë, B., Penaud, A., Fontanier, C., Turon, J. L., Cortijo, E., and Gibbard, P. L.: Timing of massive 'Fleuve Manche' discharges over the last 350 kyr: insights into the European ice-sheet oscillations and the European drainage network from MIS 10 to 2, Quaternary Sci. Rev., 28, 1238–1256, https://doi.org/10.1016/j.quascirev.2009.01.006, 2009.

Trájer, A. J.: Ecological evaluation of the development of Neanderthal niche exploitation, Quaternary Sci. Rev., 310, 108127, https://doi.org/10.1016/j.quascirev.2023.108127, 2023.

Tzedakis, P. C.: Long-term tree populations in northwest Greece through multiple Quaternary climatic cycles, Nature, 364, 437–440, https://doi.org/10.1038/364437a0, 1993.

Tzedakis, P. C.: Towards an understanding of the response of southern European vegetation to orbital and suborbital climate variability, Quaternary Sci. Rev., 24, 1585–1599, https://doi.org/10.1016/j.quascirev.2004.11.012, 2005.

Tzedakis, P. C., Frogley, M. R., Lawson, I. T., Preece, R. C., Cacho, I., and de Abreu, L.: Ecological thresholds and patterns of millennial-scale climate variability: The response of vegetation in Greece during the last glacial period, Geology, 32, 109, https://doi.org/10.1130/G20118.1, 2004.

Tzedakis, P. C., Hooghiemstra, H., and Pälike, H.: The last 1.35 million years at Tenaghi Philippon: revised chronostratigraphy and long-term vegetation trends, Quaternary Sci. Rev., 25, 3416–3430, https://doi.org/10.1016/j.quascirev.2006.09.002, 2006.

Tzedakis, P. C., Drysdale, R. N., Margari, V., Skinner, L. C., Menviel, L., Rhodes, R. H., Taschetto, A. S., Hodell, D. A., Crowhurst, S. J., Hellstrom, J. C., Fallick, A. E., Grimalt, J. O., McManus, J. F., Martrat, B., Mokeddem, Z., Parrenin, F., Regattieri, E., Roe, K., and Zanchetta, G.: Enhanced climate instability in the North Atlantic and southern Europe during the Last Interglacial, Nat. Commun., 9, 4235, https://doi.org/10.1038/s41467-018-06683-3, 2018.

Valensi, P., Aouraghe, H., Bailon, S., Cauche, D., Combier, J., Desclaux, E., Gagnepain, J., Gaillard, C., Khatib, S., Lumley, H., Moigne, A.-M., Moncel, M.-H., and Notter, O.: Les peuplements préhistoriques dans le sud-est de la France à la fin du Pléistocène moyen: 400–120 000 ans. Terra Amata, Orgnac 3, Baume Bonne, Lazaret, Cadre géochronologique et biostratigraphique, paléoenvironnements et évolution culturelle des derniers anténéandertaliens, ISBN 1841713988, 2005.

Valensi, P., Michel, V., El Guennouni, K., and Liouville, M.: New data on human behavior from a 160 000 year old Acheulean occupation level at Lazaret cave, south-east France: An archaeozoological approach, Quatern. Int., 316, https://doi.org/10.1016/j.quaint.2013.10.034, 2013.

Vernot, B., Zavala, E., Gómez-Olivencia, A., Jacobs, Z., Slon, V., Mafessoni, F., Romagné, F., Pearson, A., Petr, M., Sala, N., Pablos, A., Aranburu, A., Bermúdez de Castro, J.-M., Carbonell, E., Li, B., Krajcarz, M., Krivoshapkin, A., Kolobova, K., Kozlikin, M., and Meyer, M.: Unearthing Neanderthal population history using nuclear and mitochondrial DNA from cave sediments, Science, 372, eabf1667, https://doi.org/10.1126/science.abf1667, 2021.

Vidal-Matutano, P., Blasco, R., Sañudo, P., and Fernández Peris, J.: The Anthropogenic Use of Firewood During the European Mid-

dle Pleistocene: Charcoal Evidence from Levels XIII and XI of Bolomor Cave, Eastern Iberia (230–160 ka), Environ. Archaeol., 24, 269–284, https://doi.org/10.1080/14614103.2017.1406026, 2019.

Voelker, A. H. L. and de Abreu, L.: A Review of Abrupt Climate Change Events in the Northeastern Atlantic Ocean (Iberian Margin): Latitudinal, Longitudinal, and Vertical Gradients, in: Abrupt Climate Change: Mechanisms, Patterns, and Impacts, American Geophysical Union (AGU), 15–37, https://doi.org/10.1029/2010GM001021, 2011.

von Grafenstein, R., Zahn, R., and Tiedemann, R.: Planktonic d18O records at Sites 976 and 977, Alboran Sea: stratigraphy, forcing, and paleoceanographic implications, in: Proceedings Ocean Drilling Program Scientific Results, edited by: Zahn, R., Comas, M. C., and Klaus, A., 161, 469–479, https://doi.org/10.2973/odp.proc.sr.161.1999, 1999.

Wagner, B., Vogel, H., Francke, A., Friedrich, T., Donders, T., Lacey, J. H., Leng, M. J., Regattieri, E., Sadori, L., Wilke, T., Zanchetta, G., Albrecht, C., Bertini, A., Combourieu-Nebout, N., Cvetkoska, A., Giaccio, B., Grazhdani, A., Hauffe, T., Holtvoeth, J., Joannin, S., Jovanovska, E., Just, J., Kouli, K., Kousis, I., Koutsodendris, A., Krastel, S., Lagos, M., Leicher, N., Levkov, Z., Lindhorst, K., Masi, A., Melles, M., Mercuri, A. M., Nomade, S., Nowaczyk, N., Panagiotopoulos, K., Peyron, O., Reed, J. M., Sagnotti, L., Sinopoli, G., Stelbrink, B., Sulpizio, R., Timmermann, A., Tofilovska, S., Torri, P., Wagner-Cremer, F., Wonik, T., and Zhang, X.: Mediterranean winter rainfall in phase with African monsoons during the past 1.36 million years, Nature, 573, 256–260, https://doi.org/10.1038/s41586-019-1529-0, 2019.

Wainer, K., Genty, D., Blamart, D., Daëron, M., Bar-Matthews, M., Vonhof, H., Dublyansky, Y., Pons-Branchu, E., Thomas, L., Calsteren, P., Quinif, Y., and Caillon, N.: Speleothem record of the last 180 ka in Villars cave (SW France): Investigation of a large δ 18O shift between MIS6 and MIS5, Quaternary Sci. Rev., 30, 130–146, https://doi.org/10.1016/j.quascirev.2010.07.004, 2011.

Wainer, K., Genty, D., Blamart, D., Bar-Matthews, M., Quinif, Y., and Plagnes, V.: Millennial climatic instability during penultimate glacial period recorded in a south-western France speleothem, Palaeogeogr. Palaeocl., 376, 122–131, https://doi.org/10.1016/j.palaeo.2013.02.026, 2013.

Wang, Q., Wang, Y., Shao, Q., Liang, Y., Zhang, Z., and Kong, X.: Millennial-scale Asian monsoon variability during the late Marine Isotope Stage 6 from Hulu Cave, China, Quat. Res., 90, 394–405, https://doi.org/10.1017/qua.2018.75, 2018.

Wang, Y. J., Cheng, H., Edwards, R. L., An, Z. S., Wu, J. Y., Shen, C. C., and Dorale, J. A.: A high-resolution absolute-dated late Pleistocene Monsoon record from Hulu Cave, China, Science, 294, 2345–2348, https://doi.org/10.1126/science.1064618, 2001.

Wenzel, S.: Neanderthal presence and behaviour in central and Northwestern Europe during MIS 5e, in: Developments in Quaternary Sciences, 173–193, https://doi.org/10.13140/2.1.2747.7442, 2007.

White, M. J. and Pettitt, P. B.: The British Late Middle Palaeolithic: An Interpretative Synthesis of Neanderthal Occupation at the Northwestern Edge of the Pleistocene World, J. World Prehist., 24, https://doi.org/10.1007/s10963-011-9043-9, 2011.

Willis, K. J., Bennett, K. D., Walker, D., Gamble, C., Davies, W., Pettitt, P., and Richards, M.: Climate change and evolving human diversity in Europe during the last glacial, Philos. T. Roy. Soc. Lond. B, 359, 243–254, https://doi.org/10.1098/rstb.2003.1396, 2004.

Wilson, G. P., Frogley, M. R., Hughes, P. D., Roucoux, K. H., Margari, V., Jones, T. D., Leng, M. J., and Tzedakis, P. C.: Persistent millennial-scale climate variability in Southern Europe during Marine Isotope Stage 6, Quaternary Science Advances, 3, 100016, https://doi.org/10.1016/j.qsa.2020.100016, 2021.

Xue, G., Cai, Y., Ma, L., Cheng, X., Cheng, H., Edwards, R. L., Li, D., and Tan, L.: A new speleothem record of the penultimate deglacial: Insights into spatial variability and centennial-scale instabilities of East Asian monsoon, Quaternary Sci. Rev., 210, 113–124, https://doi.org/10.1016/j.quascirev.2019.02.023, 2019.

Yaworsky, P. M., Nielsen, E. S., and Nielsen, T. K.: The Neanderthal niche space of Western Eurasia 145 ka to 30 ka ago, Sci. Rep., 14, 7788, https://doi.org/10.1038/s41598-024-57490-4, 2024.

Yravedra, J., Rubio-Jara, S., Panera, J., Made, J. van der, and Pérez-González, A.: Neanderthal diet in fluvial environments at the end of the Middle Pleistocene/early Late Pleistocene of PRERESA site in the Manzanares Valley (Madrid, Spain), Quatern. Int., 520, 72–83, https://doi.org/10.1016/j.quaint.2018.01.030, 2019.

Zahn, R., Comas, M. C., and Klaus, A. (Eds.): Proceedings of the Ocean Drilling Program, 161 Scientific Results, Ocean Drilling Program, https://doi.org/10.2973/odp.proc.sr.161.1999, 1999.

Zhang, J., Zolitschka, B., Hogrefe, I., Tsukamoto, S., Binot, F., and Frechen, M.: High-resolution luminescence-dated sediment record for the last two glacial-interglacial cycles from Rodderberg, Germany, Quat. Geochronol., 82, 101535, https://doi.org/10.1016/j.quageo.2024.101535, 2024.

Ziegler, M., Tuenter, E., and Lourens, L.: The precession phase of the boreal summer monsoon as viewed from the eastern Mediterranean (ODP Site 968), Quaternary Sci. Rev., 29, https://doi.org/10.1016/j.quascirev.2010.03.011, 2010.

Zumaque, J., de Anne, V., Fréchette, B., Joel, G., Sanchez Goñi, M., Barhoumi, C., Peyron, O., Peros, M., Burke, A., Camuera, J., Jiménez-Moreno, G., and Ramos-Román, M. J.: Decoupled winter and summer climate changes in southern Europe during the Dansgaard-Oeschger cycles, Quaternary Sci. Rev., 359, https://doi.org/10.1016/j.quascirev.2025.109273, 2025.